

Dynamical Coupled Channels Theory

for nucleon resonances

Michael Doering

THE GEORGE
WASHINGTON
UNIVERSITY

WASHINGTON, DC

Jefferson Lab
Thomas Jefferson National Accelerator Facility

Baryons 2021

18-22 October, Sevilla^u

- Conference Link: <https://indico.cern.ch/event/1026059/>
- My contact: doring@gwu.edu. Please write me for any questions or access to material upon which this lecture is based
- Work supported by:



Department of Energy,
DOE DE-AC05-06OR23177
& DE-SC0016582



HPC support by JSC
grant *jikp07*



National Science Foundation
Grant No. PHY 2012289

Literature & Resources

- Part on quantum mechanical scattering: Some pictures & formulas taken from
 - Helmut Haberketzl, "Quantum Mechanics with Introduction to Quantum Field Theory", Lecture Notes, to be published; indicated as [HZ] (helmut@gwu.edu)
- Example codes in Mathematica, partially coming from my lectures at GW on computational physics:
 - Dropbox
<https://www.dropbox.com/sh/7h9bxxcvu124z2x/AAAiL2S5ISj8yVGYGjKejFxSa?dl=0>
- Several slides borrowed from Maxim Mai [MM] and Deborah Rönchen [DR]
- References are hyperlinks; usually, only reviews with didactic components are cited (this is a lecture, not a review)
- What this lecture is
 - highlight of interesting aspects of arguable relevance with some useful links
 -and what it isn't (systematic & self-contained)
 - But, still, with some explicit derivations and in-depth examples & connections

Content

1. Scattering basics:
 1. Scattering theory basics & application to spherical well
 2. Mathematica animation & example code (bound state vs. resonances)
 3. Resonances as poles: Analytic continuation & the meson baryon amplitude
2. Phenomenology of resonances:
 1. Spectrum of excited baryons from experiment: missing (?) resonances
 2. A dynamical-coupled channel model
 3. Statistical aspects: Model selection
3. Three-body aspects for dynamical coupled-channel models
 1. Three-body unitarity for the construction of amplitudes
 2. Analytic continuation for three-body amplitudes

Skipped content (Spare slides)

- Causality: Why are poles on the second Riemann sheet?
- Analyticity: Mandelstam variables and plane
- Crossing symmetry: Representations of the pion-nucleon amplitude
- Roy(-like) equations
- Application of DCC-like amplitudes in lattice QCD: three body resonances

Scattering energy named in this talk: $W = z = E = \sqrt{s}$

Interesting light baryons

$\Delta(1232)3/2^-$

First excited baryon
discovered
Standard Breit-Wigner
(BW) resonance [\[Crede\]](#)

$N(1440)1/2^+$, “Roper”

Enigmatic; absent in many
Lattice QCD and quark
model calculations; non-BW
[\[Burkert\]](#)

$\Lambda(1405)$

Two pole structure
complicated
production [\[Mai\]](#)

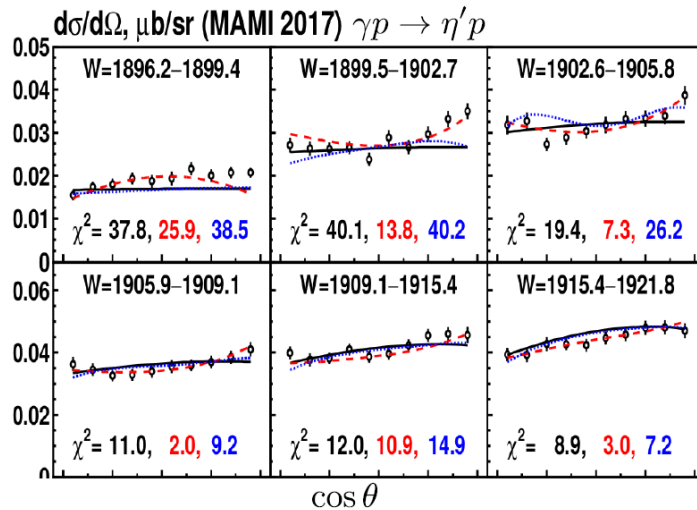
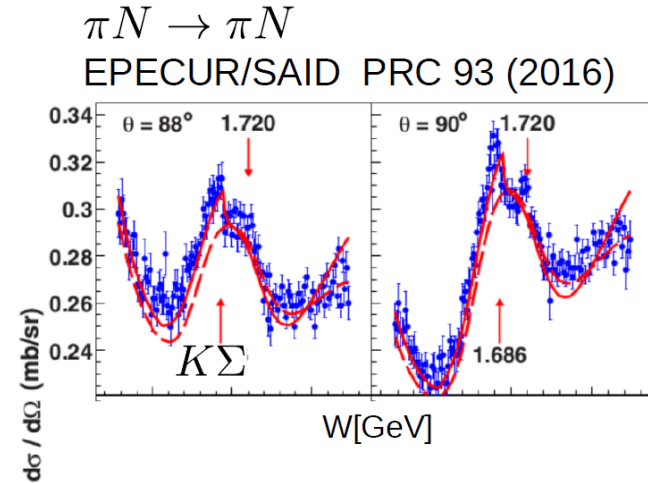
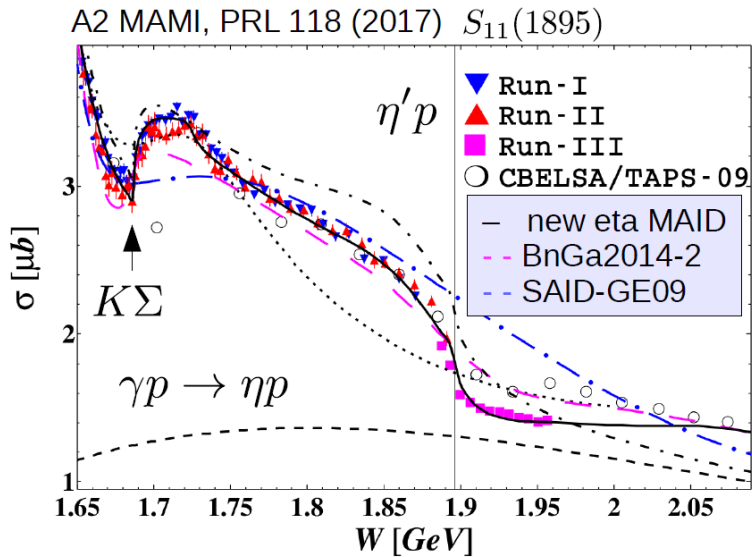
$N(1535)1/2^-$, $N(1650)1/2^-$

Nearby, overlapping
resonances with same
quantum numbers

$N(1900)3/2^+$

Recently discovered
in large experimental
baryon searches for
“missing resonance”

Resonances or not?



BnGa
PLB785 (2018):

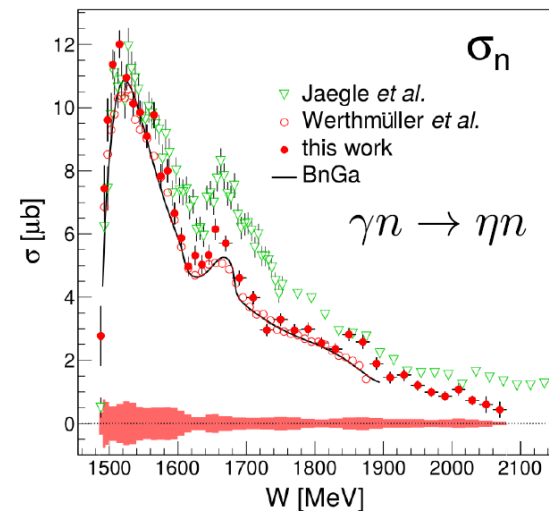
No narrow
resonance

3/2⁻ narrow
Resonance

5/2⁻ narrow
Resonance

Data: A2.Mami
PRL 118 (2017)

[CBELSA/TAPS EPJA 53 (2017)]



1.1. QM Scattering: Basics

- Radiation condition: $\psi_{\mathbf{k}}^{(+)}(\mathbf{r}) \xrightarrow{r \rightarrow \infty} e^{i\mathbf{k} \cdot \mathbf{r}} + \frac{e^{ikr}}{r} f(\theta)$
- Scattering amplitude & partial-wave (PW) expansion:

$$f(\theta) = \sum_{\ell=0}^{\infty} (2\ell + 1) t_{\ell} P_{\ell}(\xi) , \quad t_{\ell} = \frac{1}{k \cot \delta_{\ell} - ik}$$

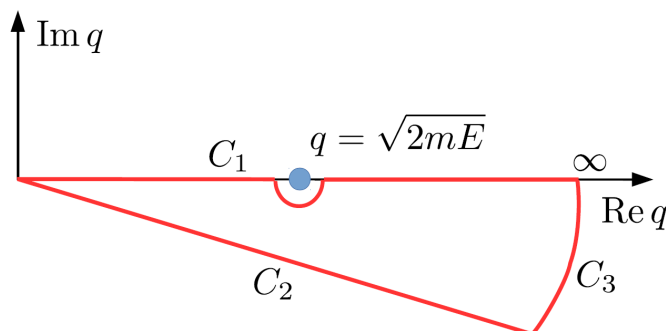
Legendre polynomials P_{ℓ} and $\xi = \cos \theta$.

- Lippmann-Schwinger equation (LSE)

$$T(\mathbf{p}', \mathbf{p}) = V(\mathbf{p}', \mathbf{p}) + \int d^3q V(\mathbf{p}', \mathbf{q}) \frac{1}{E - \frac{q^2}{2m} + i\epsilon} T(\mathbf{q}, \mathbf{p})$$

- PW-projected LSE

$$T_{\ell}(p', p) = V_{\ell}(p', p) + \int_0^{\infty} dq q^2 \frac{V_{\ell}(p', q)}{E - \frac{q^2}{2m} + i\epsilon} T_{\ell}(q, p)$$



- Solve, e.g., by contour deformation

How to solve the LSE

- Example code in Mathematica: Implementation of Haftl-Tabakin scheme [\[Haftl\]](#)

$$T_{\ell}(p', p) = V_{\ell}(p', p) + \int_0^{\infty} dq q^2 \frac{V_{\ell}(p', q)}{E - \frac{q^2}{2m} + i\epsilon} T_{\ell}(q, p)$$

- Gauss integration $\int f(x) dx \approx \sum_{i=1}^n f(x_i) w_i$ for n off-shell momenta and one on-shell momentum $n + 1$

$$\bar{V} = \begin{pmatrix} V_{11} & \dots & V_{1n} & V_{1,n+1} \\ \vdots & \ddots & \vdots & \vdots \\ V_{n1} & \dots & V_{nn} & \vdots \\ V_{n+1,1} & \dots & \dots & V_{n+1,n+1} \end{pmatrix}$$

$$\bar{G} = \begin{pmatrix} \frac{q_1^2 w_1}{z - E_1} & 0 & \dots & 0 \\ 0 & \ddots & & \vdots \\ \vdots & & \frac{q_n^2 w_n}{z - E_n} & \vdots \\ 0 & \dots & \dots & 0 \end{pmatrix} \quad (z = E)$$

$$\bar{T} = \begin{pmatrix} T_{11} & \dots & T_{1n} & T_{1,n+1} \\ \vdots & \ddots & \vdots & \vdots \\ T_{n1} & \dots & T_{nn} & \vdots \\ T_{n+1,1} & \dots & \dots & T_{n+1,n+1} \end{pmatrix}$$

[DR]

- Gauss nodes q_1, \dots, q_n chosen along contour from 0 to ∞
- On-shell point chosen as

$$E = \frac{q_{n+1}^2}{2m}$$

where E is scattering energy

How to solve the LSE (2)

$$T_\ell(p', p) = V_\ell(p', p) + \int_0^\infty dq q^2 \frac{V_\ell(p', q)}{E - \frac{q^2}{2m} + i\epsilon} T_\ell(q, p)$$

Discretize the integral: $\int dq q^2 V(p', q) G(q, E) T(q, p) \rightarrow \bar{V} \bar{G} \bar{T}$

Gauss integration $\int f(x) dx \approx \sum_{i=1}^n f(x_i) w_i$ for n off-shell momenta and one on-shell momentum $n + 1$

$$\bar{V} \bar{G} \bar{T} = \begin{pmatrix} \sum_{i=1}^n V_{1i} \frac{q_i^2 w_i}{z - E_i} T_{i1} & \cdots & \sum_{i=1}^n V_{1i} \frac{q_i^2 w_i}{z - E_i} T_{in} & \sum_{i=1}^n V_{1i} \frac{q_i^2 w_i}{z - E_i} T_{i,n+1} \\ \vdots & \ddots & \vdots & \vdots \\ \sum_{i=1}^n V_{ni} \frac{q_i^2 w_i}{z - E_i} T_{i1} & \cdots & \sum_{i=1}^n V_{ni} \frac{q_i^2 w_i}{z - E_i} T_{in} & \vdots \\ \sum_{i=1}^n V_{n+1,i} \frac{q_i^2 w_i}{z - E_i} T_{i1} & \cdots & \cdots & \sum_{i=1}^n V_{n+1,i} \frac{q_i^2 w_i}{z - E_i} T_{i,n+1} \end{pmatrix}$$

[DR]

How to solve the LSE (3)

- On-shell \rightarrow on-shell for physical amplitude

$$T_{ik} = V_{ik} + \sum_{j=1}^n V_{ij} \frac{q_j^2 w_j}{z - E_j} T_{jk} \quad \text{off-shell} \rightarrow \text{off-shell}$$

$$T_{n+1,k} = V_{n+1,k} + \sum_{j=1}^n V_{n+1,j} \frac{q_j^2 w_j}{z - E_j} T_{jk} \quad \text{off-shell} \rightarrow \text{on-shell}$$

$$T_{i,n+1} = V_{i,n+1} + \sum_{j=1}^n V_{ij} \frac{q_j^2 w_j}{z - E_j} T_{j,n+1} \quad \text{on-shell} \rightarrow \text{off-shell}$$

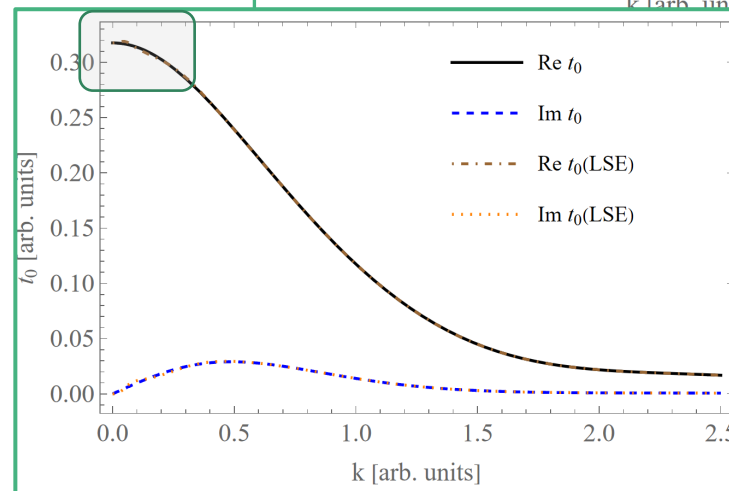
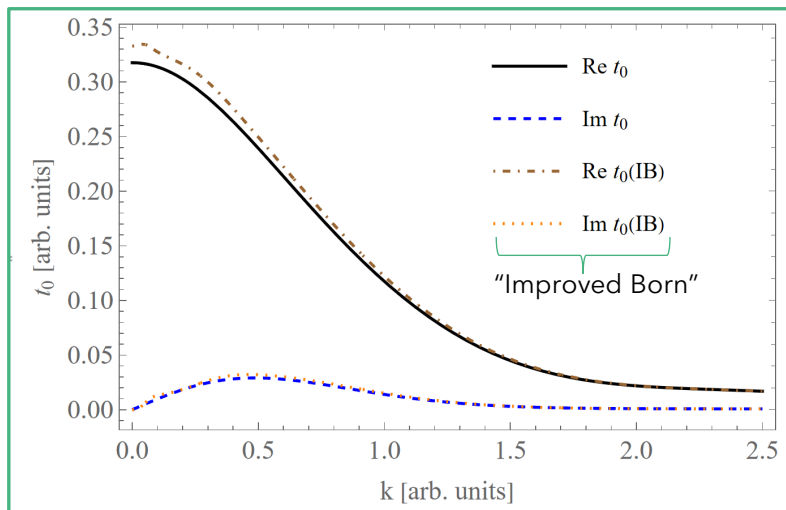
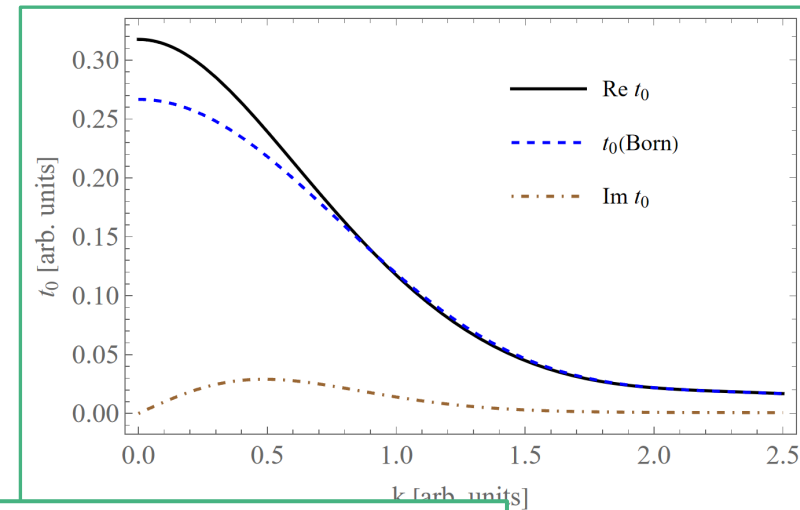
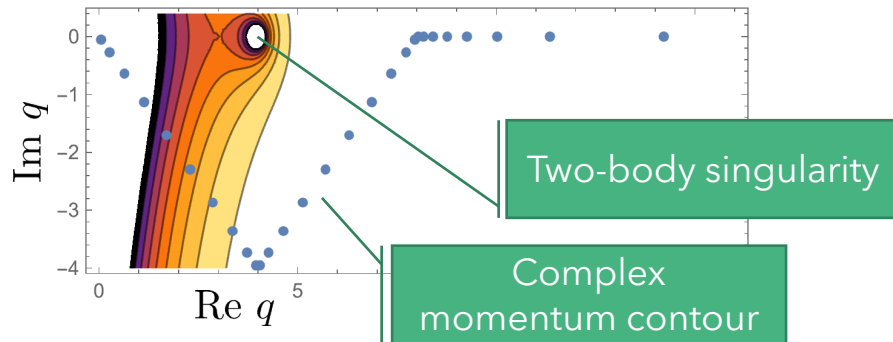
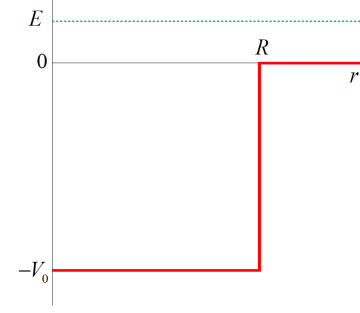
$$\boxed{T_{n+1,n+1}} = V_{n+1,n+1} + \sum_{j=1}^n V_{n+1,j} \frac{q_j^2 w_j}{z - E_j} T_{j,n+1} \quad \text{on-shell} \rightarrow \text{on-shell}$$

- We can now invert the matrix:

$$\bar{\mathbf{T}} = (\mathbf{1} - \bar{\mathbf{V}}\bar{\mathbf{G}})^{-1}\bar{\mathbf{V}}$$

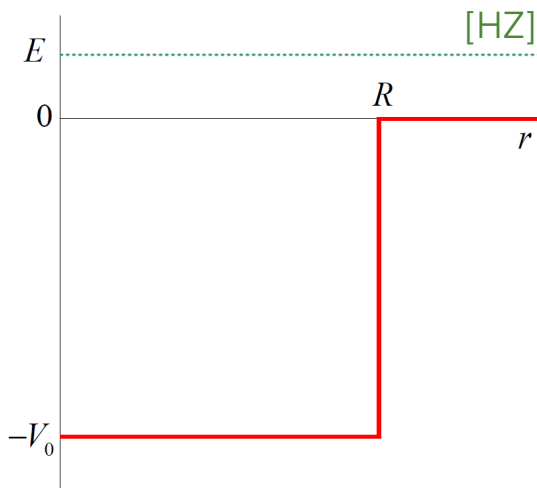
CompPhys-project

- Spherical well with LSE compared to analytic solution
- "LSE_for_Spherical_Well.nb"



Spherical well

Potential in radial coordinates:



$$V(r) = \begin{cases} -V_0 & \text{for } r < R, \\ 0 & \text{for } r > R, \end{cases}$$

Scattering phase shifts ($E > 0$)

$$\tan \delta_\ell = \frac{k j'_\ell(kR) - \gamma_\ell j_\ell(kR)}{k n'_\ell(kR) - \gamma_\ell n_\ell(kR)}$$

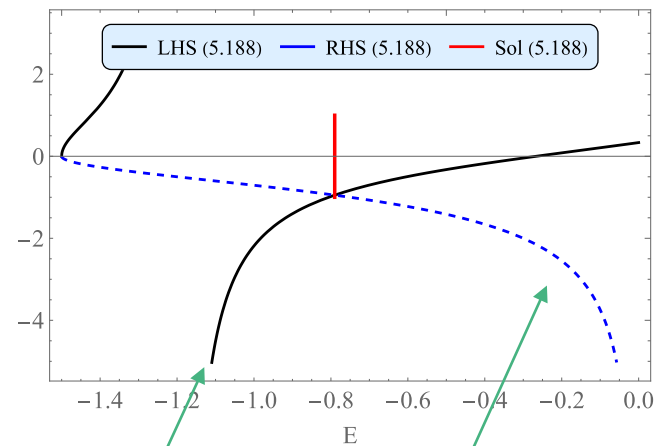
Matching

Sph. Bessel-f.

Wave number

v. Neumann-f.

Bound state energies ($E < 0$) [note: $a=R$]



$$v = a^2 v_0 = \frac{2m}{\hbar^2} V_0 a^2$$

$$\lambda = a^2 \kappa^2 = -\frac{2ma^2}{\hbar^2} E > 0$$

$$\tan \sqrt{v - \lambda} = -\sqrt{\frac{v - \lambda}{\lambda}}$$

Breit-Wigner Resonances

- Small energy $kR \ll 1$
$$\tan \delta_\ell \approx \underbrace{\frac{\ell - \gamma_\ell R}{\ell + 1 + \gamma_\ell R}}_{=0} \frac{(kR)^{2\ell+1}}{(2\ell+1)!!(2\ell-1)!!}$$

- Expansion around the pole:

$$\tan \delta_\ell \approx \frac{1}{(E - E_R)g'_\ell(E_R)} \frac{(kR)^{2\ell+1}}{[(2\ell-1)!!]^2}$$

- Or:
$$\tan \delta_\ell \approx -\frac{\Gamma_\ell}{2(E - E_R)} \quad \text{where} \quad \Gamma_\ell = -\frac{2(kR)^{2\ell+1}}{g'_\ell(E_R)[(2\ell-1)!!]^2}$$

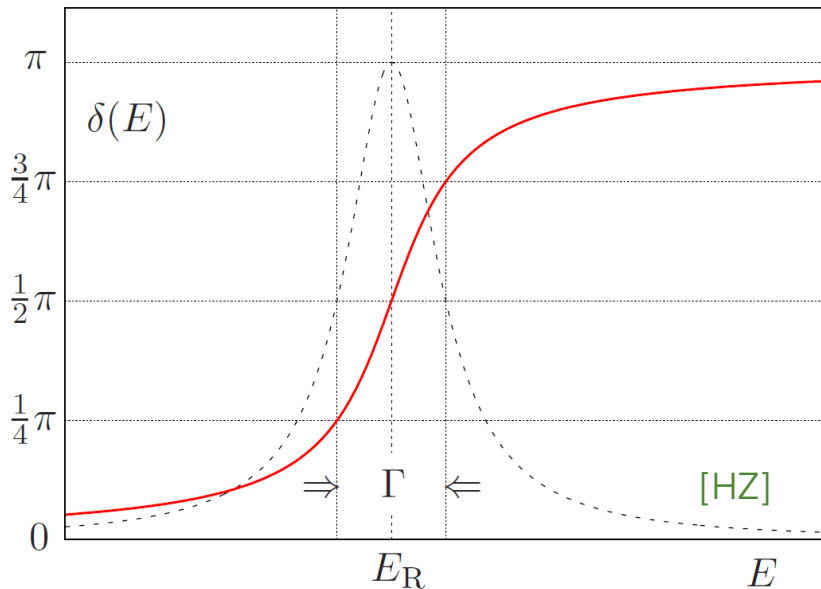
- For t-matrix and cross section:

$$t_\ell \approx \frac{1}{k} \frac{\frac{\Gamma_\ell}{2}}{E_R - E - i\frac{\Gamma_\ell}{2}}$$

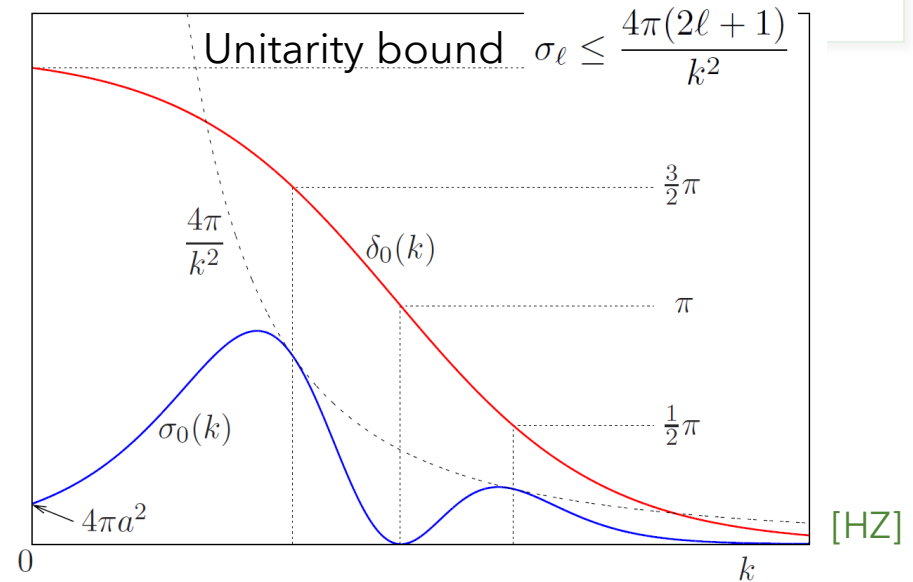
$$\sigma \approx \frac{4\pi}{k^2} (2\ell_0 + 1) \frac{\frac{\Gamma_{\ell_0}^2}{4}}{(E - E_R)^2 + \frac{\Gamma_{\ell_0}^2}{4}}$$

[HZ]

BW resonances and Ramsauer-Townsend



$$\tan \delta_\ell \approx -\frac{\Gamma_\ell}{2(E - E_R)}$$



S-wave, low energy:

$$f(\theta) \xrightarrow{k \rightarrow 0} t_0 P_0 = t_0 = \frac{\sin \delta_0}{k} e^{i\delta_0} \approx -a e^{i\delta_0}$$

$$\sigma_0(k) = \frac{4\pi}{k^2} \sin^2 \delta_0(k)$$

Typical Breit-Wigner resonances

ρ -meson
photoproduction

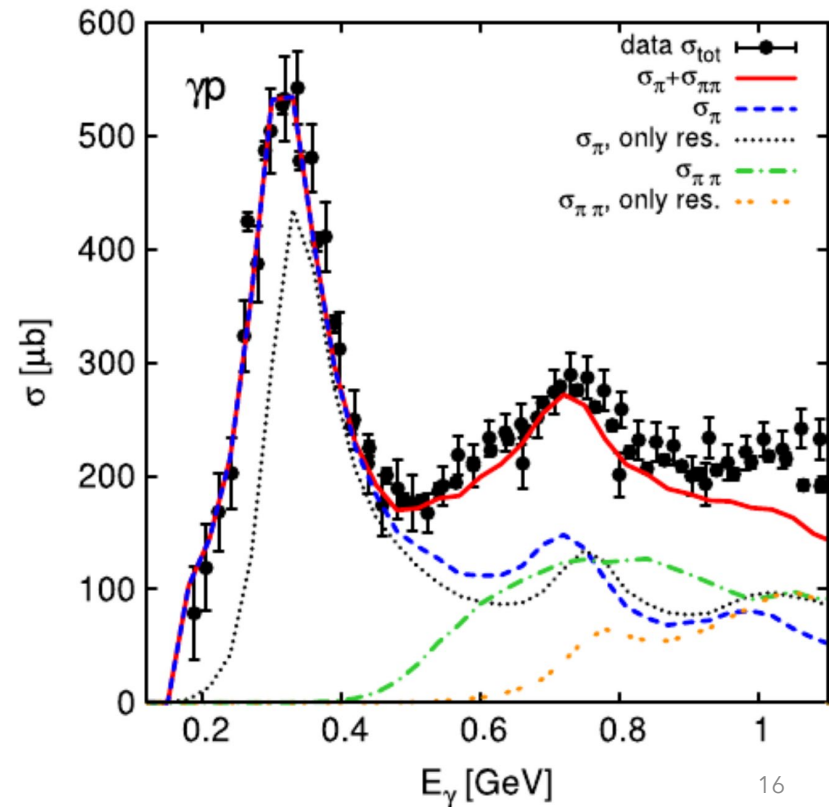
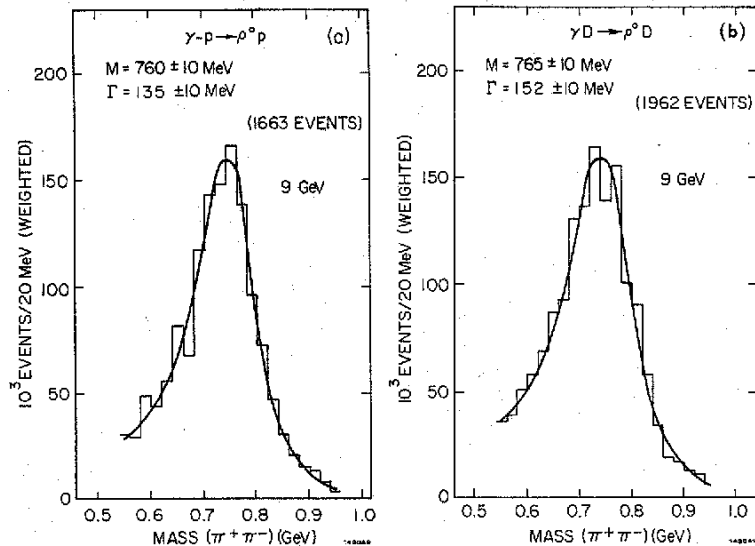
$$\left. \begin{aligned} M &= 760 \pm 10 \text{ MeV} \\ \Gamma &= 135 \pm 10 \text{ MeV} \end{aligned} \right\}$$

Hydrogen, 9 BeV.

$$\left. \begin{aligned} M &= 765 \pm 10 \\ \Gamma &= 152 \pm 10 \end{aligned} \right\}$$

Deuterium, 9 BeV.

Δ -baryon
photoproduction



Deficiencies of Breit-Wigner

- Breit-Wigner resonances are an idealized case
 - No background (see Laurent expansion previous slide)
 - Reaction dependent: Shape changes in different channels
 - No energy-energy dependent width in simplest BW form. Width MUST be energy dependent even for S-wave (unitarity)
 - Adding Breit-Wigner resonances violates unitarity
 - Close-by threshold have an influence (Generalization: Flatté)

$$A_i \sim \frac{M_R \sqrt{\Gamma_0 \Gamma_i}}{M_R^2 - E^2 - iM_R(\Gamma_1 + \Gamma_2)}, \quad i = 1, 2 \quad 1: \pi\eta, 2: \bar{K}K$$

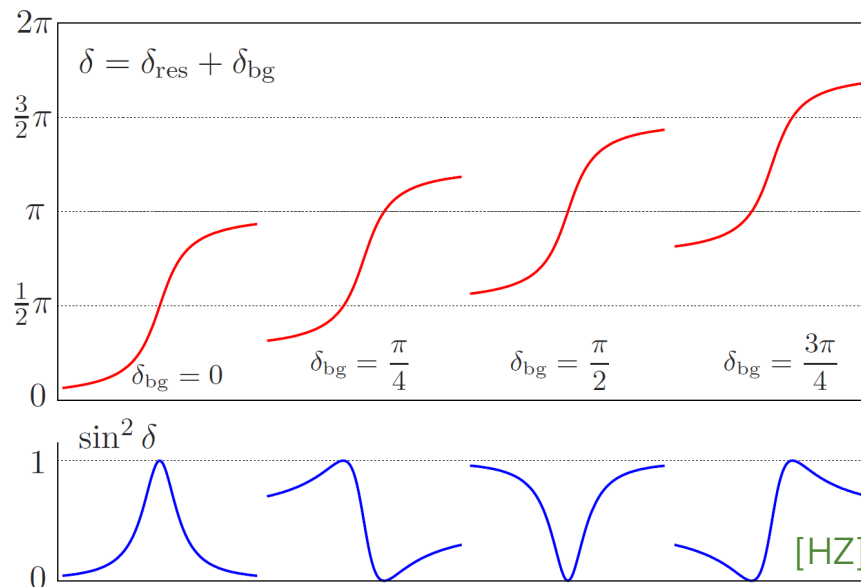
$$\Gamma_1 = g_1 k_1, \quad k_1 = \frac{1}{2E} \sqrt{[E^2 - (m_\eta + m_\pi)^2][E^2 - (m_\eta - m_\pi)^2]} \quad \Gamma_2 = g_2 k_2 \quad k_2 = \sqrt{\frac{E^2}{4} - m_K^2}$$

[Lesniak]

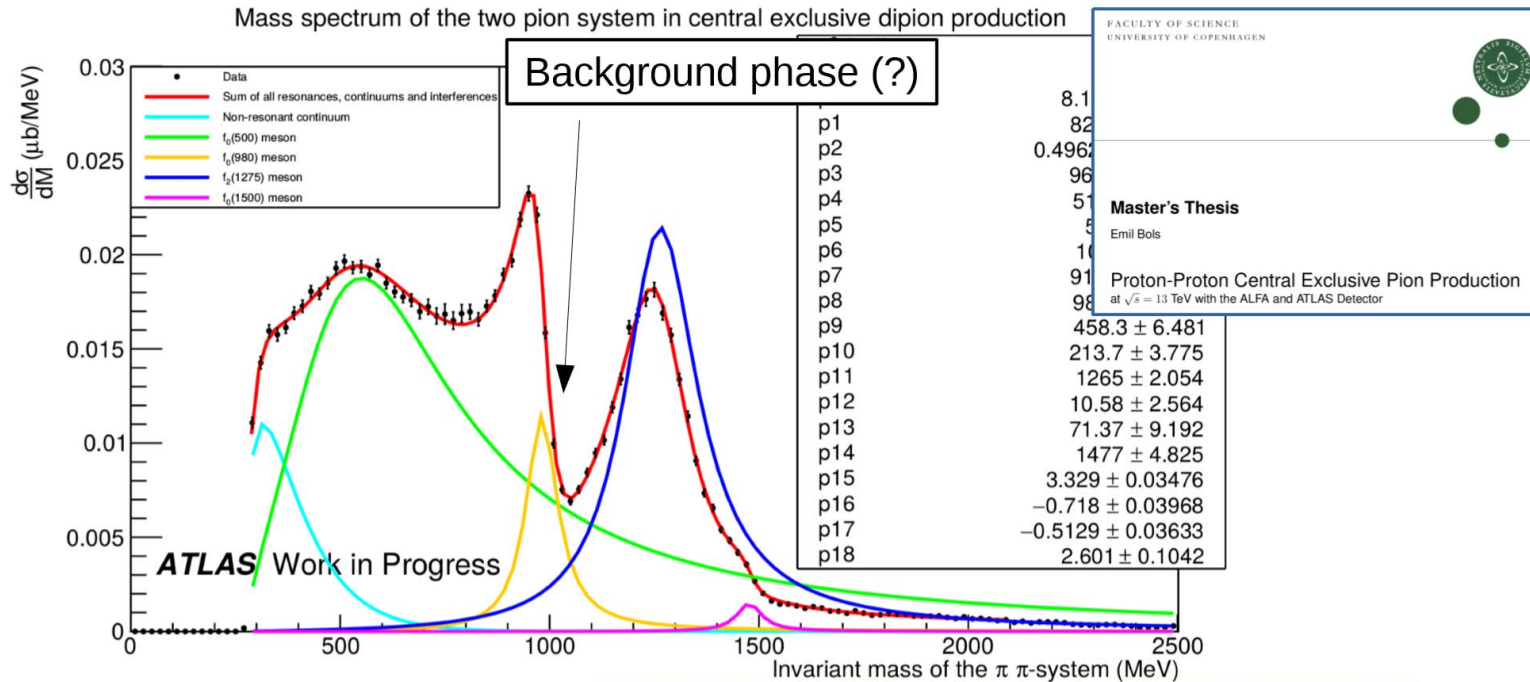
- Coupled-channel environment respected
- Unitarity respected (as long as no other background is added ;)
- Example of “analytic continuation”: k_2 is complex below $\bar{K}K$ threshold!

Background

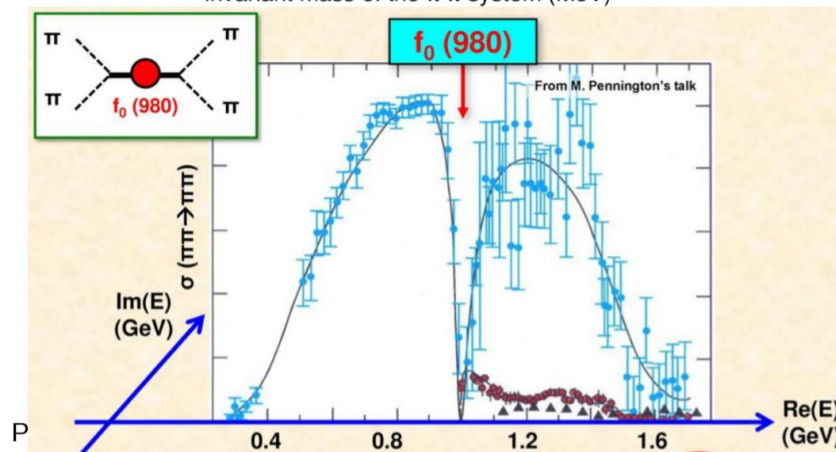
- Refers to non-resonant contributions to scattering amplitude (= physical effects), not experimental background
 - Sometimes resonances and background are added at the level of cross sections, but, of course, they add at level of amplitudes (interference)
- Resonances are by no means bumps in cross sections:



More complicated cases



Opposite pictures



Source:
H. Kamano

1.2 from resonances to bound state

A computational physics exercise:

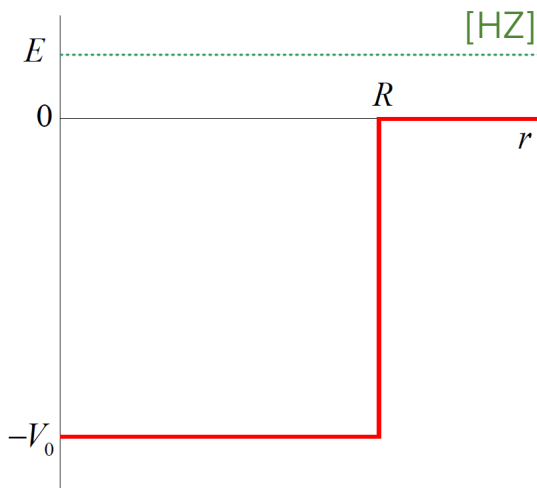
In this exercise you will learn about analytic properties of the scattering amplitude. First, have a look at this [video](#) – you will produce something similar. The exercise serves to get intuition about scattering/bound state problems and the underlying analytic structure in terms of singularities that manifest themselves as resonances and bound states – and how one transforms into the other as the potential depth changes. For simplicity, you may set $\hbar = m = 1$ in the entire problem. This is also done in the video. Note: here we look at the S -wave only.

Our example is the spherical square well. We want to make an animation that shows the partial-wave amplitude $t_0(k)$ as a function of $k \in \mathbb{C}$. Treating the problem in the complex k -plane is slightly simpler because there is only one Riemann sheet while the complex $E = \hbar^2 k^2 / (2m)$ -plane has two Riemann sheets.

1. *Bound state problem:* From topic 5, solve the bound-state problem numerically for a well that allows for at least one S -wave bound state. Check the bound state condition to make sure the state exists. Make a plot in which you show the RHS and LHS of Eq. (5.188) for illustration.
2. *The power of analyticity:* Bound state energies are pole positions of t_0 on the positive imaginary k -axis. For the same well as before, search numerically for poles and confirm that their positions (or, position if you have a well with only one bound state) coincide with the bound state energies determined in 1.
3. *Pole trajectories:* Trace the pole movements (“trajectories”) in the complex k -plane by plotting $\log |t_0|(k)$ for different $0 < V_0 < V_{\max}$ (make an animation). The logarithm only serves to make poles more visible in the contour plot. This would look like in the [video](#), but you do not have to look for poles for every value of V_0 which is quite cumbersome and takes a lot of time. However, do the animation like in that video, i.e., complex plane to the left and phase shift to the right, to see what effects poles have on the phase shift. Choose the maximal depth of the well, V_{\max} , such that there you have at least two bound states.

Reminder:

Potential in radial coordinates:



$$V(r) = \begin{cases} -V_0 & \text{for } r < R, \\ 0 & \text{for } r > R, \end{cases}$$

Scattering phase shifts ($E > 0$)

$$\tan \delta_\ell = \frac{k j'_\ell(kR) - \gamma_\ell j_\ell(kR)}{k n'_\ell(kR) - \gamma_\ell n_\ell(kR)}$$

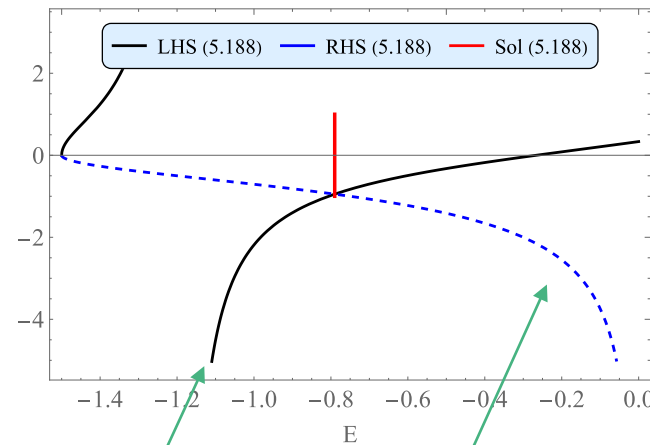
Matching

Sph. Bessel-f.

Wave number

v. Neumann-f.

Bound state energies ($E < 0$) [note: $a=R$]



$$\tan \sqrt{v - \lambda} = -\sqrt{\frac{v - \lambda}{\lambda}}$$

$$v = a^2 v_0 = \frac{2m}{\hbar^2} V_0 a^2$$

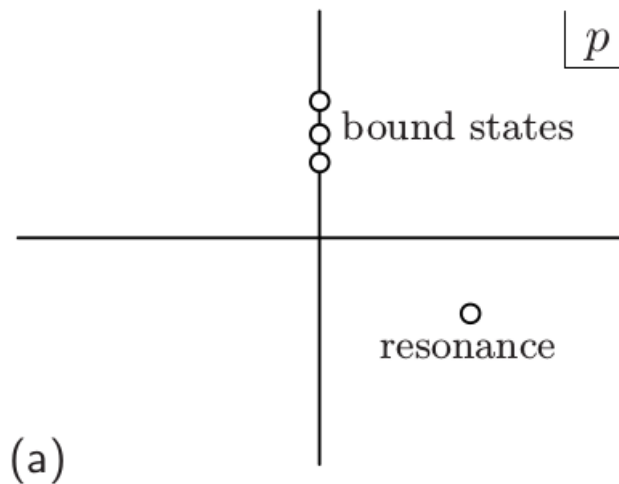
$$\lambda = a^2 \kappa^2 = -\frac{2ma^2}{\hbar^2} E > 0$$

QMII

QMI

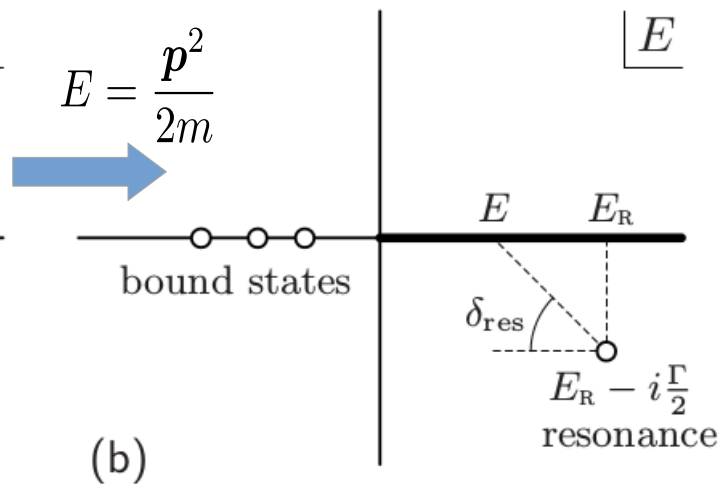
Complex momentum vs. energy plane

One Riemann sheet



(a)

Two Riemann sheets



(b)

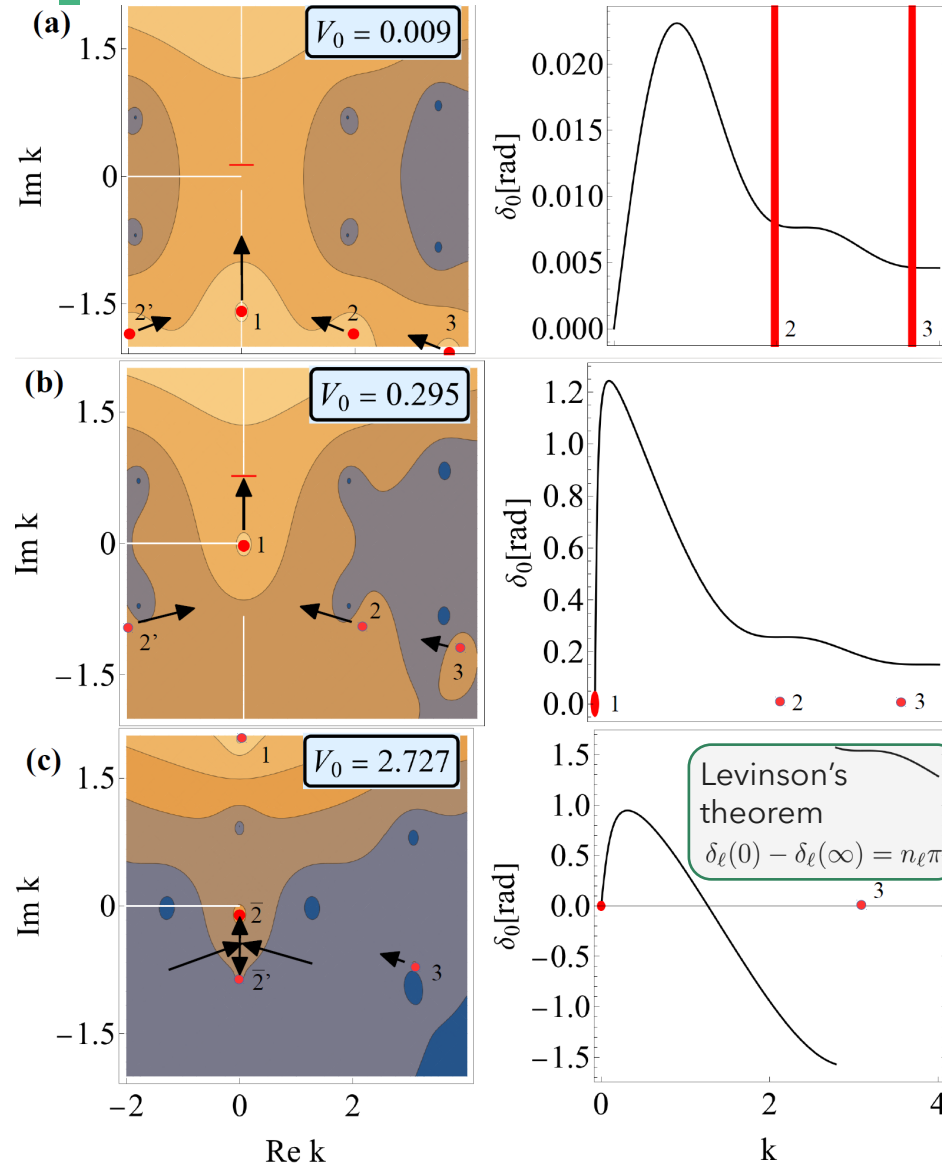
[HZ]

Resonances and bound states



$$E = \frac{(\hbar k)^2}{2m}$$

From resonances to bound states



Left column: S -wave T -matrix, $|t_0|$, in the complex-momentum plane (arb. units).
Right column: phase shift.

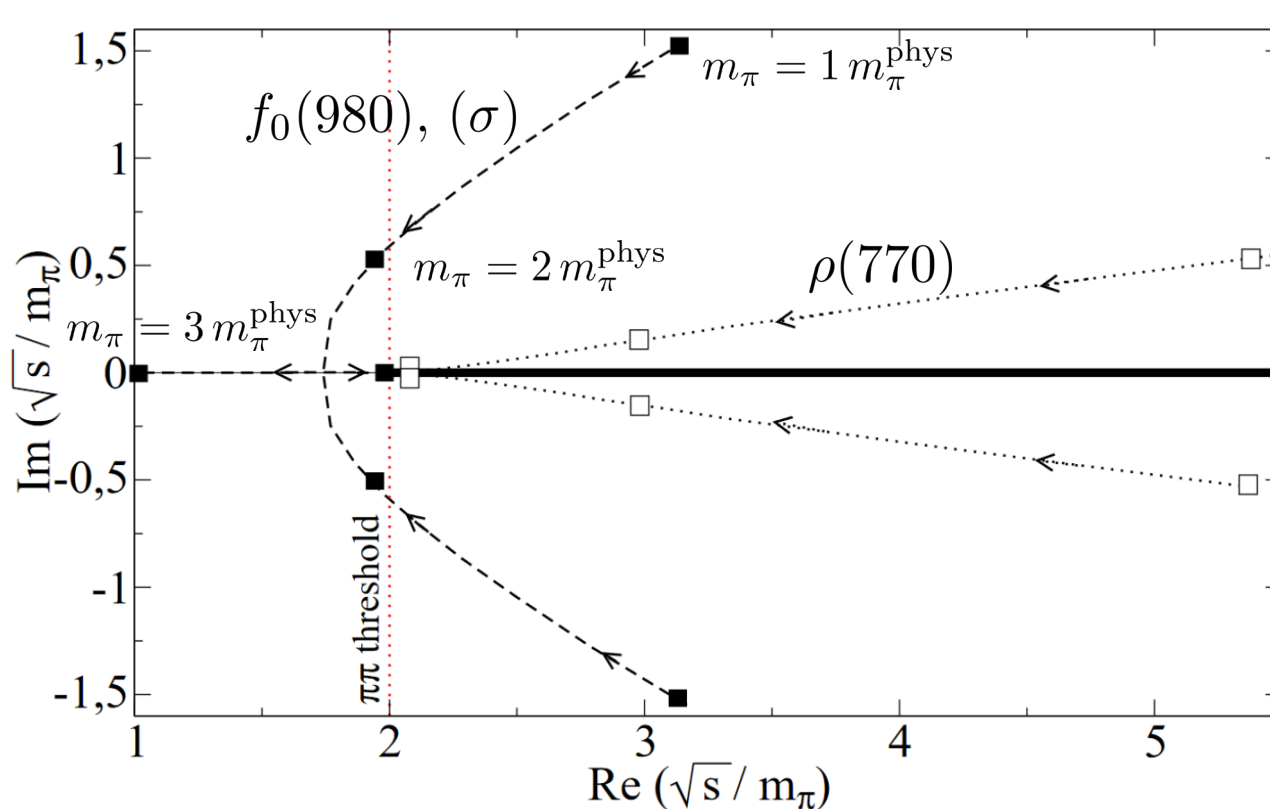
(a) For a shallow potential, there is no bound state, but only virtual state 1 and resonances 2 and 3.

In (b), infinite scattering length is reached which motivates a discussion of universality. [\[Braaten\]](#)

In (c), pole 1 became a deeply bound state. Pole 2 and its mirror pole $2'$ have met on the imaginary k -axis and then separated again as virtual states $\bar{2}$ and $\bar{2}'$, with $\bar{2}$ on its way to become a bound state and $\bar{2}'$ a deeper-bound virtual state. Such intriguing S -wave pole trajectories have only been discovered ten years ago.

Chiral trajectories of light mesons

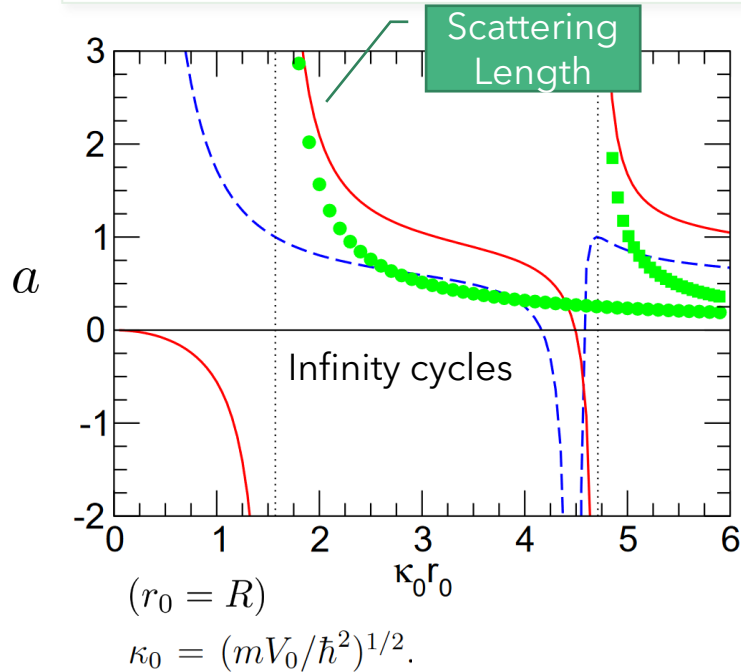
- Quark-mass dependence as predicted from “Inverse amplitude method” with one-loop ChPT
- [Hanhart et al., [0801.2871](#)]



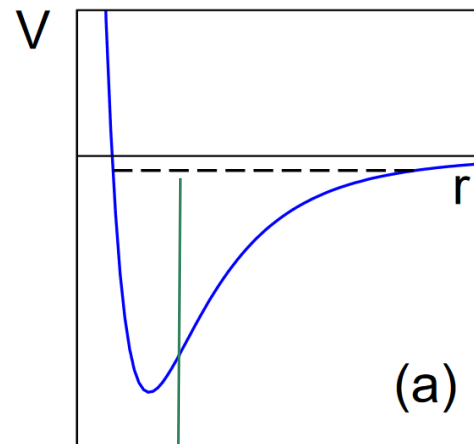
- Axes: \sqrt{s} vs. k
 - Resonances \rightarrow Virtual state \rightarrow bound state
 - But rho-resonance: rather featureless conversion to bound state
 - Wide scalar mesons are not at all conventional Breit-Wigner resonances
 - Prominent molecular component
- [Morgan/Pennington]
[Baru] [Guo]

Feshbach resonances [Braaten]

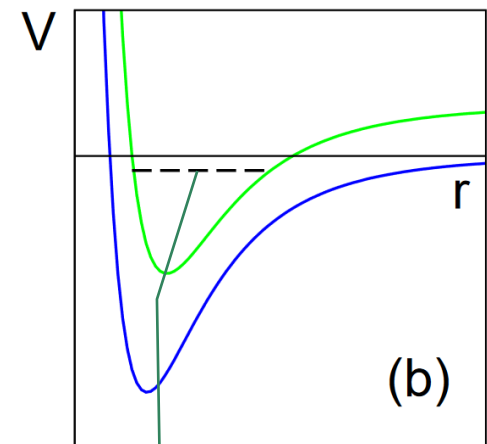
$$a = R \left(1 - \frac{\tan \kappa_0 R}{\kappa_0 R} \right), \text{ where } \kappa_0 = \sqrt{\frac{2mV_0}{\hbar^2}}$$



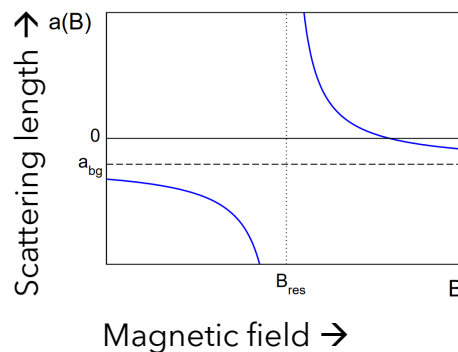
Mechanisms to generate large scattering length



Shape resonance



Feshbach resonance: bound state in a weakly-coupled, closed channel



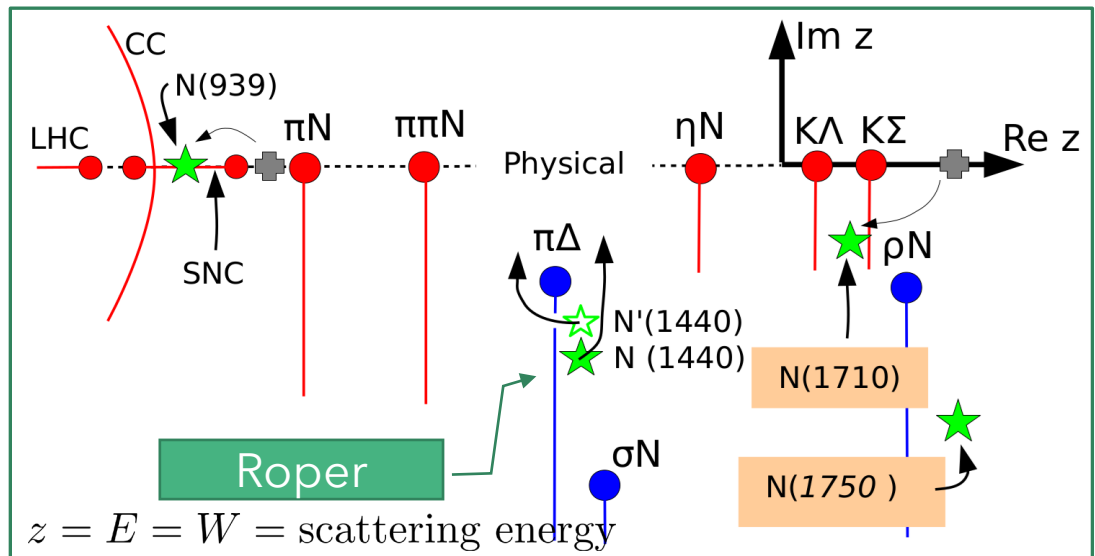
1.3 Baryon resonances as poles

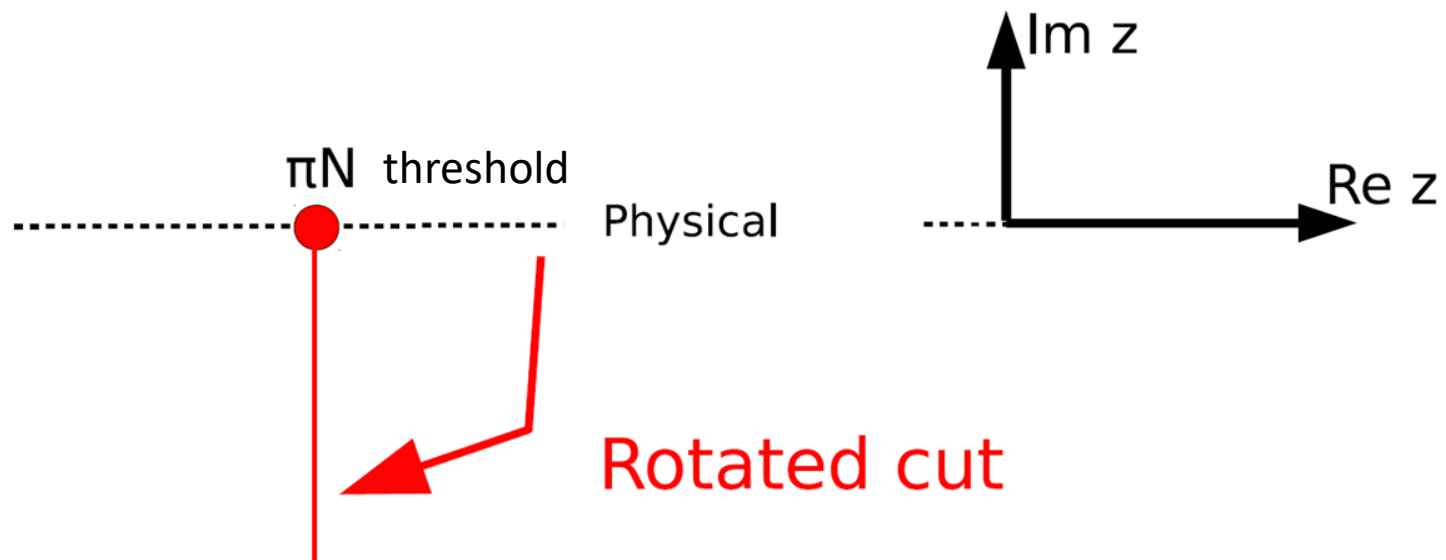
[see spare slides on crossing symmetry and causality]

- Defining resonances as poles in amplitudes at complex energies resolves all mentioned problems
 - Real part of pole position \longleftrightarrow Mass
 - 2x Imaginary part of pole position \longleftrightarrow Width
 - Pole residue \longleftrightarrow Branching ratio into different channels because amplitudes factorize at poles

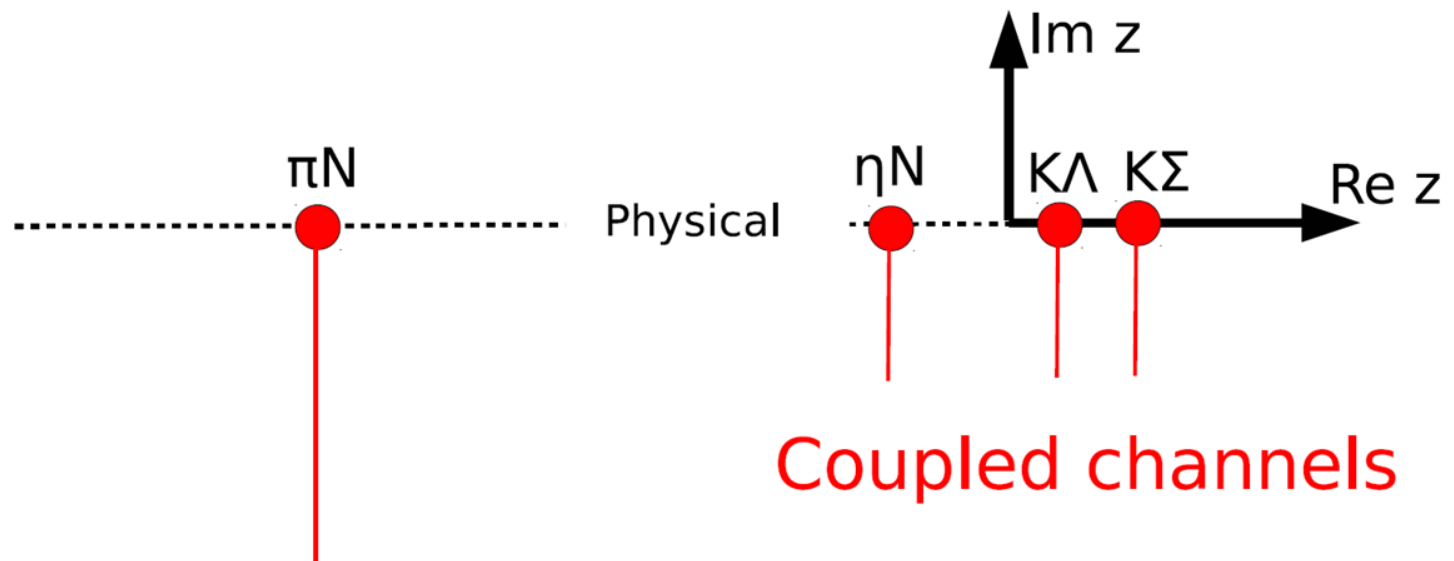
- Next goal: What is this?

- Red: Real thresholds
- Blue: sub-channel thres.
- Why is Roper double?
- What happens below threshold?

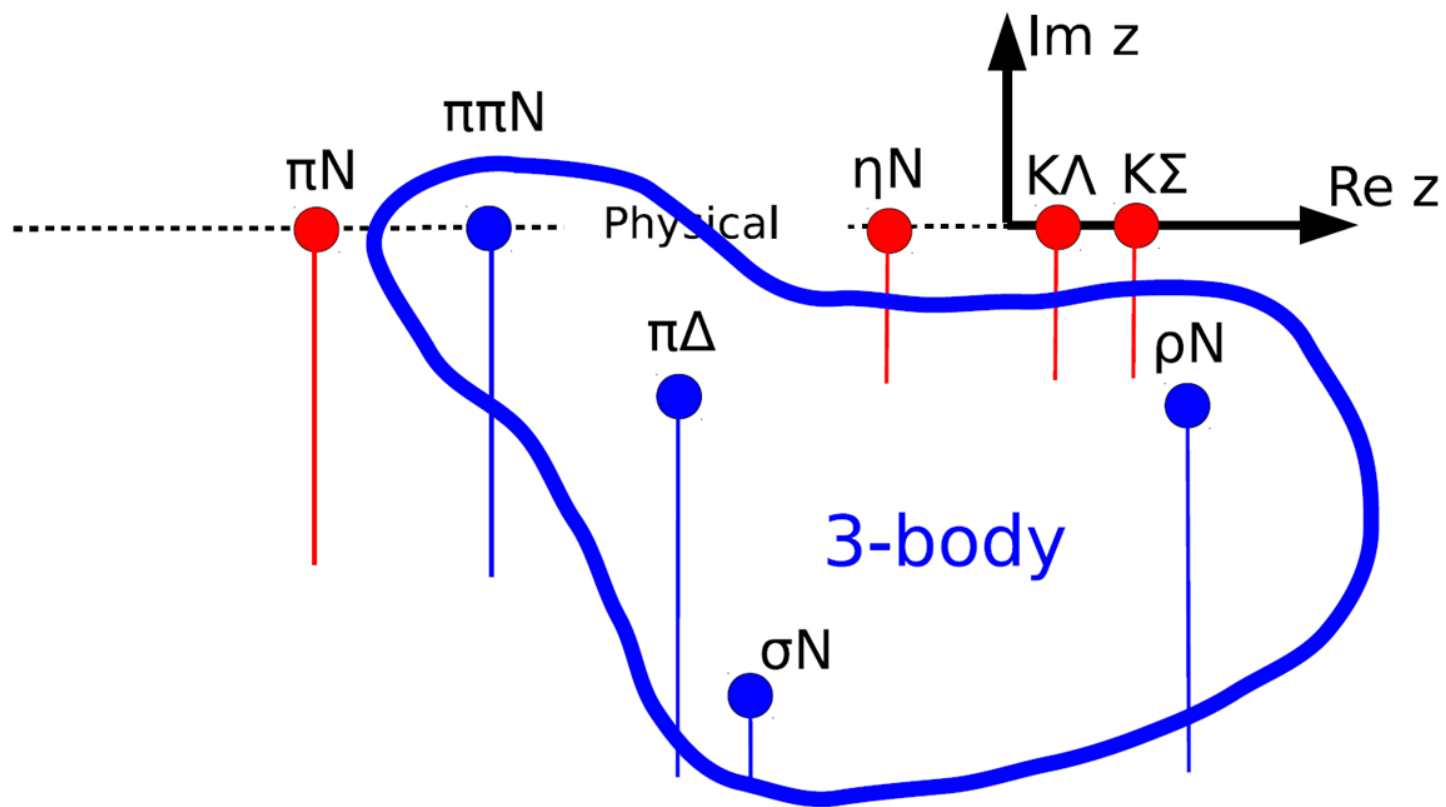




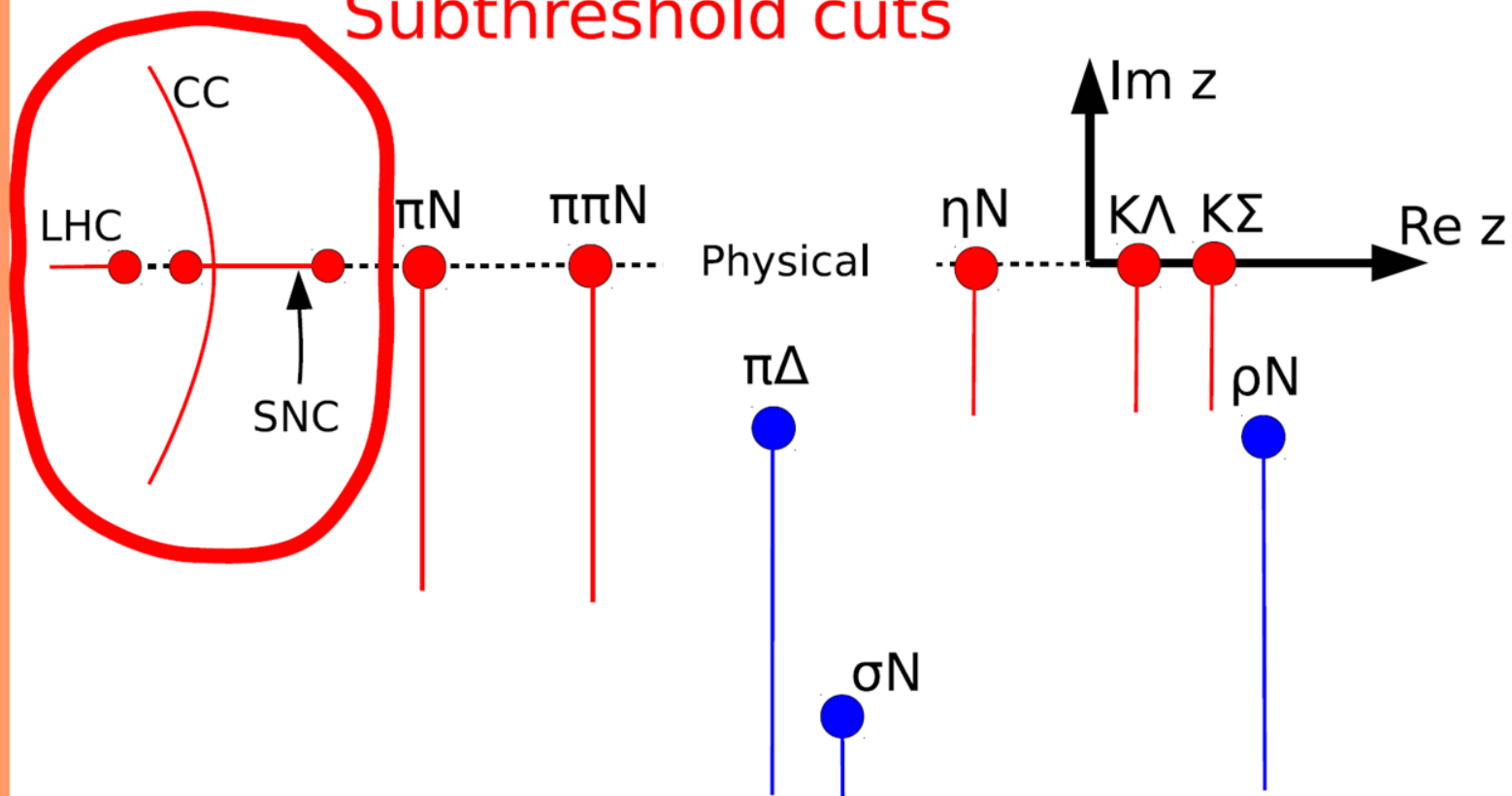
- Thresholds are fixed by kinematics
- Position of cuts are by convention

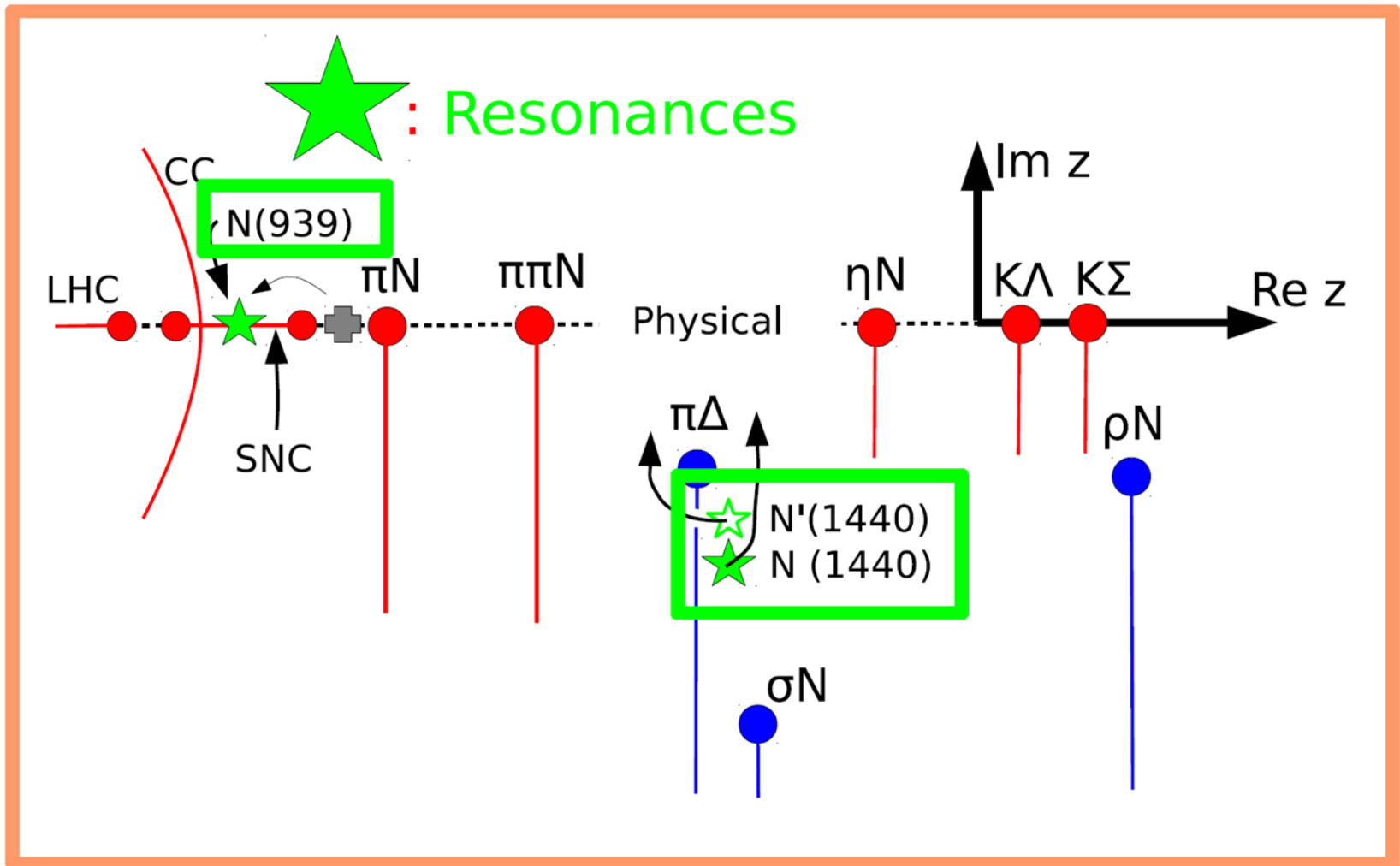


- And many others: ωN , $\eta' N$, ...



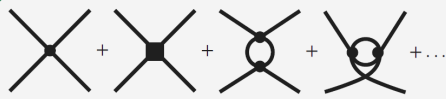
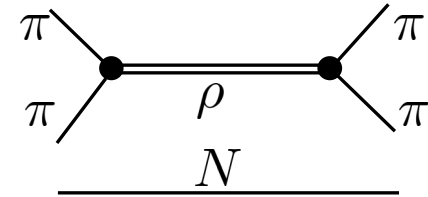
Subthreshold cuts





- The nucleon is a bound state in the P11 partial wave
- The Roper resonance $N(1440)$ is very unusual and non-Breit-Wigner

Analytic continuation (2B)



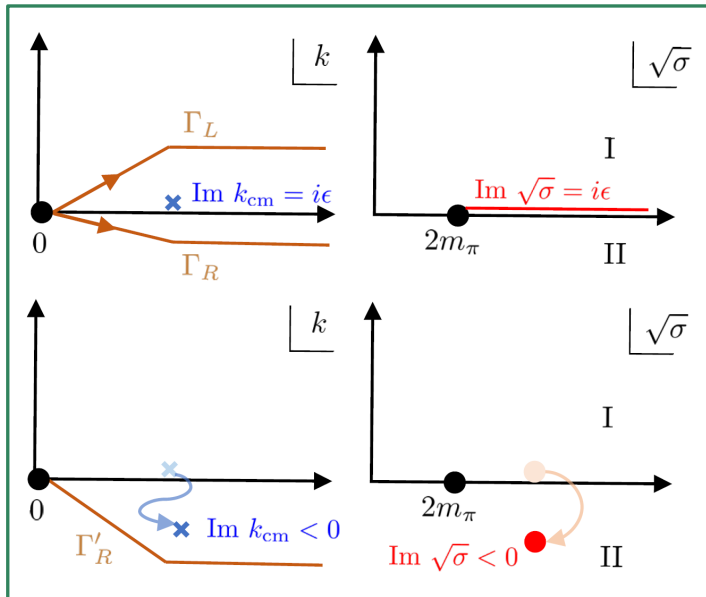
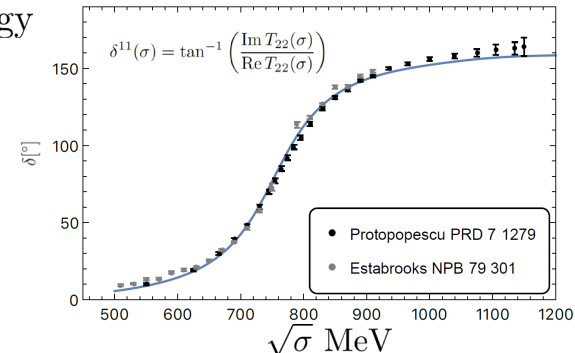
Inverse Amplitude Method [Dobado]
 $\sqrt{\sigma} = z = \text{sub-system scattering energy}$

$$T_{22}(\sigma) = \tilde{v}(k_{\text{cm}}) \tau(\sigma) \tilde{v}^*(k_{\text{cm}}), \quad k_{\text{cm}} = \sqrt{\frac{\sigma}{4} - m_{\pi}^2},$$

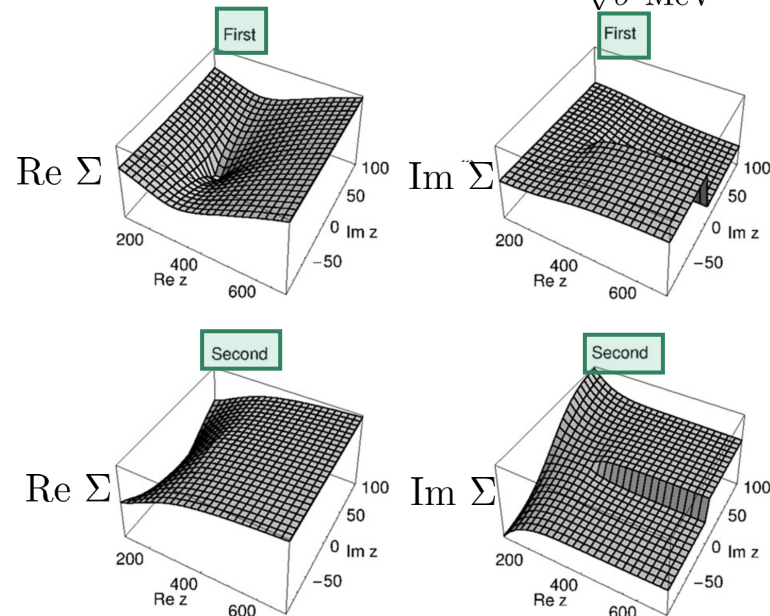
$$\tau^{-1}(\sigma) = K^{-1} - \Sigma,$$

$$\Sigma = \int_0^{\infty} \frac{dk k^2}{(2\pi)^3} \frac{1}{2E_k} \frac{\sigma^2}{\sigma'^2} \frac{\tilde{v}(k)^* \tilde{v}(k)}{\sigma - 4E_k^2 + i\epsilon}$$

$$E_k = \sqrt{k^2 + m_{\pi}^2}$$



"Adiabatic" contour deformation
 (remember for 3-body case later!)



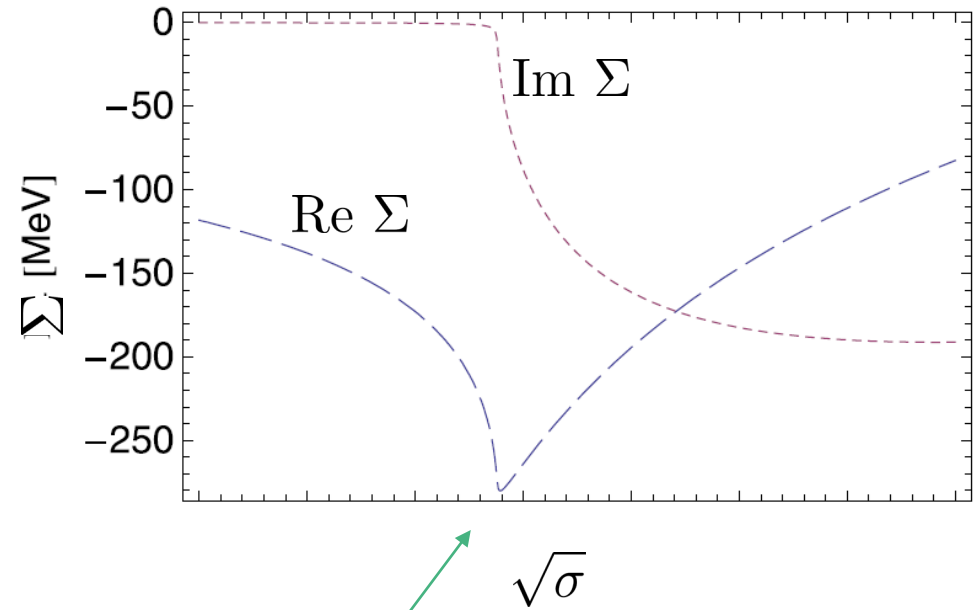
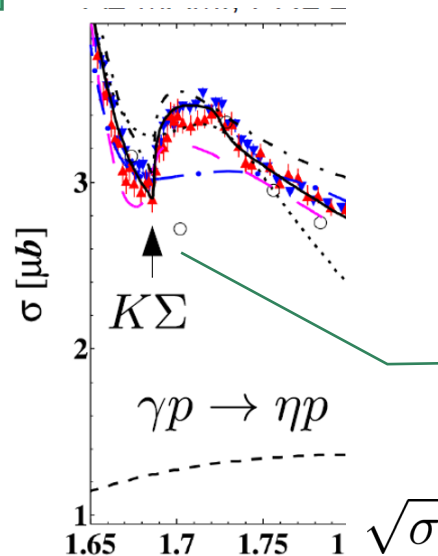
Threshold effects in S-wave

$$T_{22}(\sigma) = \tilde{v}(k_{\text{cm}})\tau(\sigma)\tilde{v}^*(k_{\text{cm}}), \quad k_{\text{cm}} = \sqrt{\frac{\sigma}{4} - m_{\pi}^2},$$

$$\tau^{-1}(\sigma) = K^{-1} - \Sigma,$$

$$\Sigma = \int_0^{\infty} \frac{dk k^2}{(2\pi)^3} \frac{1}{2E_k} \frac{\sigma^2}{\sigma'^2} \frac{\tilde{v}(k)^*\tilde{v}(k)}{\sigma - 4E_k^2 + i\epsilon}$$

Assume S-wave



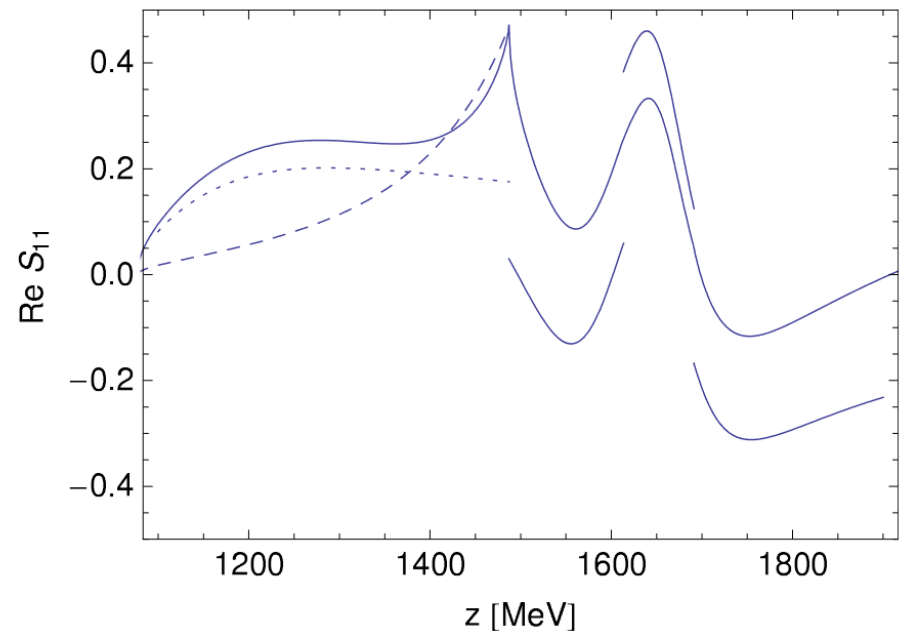
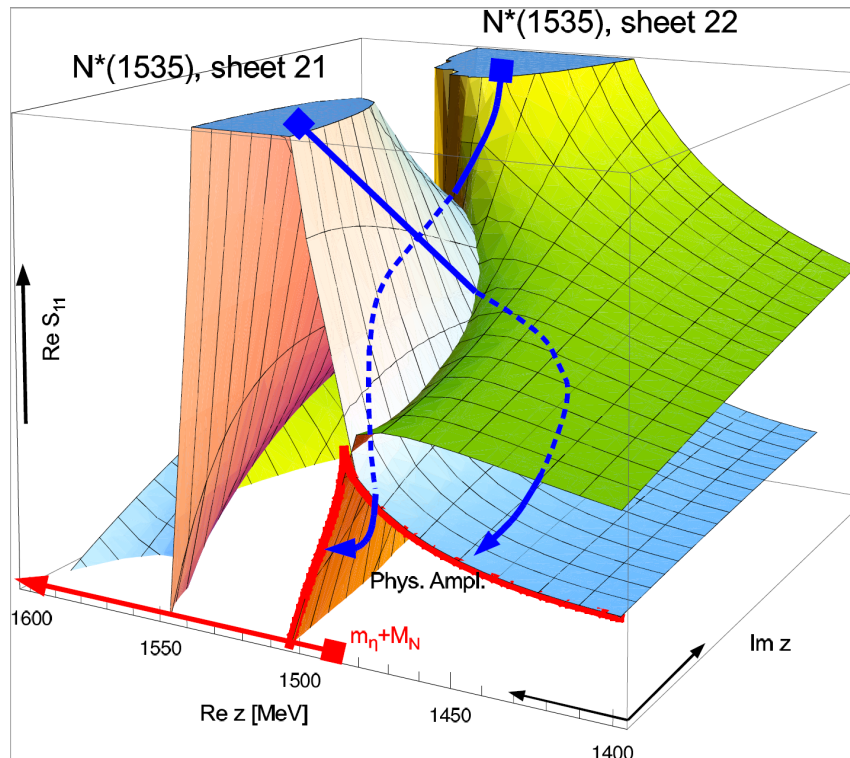
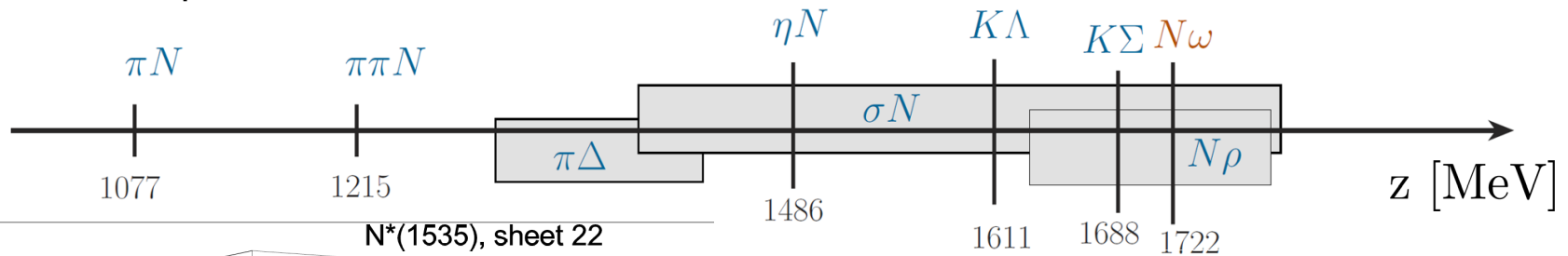
Threshold

Classification of analytic structures

- Thresholds, ✓ Triangle singularities ?
- Classification of poles:
 - Resonances (2nd sheet, above threshold) $\Delta(1232), \rho(770), \dots$ ✓
 - Bound states (1st sheet, below threshold) N, d ✓
 - Virtual states (2nd sheet, below threshold): threshold enhancements ✓
 - Shadow poles (distant unphysical sheets), sometimes visible as enhanced cusps (“shoulder” of a resonance) $N(1535)1/2^-$?
 - Quasibound states: Bound w.r.t. a channel that opens at higher masses + strong coupling to that channel; open w.r.t. to another channel to which the state couples rather weakly. $N(1535)1/2^-, \Lambda(1405)1/2^-$?
 - Resonances with two-pole structure $\Lambda(1405)1/2^-$?

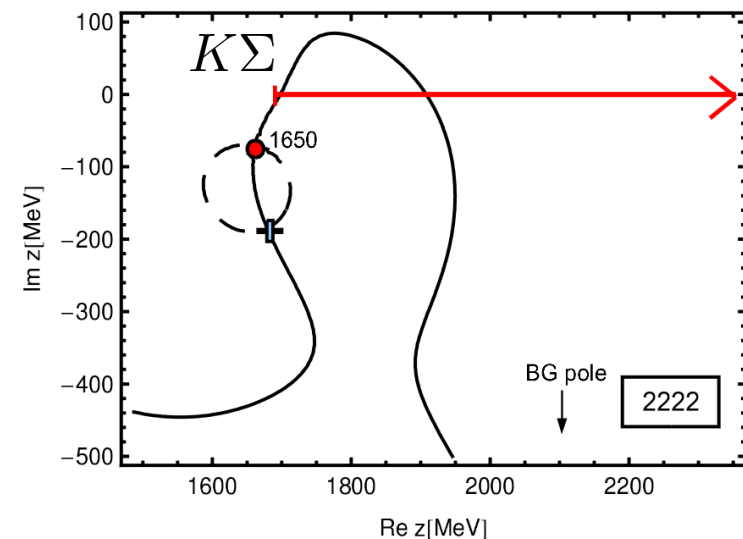
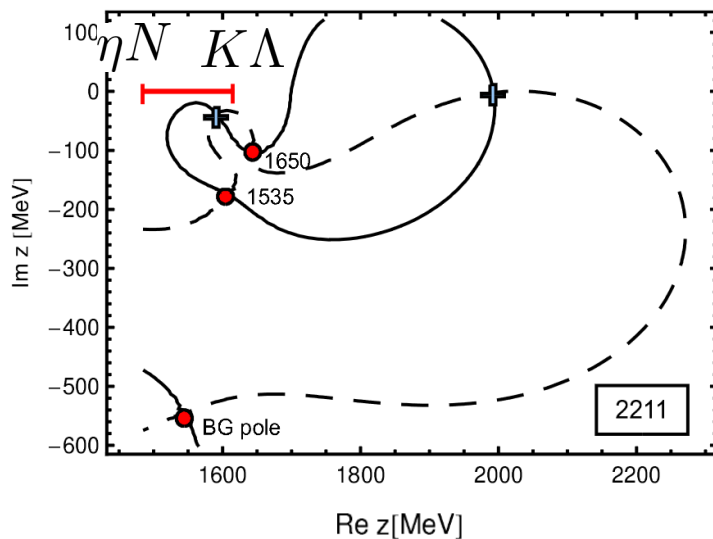
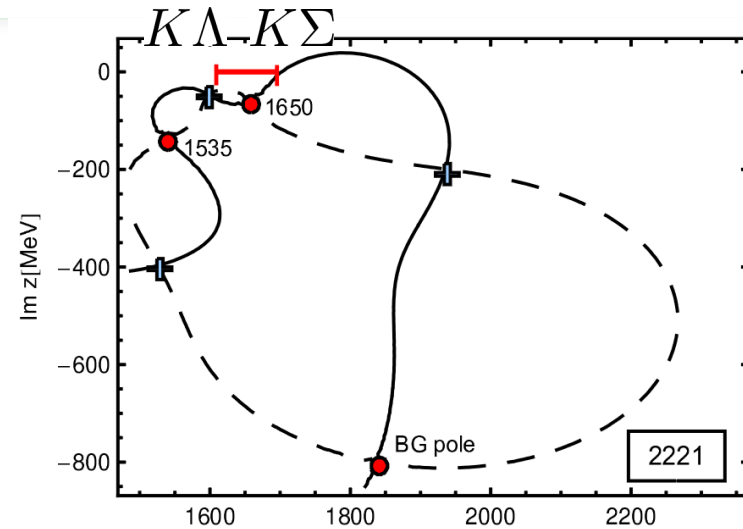
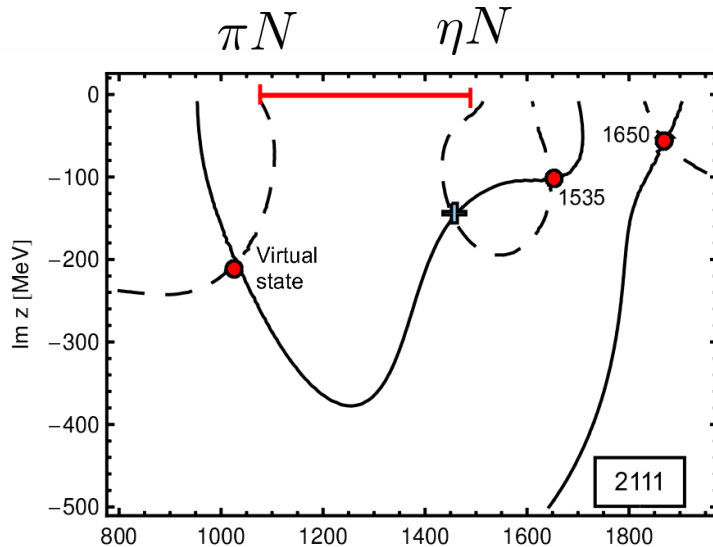
Shadow poles

- Replica of a regular resonance pole on a hidden sheet
- Visible through "shoulder" only
- Example: $N(1535)$ close to the ηN threshold



Quasibound state - S11 partial wave

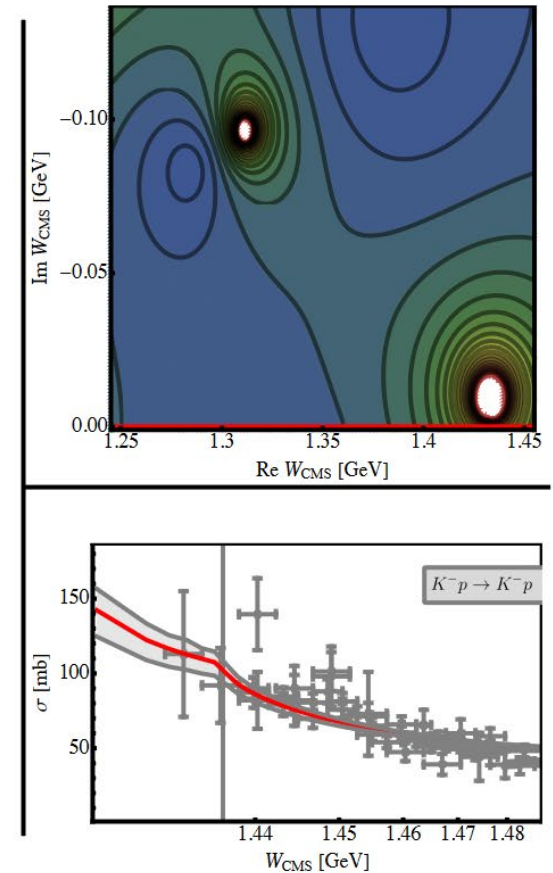
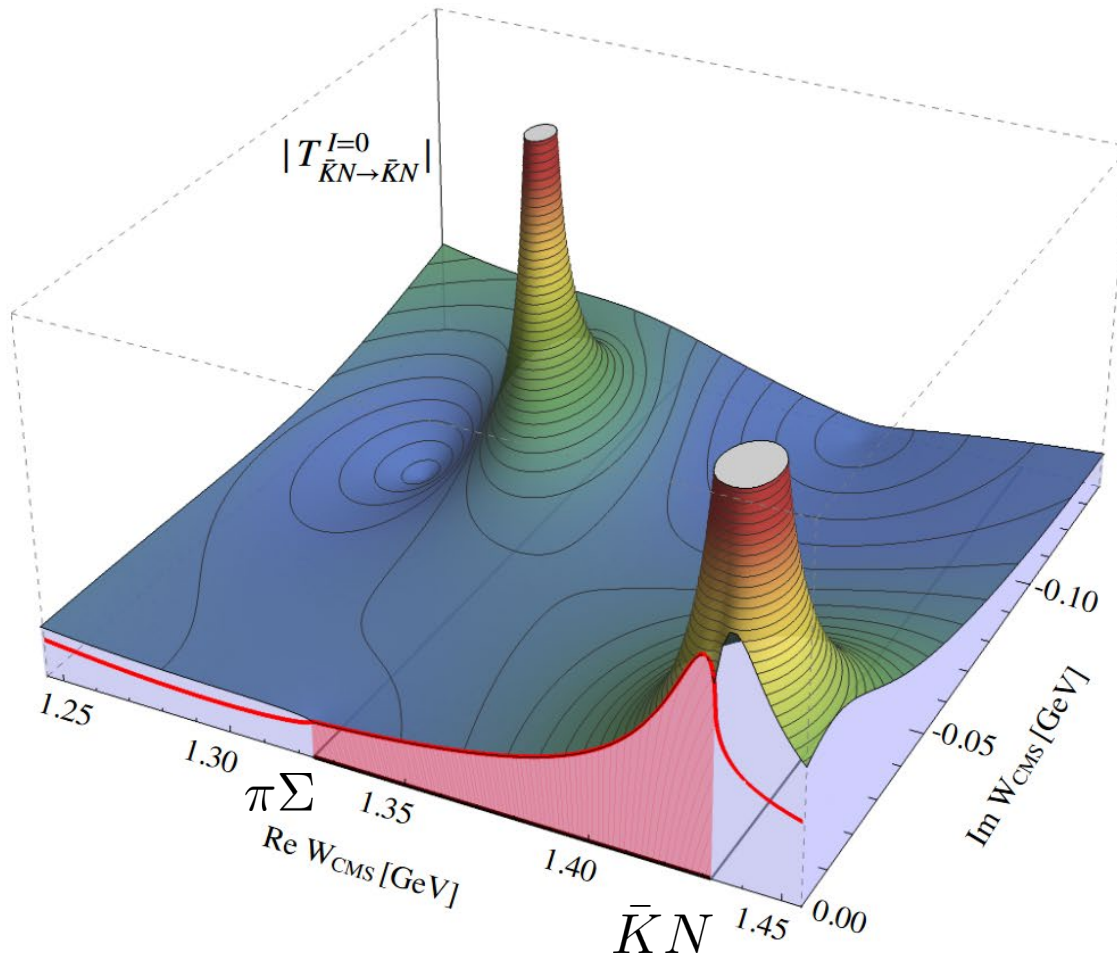
One of many possible examples: [Doring]



Two-pole structures: $\Lambda(1405)$

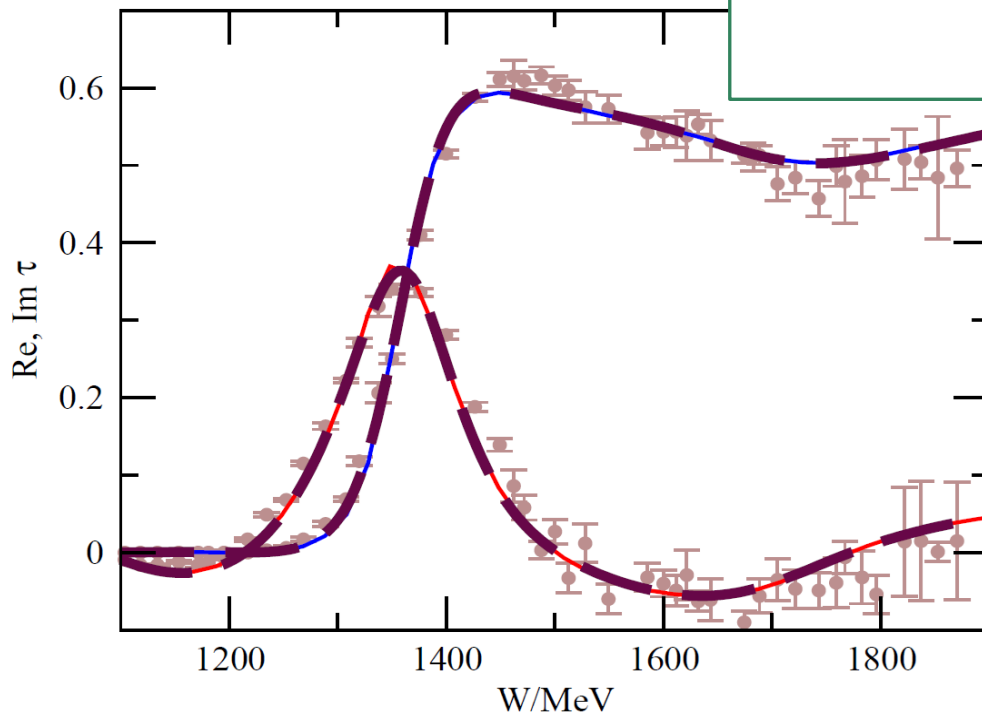
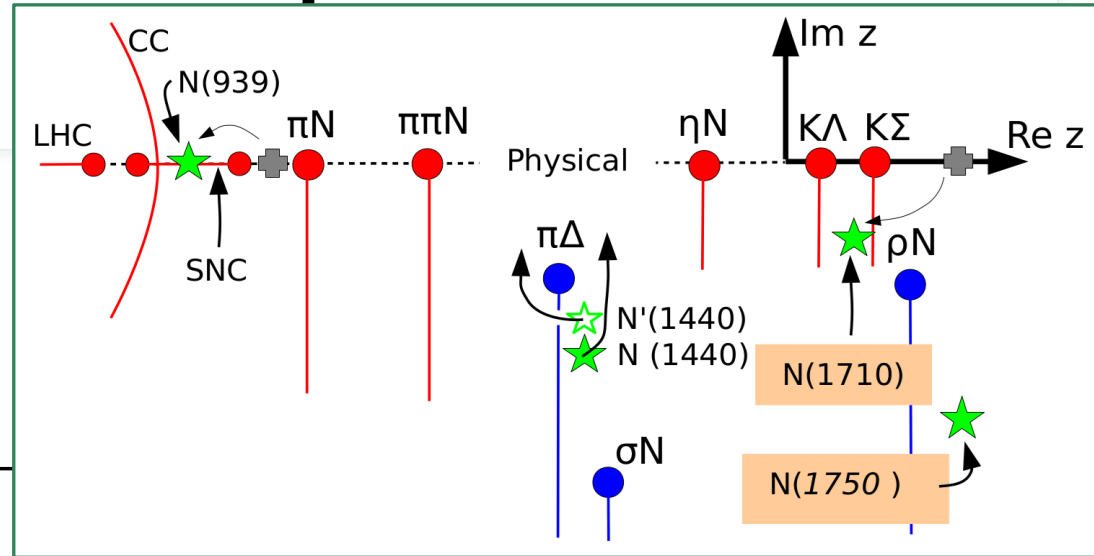
- Two resonance poles (almost) on the same Riemann sheet

Hadronic molecule [Mai]



Two-pole structure & complex threshold: Roper [SAID]

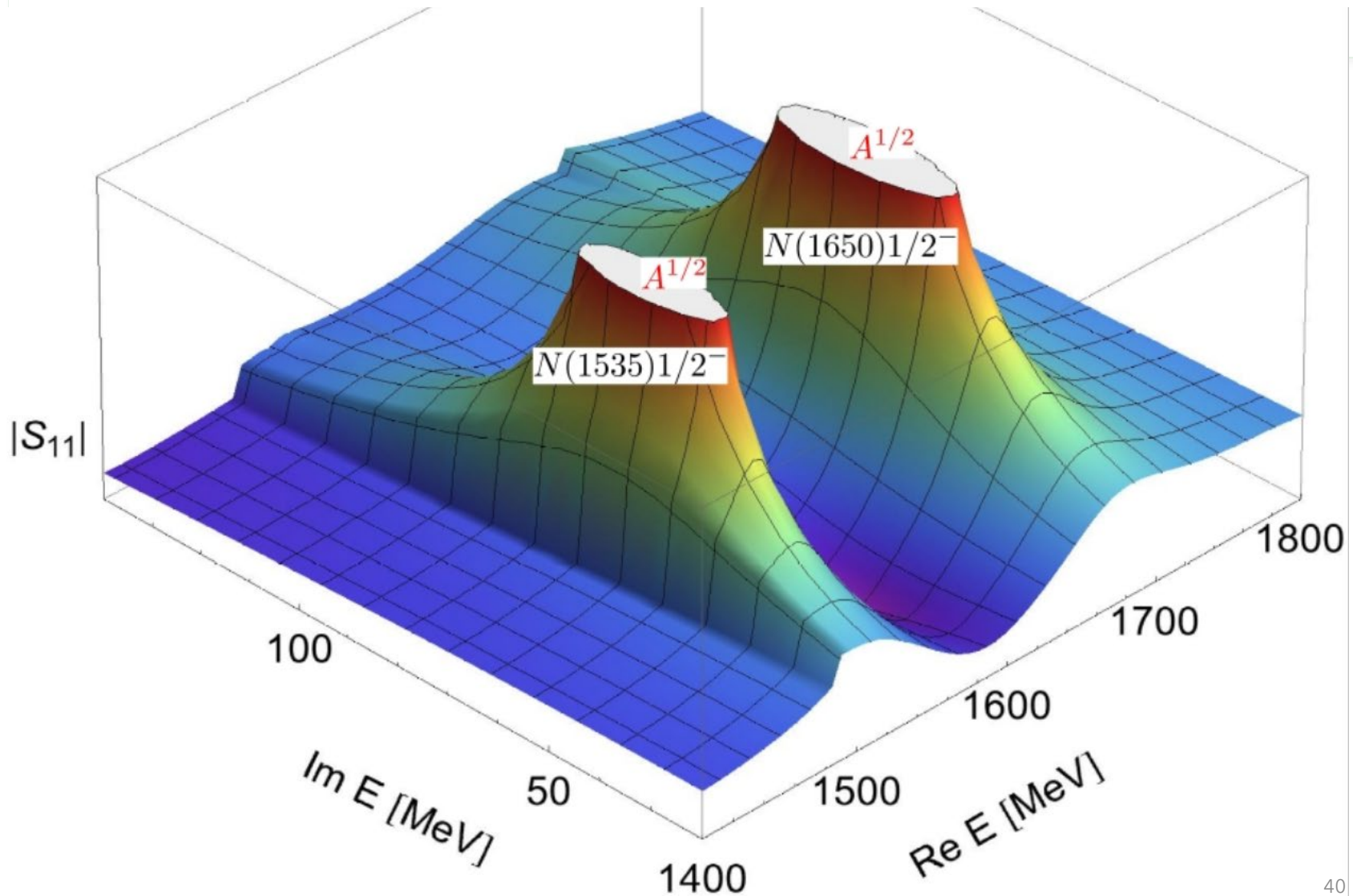
- Or rather shadow pole? Debatable...



Strategy: To reliably extract resonances from data....

- manifestly include all known analytic structures into the model amplitude before fitting to data
- Respect unitarity, analyticity,...

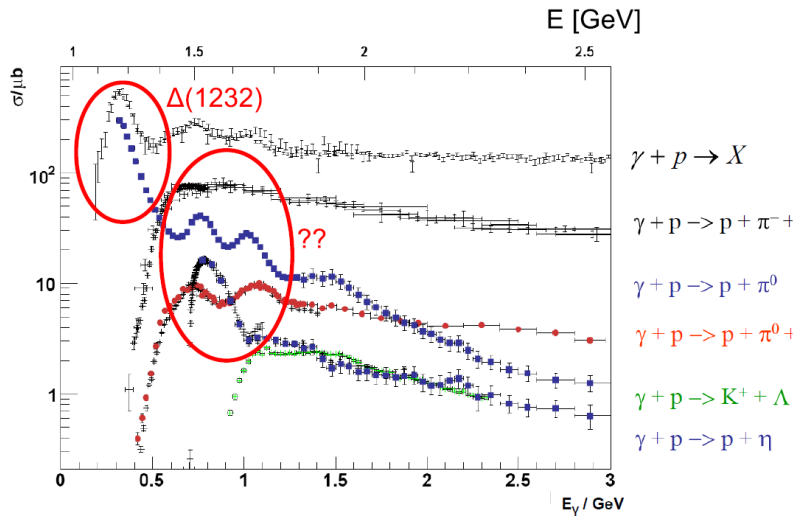
Two nearby resonances



2. Phenomenology of resonances

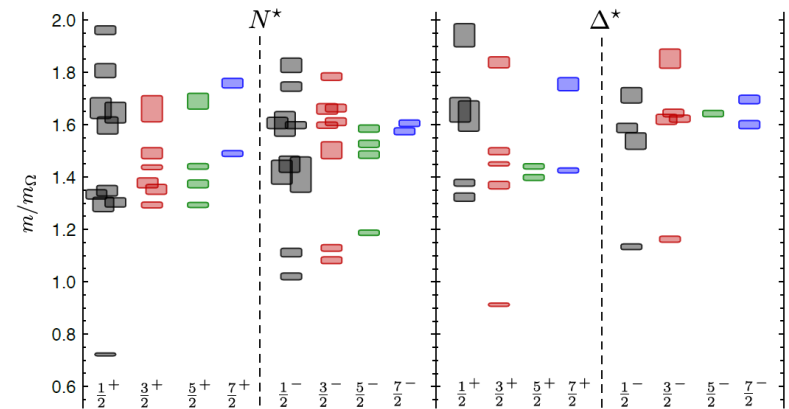
2.1 Spectrum of excited baryons

Experimental study of hadronic reactions



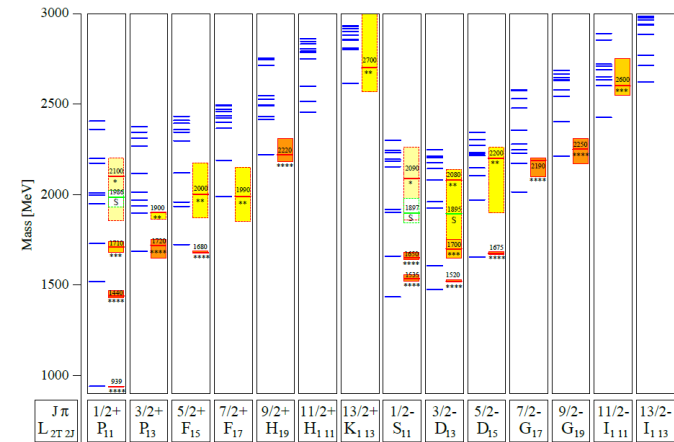
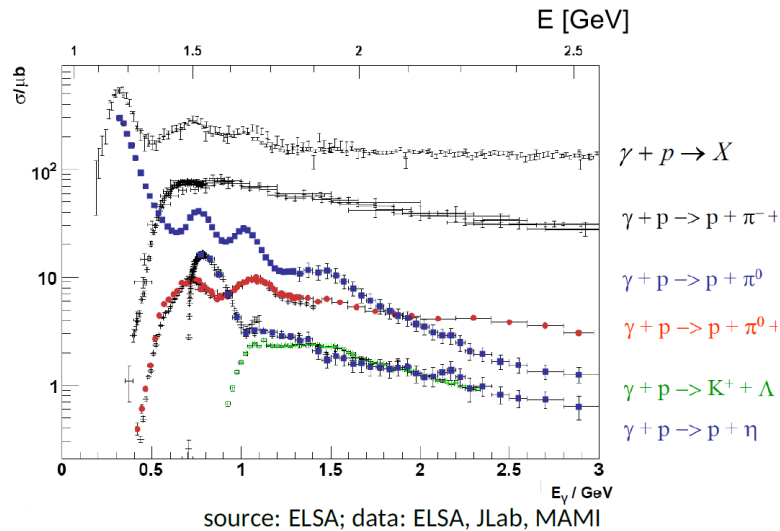
source: ELSA; data: ELSA, JLab, MAMI

Theoretical predictions of excited hadrons
e.g. from lattice calculations:
(with some limitations)



$m_\pi = 396 \text{ MeV}$ [Edwards et al., Phys.Rev. D84 (2011)]

From experimental data to the resonance spectrum



Löring et al. EPJ A 10, 395 (2001), experimental spectrum: PDG 2000

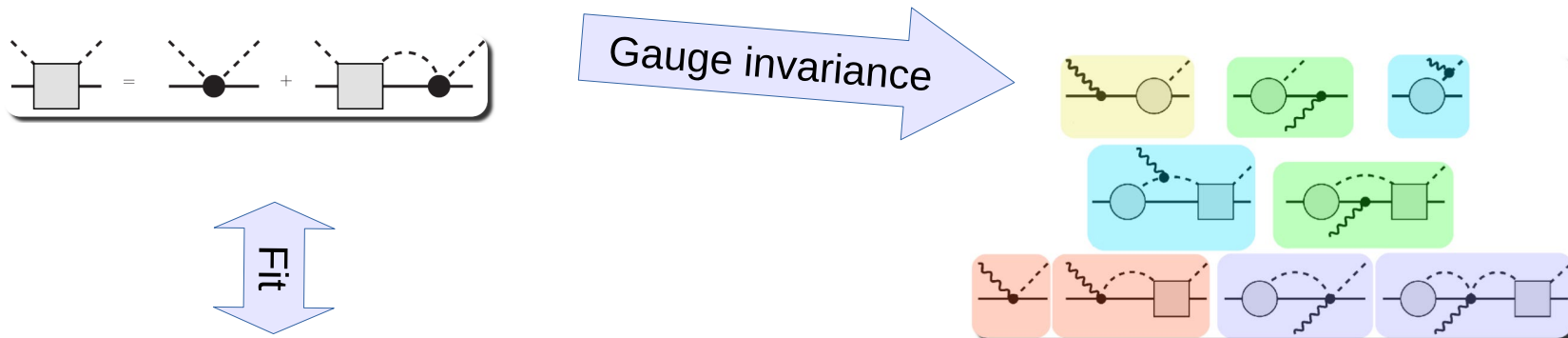
Different modern analyses frameworks:

- **unitary isobar models:** unitary amplitudes + Breit-Wigner resonances
MAID, Yerevan/JLab, KSU, JM model (πN & $\pi \pi N$)
- **(multi-channel) K -matrix:** GWU/SAID, BnGa (phenomenological),
Gießen (microscopic Bgd)
- **dynamical coupled-channel (DCC):** 3d scattering eq., off-shell intermediate states
ANL-Osaka (EBAC), Dubna-Mainz-Taipeh, Jülich-Bonn
- **other groups:** JPAC (high energies), Mainz-Tuzla-Zagreb PWA (MAID + fixed- t
dispersion relations, L+P), Gent, truncated PWA

Using ONLY meson-baryon degrees of freedom (no explicit quark dynamics):

Manifestly gauge invariant approach based on full BSE solution

[Ruic, M. Mai, U.-G. Meissner PLB 704 (2011)]



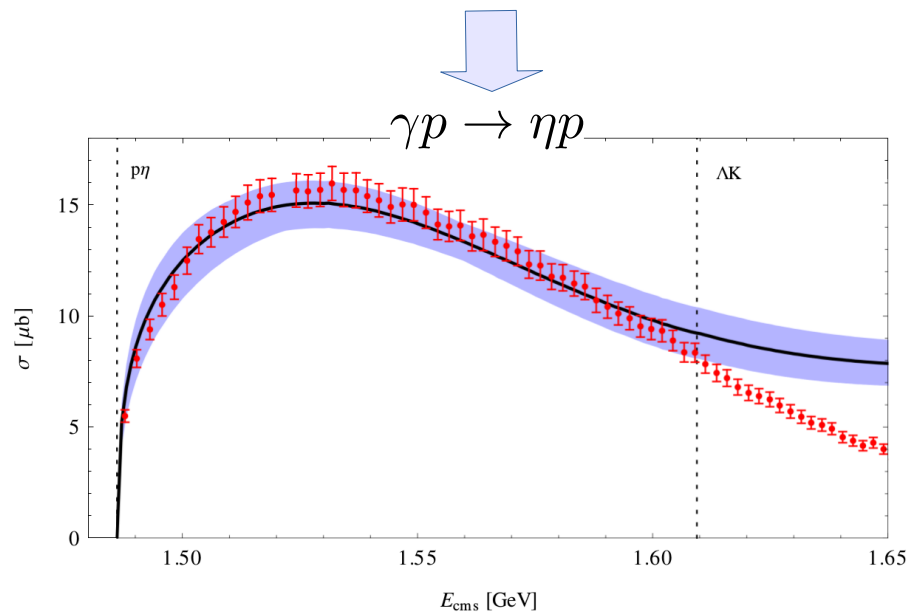
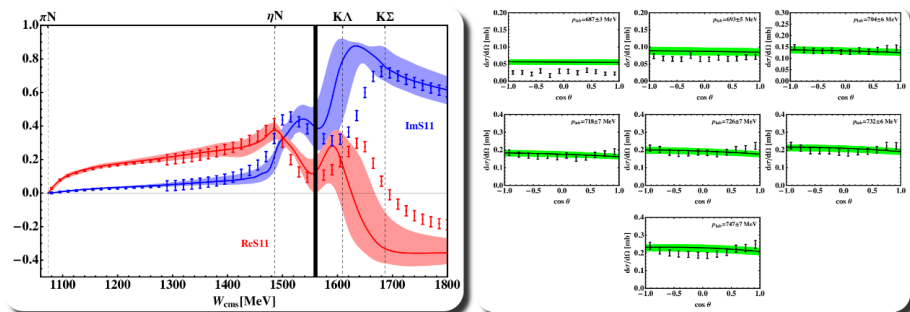
► Exact unitary meson-baryon scattering amplitude T with parameters, fixed to reproduce:

- πN -partial wave S_{11} and S_{31} for $\sqrt{s} < 1560$ MeV

Arndt et al. (2012)

- $\pi^- p \rightarrow \eta n$ differential cross sections

Prakhov et al. (2005)

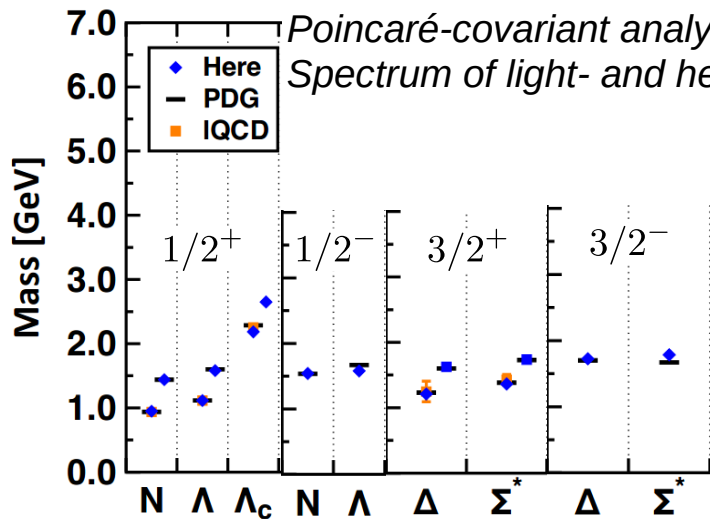
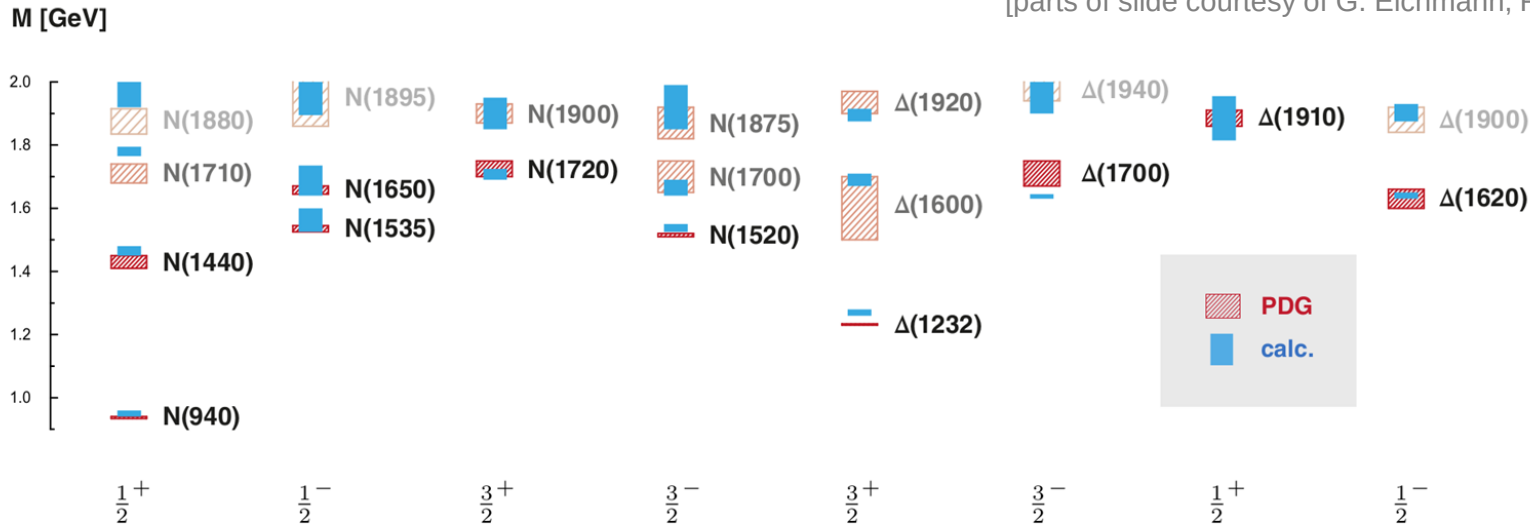


→ Making the “Missing resonance problem” worse ?!

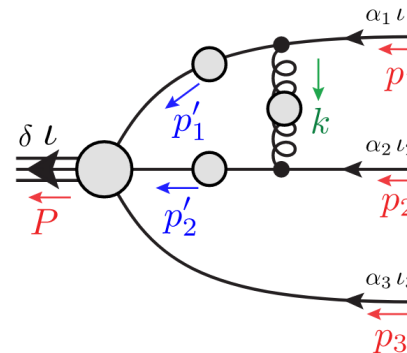
Results in dynamical quark picture

Quark-diquark with reduced pseudoscalar + vector diquarks: [GE, Fischer, Sanchis-Alepuz, PRD 94 \(2016\)](#)

[parts of slide courtesy of G. Eichmann, Few Body 2018]

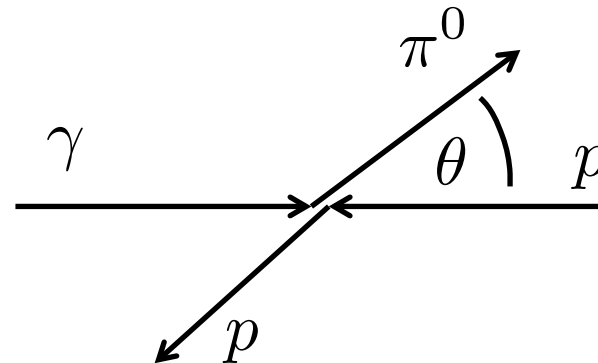
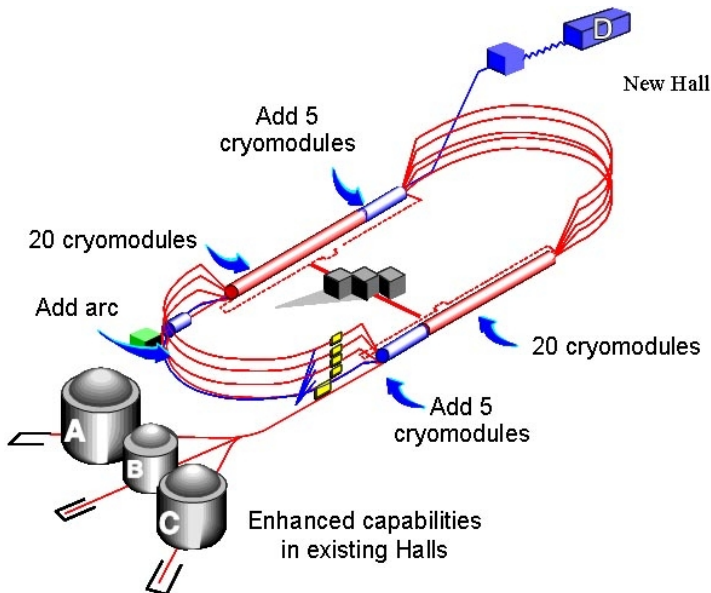
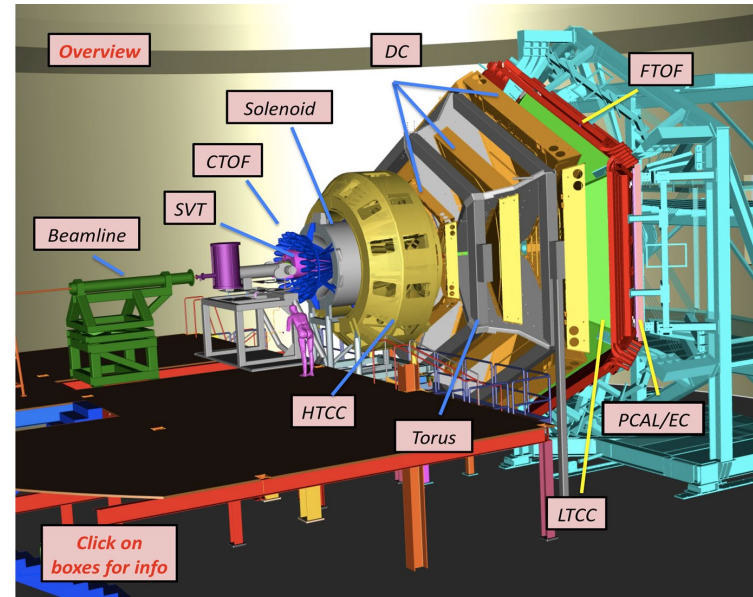


Poincaré-covariant analysis of heavy-quark baryons, Qin, Roberts, Schmidt, PRD (2018)
Spectrum of light- and heavy-baryons, Qin, Roberts, Schmidt, Few Body Syst. 60 (2019)



Photoproduction experiments

(Jlab, Mami, Elsa, GRAAL,...)



Degrees of freedom

- Energy
- Scattering angle
- Polarizations

Typical data situation

Reaction type

Observable:

Differential cross section

$$\frac{d\sigma}{d\Omega} [\mu\text{b/sr}]$$

Data from
different
experiments

Models from different
analysis groups
(GW-based and others)

Excluded regions

large variations
~ 2 orders of magnitude

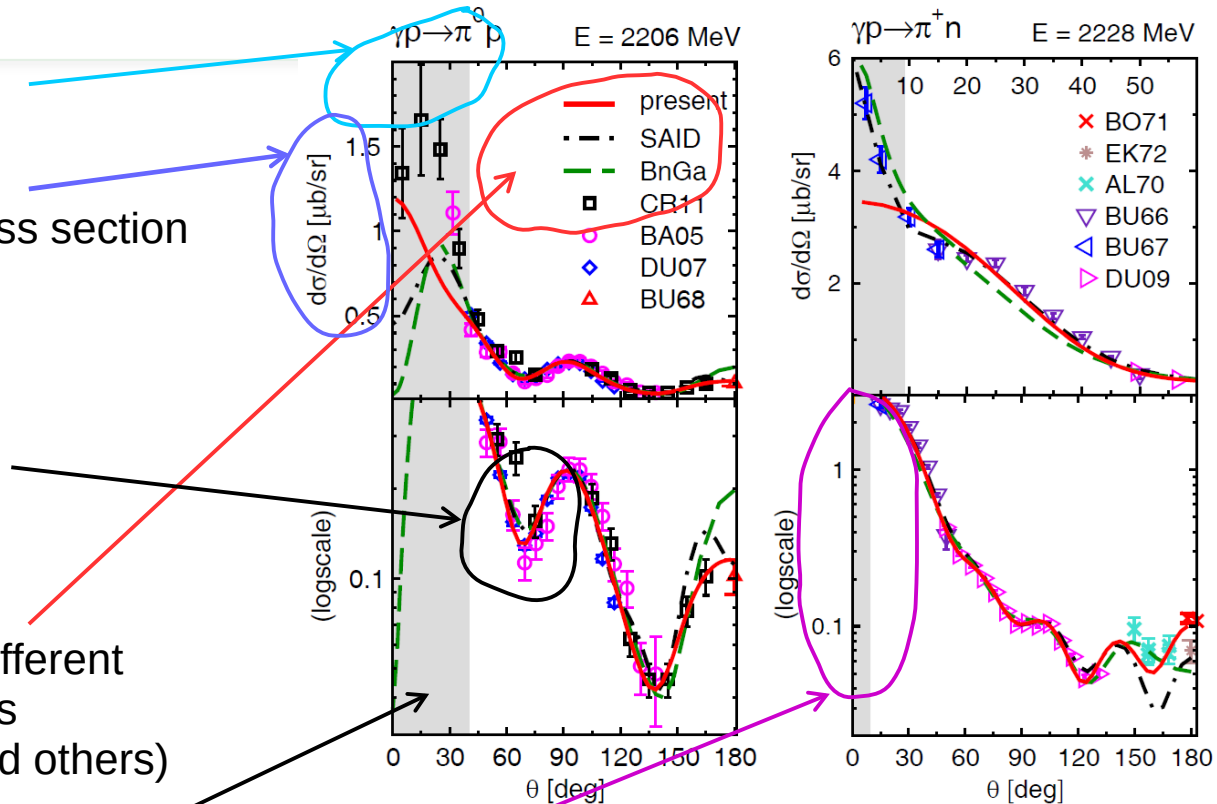
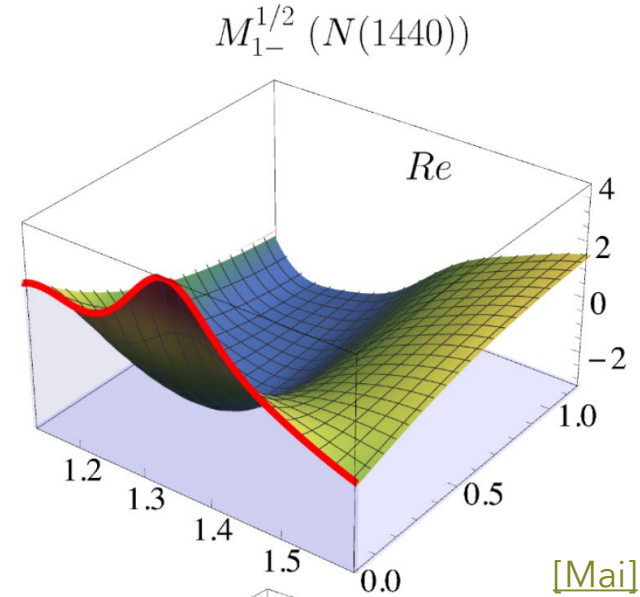
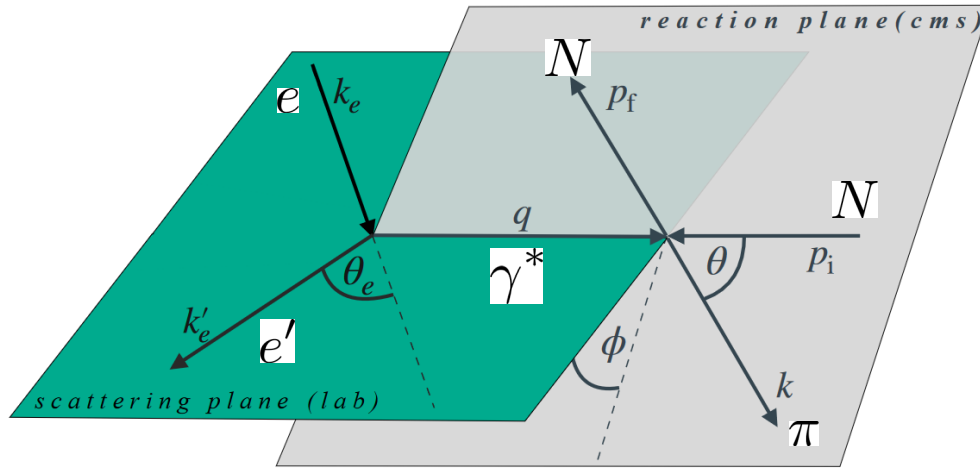
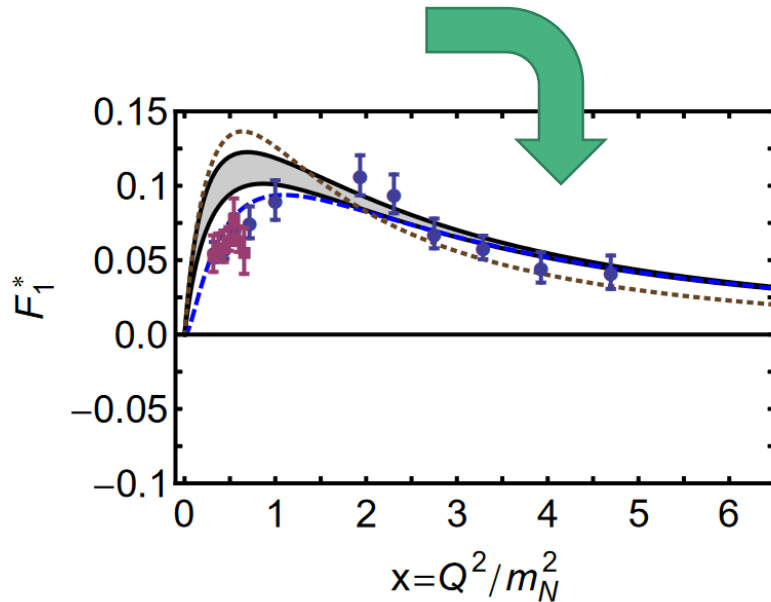


Fig. 2. High-energy behavior in the reaction $\gamma p \rightarrow \pi^0 p$ (left) and $\gamma p \rightarrow \pi^+ n$ (right). Solid (red) line: fit 2; dash-dotted (black) line: GWU/SAID CM12 [3]; dashed (green) line: Bonn-Gatchina [119]. Data $\pi^0 p$: CR11 [120], BA05 [126], DU07 [127], BU68 [128]. Data $\pi^+ n$: BO71 [129], EK72 [130], AL70 [131], BU66 [132], BU67 [133], DU09 [134]. The regions excluded in our fit are shown as shaded areas.

Electroproduction reveals resonance structure

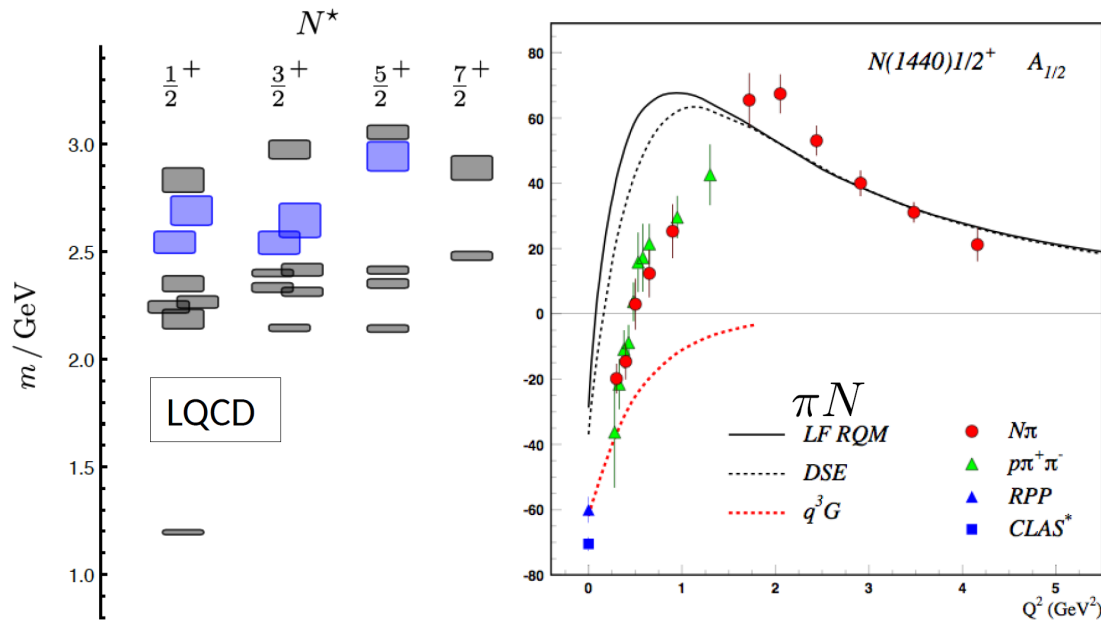


[Mai]



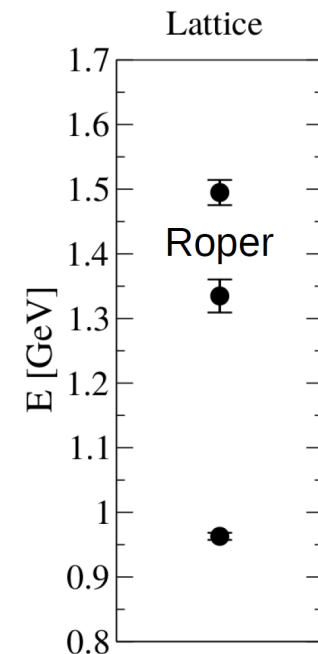
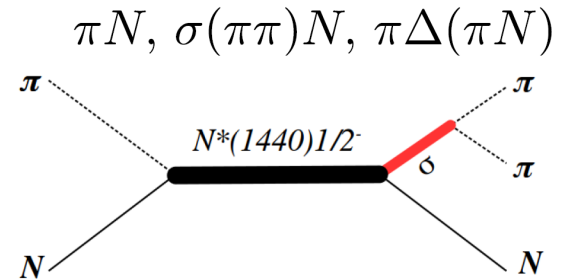
Proton-Roper Transition [Burkert] [Segovia]

Hybrid baryons & 1st lattice results



J.J. Dudek and R.G. Edwards,
PRD85 (2012)

Rel. quark model: Aznauryan (2007)
Dyson-Schwinger: Wilson, Cloet, Chang,
C. D. Roberts (2012)
[source: Int. J. Mod. Phys. (2013)]



Data: [Lang et al., Phys.Rev. D95 (2017), 014510]

Hybrid states: same J^P values as q^3 baryons.
Identification? Measure Q^2 dependence of
electro-couplings (**CLAS 12**)

2.2. Dynamical coupled-channel approaches

- ANL-Osaka (former: EBAC)
- Dubna-Mainz-Taipei model [\[Tiator\]](#)
- Jülich-Bonn [\[Rönchen\]](#)/Jülich-Bonn-Washington (latest edition with electroproduction, [\[Mai\]](#))
- ... (there are more!)
- Characteristics:
 - Direct fit to data (pion & photon-induced)
 - Simultaneous fit to data on different final states
 - Integral scattering equation as needed for proper treatment of three-body channels ($\pi\pi N$): One does need two independent integrations for 3B kinematics

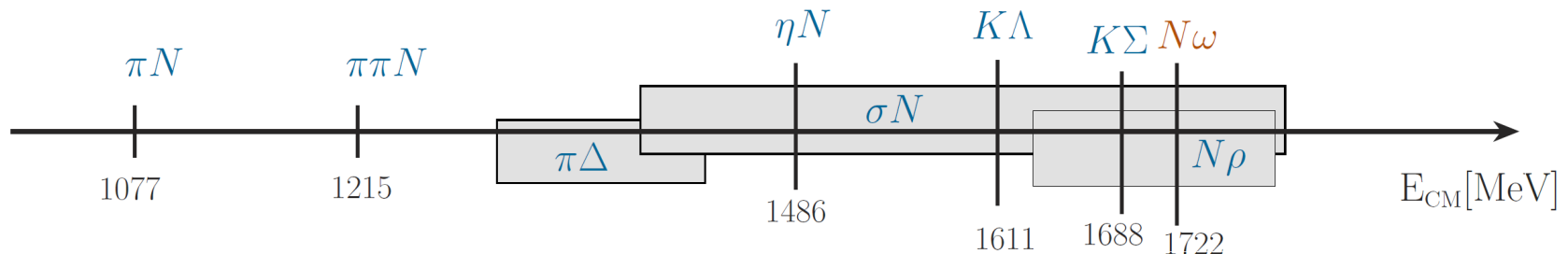
JBW DCC approach (Jülich-Bonn-Washington)

Dynamical coupled-channels (DCC): simultaneous analysis of different reactions

The scattering equation in partial-wave basis

$$\langle L' S' p' | T_{\mu\nu}^{IJ} | L S p \rangle = \langle L' S' p' | V_{\mu\nu}^{IJ} | L S p \rangle + \sum_{\gamma, L'' S''} \int_0^\infty dq \, q^2 \langle L' S' p' | V_{\mu\gamma}^{IJ} | L'' S'' q \rangle \frac{1}{E - E_\gamma(q) + i\epsilon} \langle L'' S'' q | T_{\gamma\nu}^{IJ} | L S p \rangle$$

■ channels ν, μ, γ :



Compare with Lippman-Schwinger equation:

$$T_\ell(p', p) = V_\ell(p', p) + \int_0^\infty dq \, q^2 \frac{V_\ell(p', q)}{E - \frac{q^2}{2m} + i\epsilon} T_\ell(q, p)$$

JBW DCC approach (Jülich-Bonn-Washington)

The scattering equation in partial-wave basis

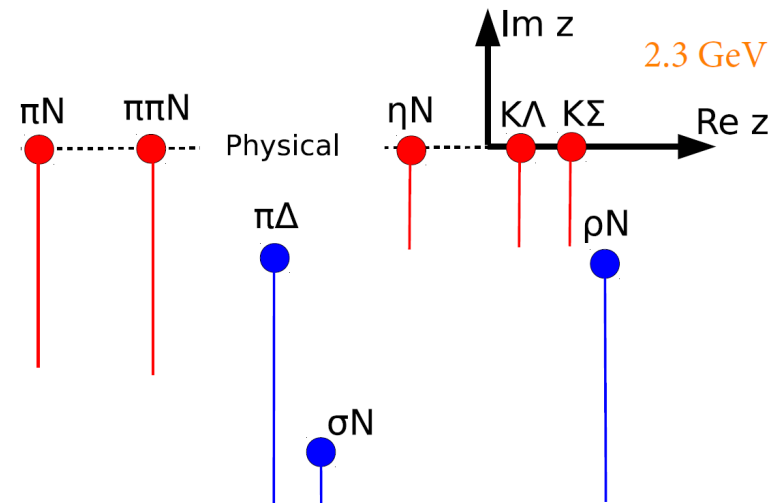
$$\langle L' S' p' | T_{\mu\nu}^{IJ} | L S p \rangle = \langle L' S' p' | V_{\mu\nu}^{IJ} | L S p \rangle + \sum_{\gamma, L'' S''} \int_0^\infty dq \, q^2 \langle L' S' p' | V_{\mu\gamma}^{IJ} | L'' S'' q \rangle \frac{1}{E - E_\gamma(q) + i\epsilon} \langle L'' S'' q | T_{\gamma\nu}^{IJ} | L S p \rangle$$

3-body $\pi\pi N$ channel:

- parameterized effectively as $\pi\Delta$, σN , ρN
- $\pi N/\pi\pi$ subsystems fit the respective phase shifts

↳ branch points move into complex plane

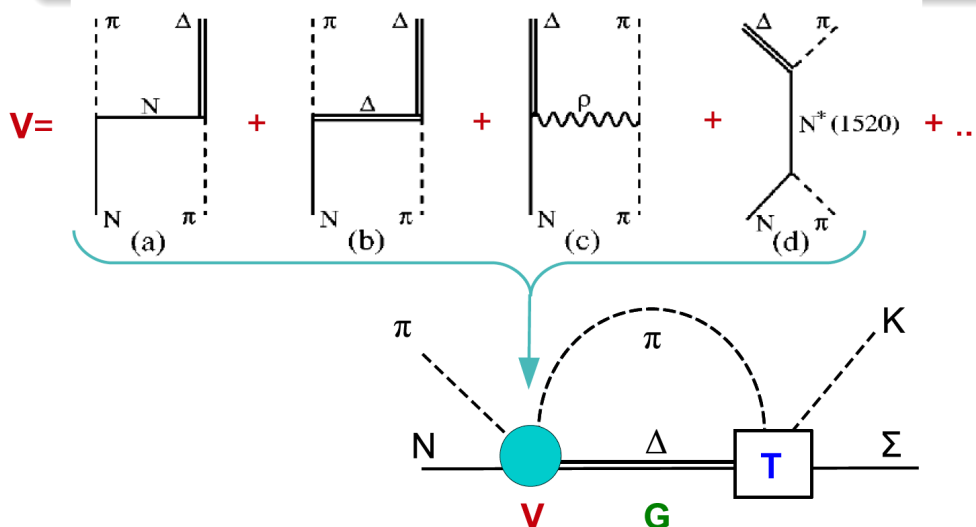
Inclusion of branch points important to avoid false resonance signal!



JBW DCC approach (Jülich-Bonn-Washington)

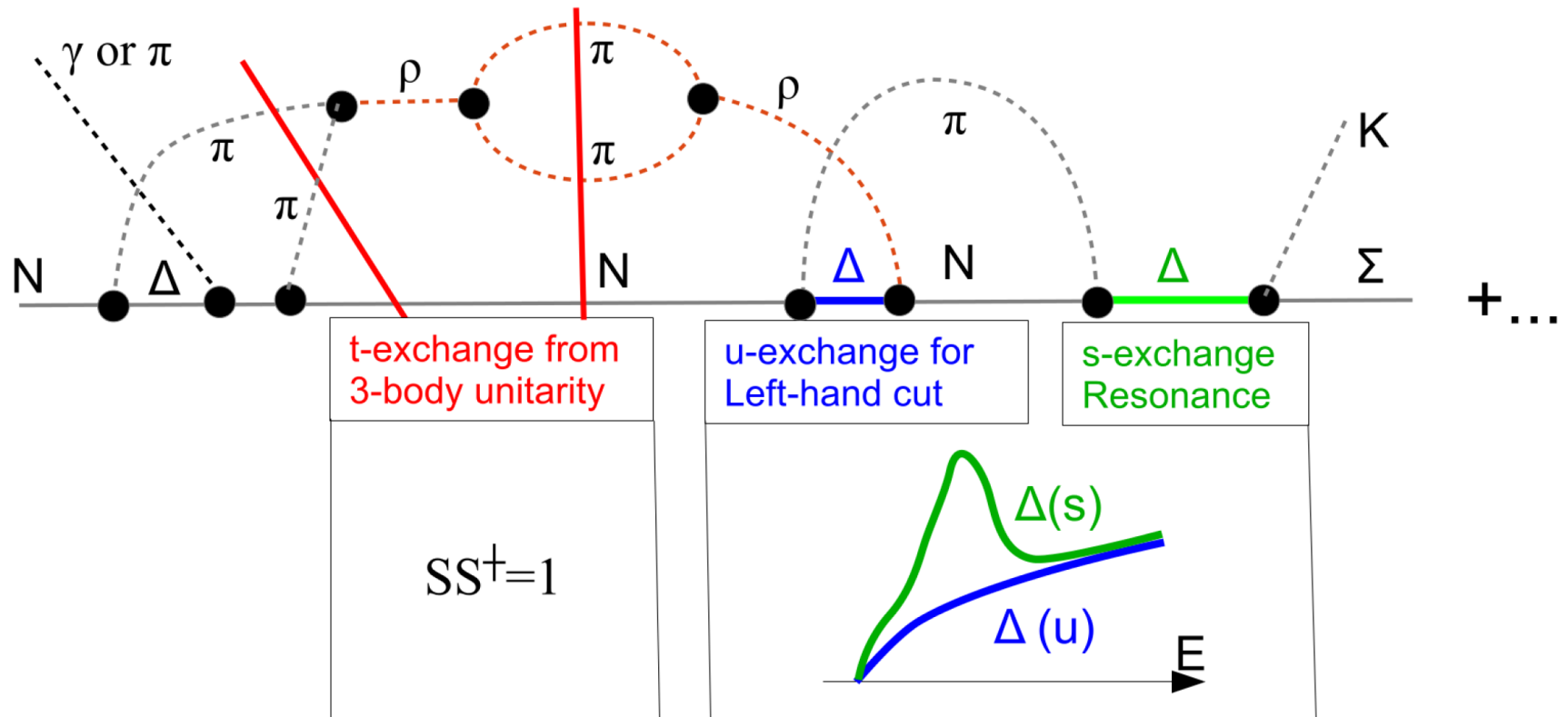
The scattering equation in partial-wave basis

$$\langle L' S' p' | T_{\mu\nu}^{IJ} | L S p \rangle = \langle L' S' p' | V_{\mu\nu}^{IJ} | L S p \rangle + \sum_{\gamma, L'' S''} \int_0^\infty dq \, q^2 \langle L' S' p' | V_{\mu\gamma}^{IJ} | L'' S'' q \rangle \frac{1}{E - E_\gamma(q) + i\epsilon} \langle L'' S'' q | T_{\gamma\nu}^{IJ} | L S p \rangle$$



- potentials V constructed from effective \mathcal{L}
- s -channel diagrams: T^P
genuine resonance states
- t - and u -channel: T^{NP}
dynamical generation of poles
partial waves strongly correlated
- contact terms

Another Visualization



Channel space

- Jülich-Bonn-Washington approach has the same channel space as ANL/Osaka (former EBAC) approach

μ	$J^P = \frac{1}{2}^- \quad \frac{1}{2}^+$	$\frac{3}{2}^+ \quad \frac{3}{2}^-$	$\frac{5}{2}^- \quad \frac{5}{2}^+$	$\frac{7}{2}^+ \quad \frac{7}{2}^-$	$\frac{9}{2}^- \quad \frac{9}{2}^+$
1 πN	$S_{11} \quad P_{11}$	$P_{13} \quad D_{13}$	$D_{15} \quad F_{15}$	$F_{17} \quad G_{17}$	$G_{19} \quad H_{19}$
2 $\rho N(S = 1/2)$	$S_{11} \quad P_{11}$	$P_{13} \quad D_{13}$	$D_{15} \quad F_{15}$	$F_{17} \quad G_{17}$	$G_{19} \quad H_{19}$
3 $\rho N(S = 3/2, J - L = 1/2)$	$— \quad P_{11}$	$P_{13} \quad D_{13}$	$D_{15} \quad F_{15}$	$F_{17} \quad G_{17}$	$G_{19} \quad H_{19}$
4 $\rho N(S = 3/2, J - L = 3/2)$	$D_{11} \quad —$	$F_{13} \quad S_{13}$	$G_{15} \quad P_{15}$	$H_{17} \quad D_{17}$	$I_{19} \quad F_{19}$
5 ηN	$S_{11} \quad P_{11}$	$P_{13} \quad D_{13}$	$D_{15} \quad F_{15}$	$F_{17} \quad G_{17}$	$G_{19} \quad H_{19}$
6 $\pi \Delta(J - L = 1/2)$	$— \quad P_{11}$	$P_{13} \quad D_{13}$	$D_{15} \quad F_{15}$	$F_{17} \quad G_{17}$	$G_{19} \quad H_{19}$
7 $\pi \Delta(J - L = 3/2)$	$D_{11} \quad —$	$F_{13} \quad S_{13}$	$G_{15} \quad P_{15}$	$H_{17} \quad D_{17}$	$I_{19} \quad F_{19}$
8 σN	$P_{11} \quad S_{11}$	$D_{13} \quad P_{13}$	$F_{15} \quad D_{15}$	$G_{17} \quad F_{17}$	$H_{19} \quad G_{19}$
9 $K\Lambda$	$S_{11} \quad P_{11}$	$P_{13} \quad D_{13}$	$D_{15} \quad F_{15}$	$F_{17} \quad G_{17}$	$G_{19} \quad H_{19}$
10 $K\Sigma$	$S_{11} \quad P_{11}$	$P_{13} \quad D_{13}$	$D_{15} \quad F_{15}$	$F_{17} \quad G_{17}$	$G_{19} \quad H_{19}$

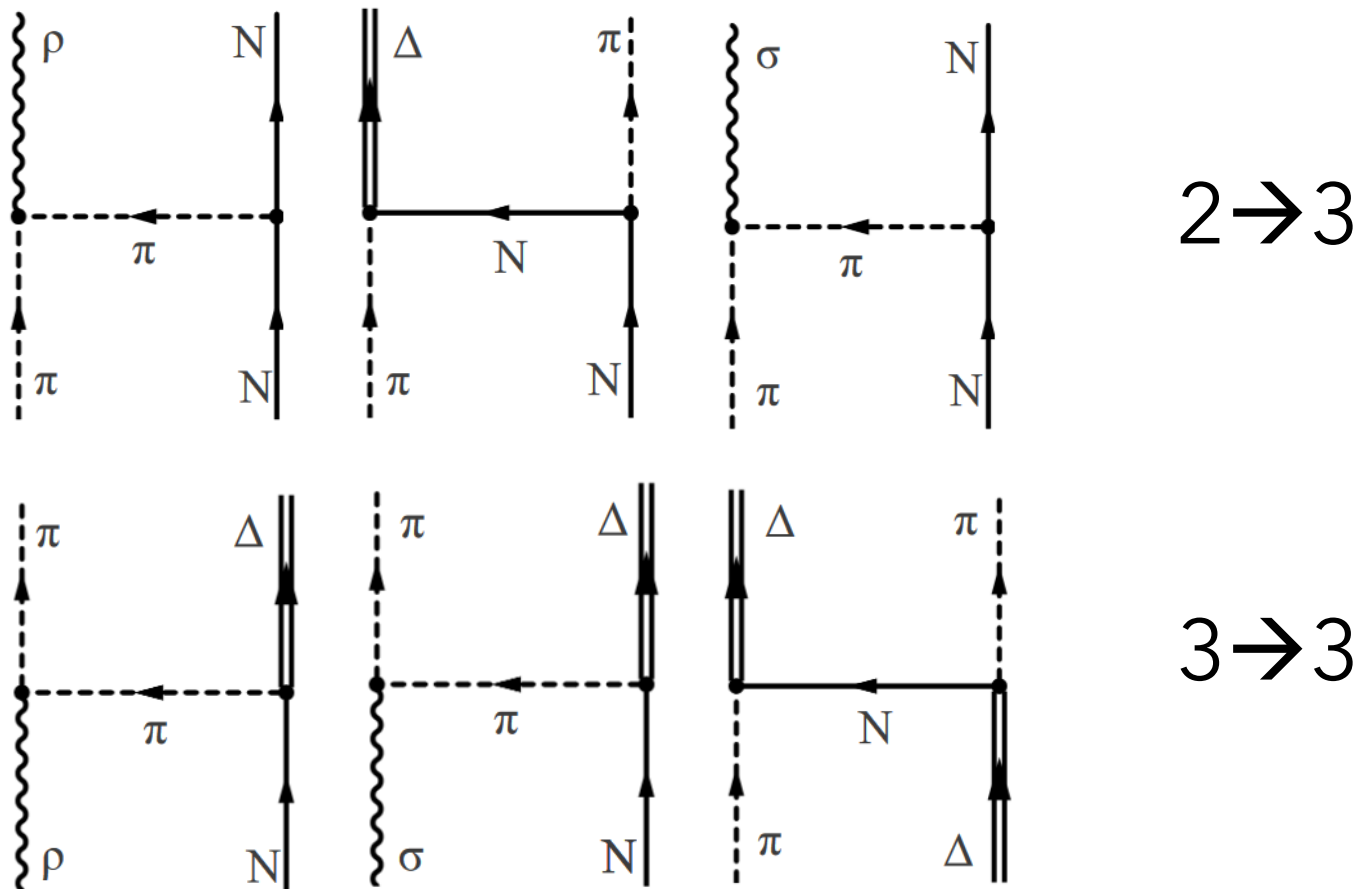
S-, t- and u-channel exchanges

- 21 s-channel states (**resonances**) coupling to πN , ηN , $K\Lambda$, $K\Sigma$, $\pi\Delta$, ρN .
- t- and u-channel **exchanges** ("background"):

	πN	ρN	ηN	$\pi\Delta$	σN	$K\Lambda$	$K\Sigma$
πN	$N, \Delta, (\pi\pi)_\sigma, (\pi\pi)_\rho$	$N, \Delta, \text{Ct.}, \pi, \omega, a_1$	N, a_0	N, Δ, ρ	N, π	Σ, Σ^*, K^*	$\Lambda, \Sigma, \Sigma^*, K^*$
ρN		$N, \Delta, \text{Ct.}, \rho$	-	N, π	-	-	-
ηN			N, f_0	-	-	K^*, Λ	Σ, Σ^*, K^*
$\pi\Delta$				N, Δ, ρ	π	-	-
σN					N, σ	-	-
$K\Lambda$		Is there a system behind this?				$\Xi, \Xi^*, f_0, \omega, \phi$	Ξ, Ξ^*, ρ
$K\Sigma$							$\Xi, \Xi^*, f_0, \omega, \phi, \rho$

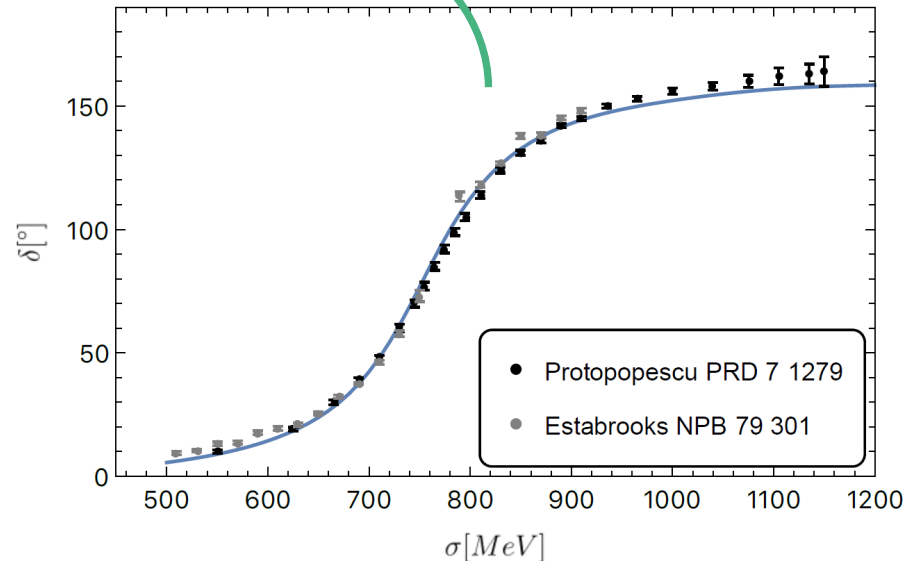
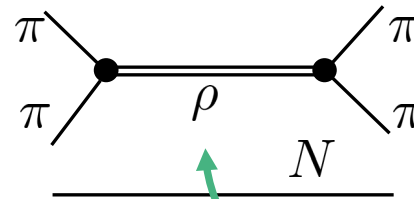
2 → 3 and 3 → 3 body unitarity

- See last part of this lecture: Unitarity requires certain transition amplitudes

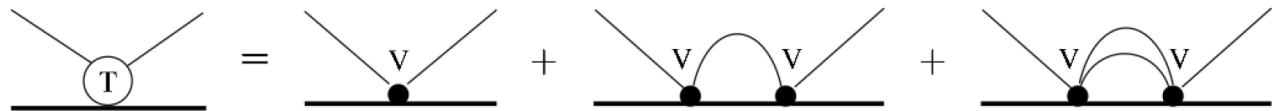
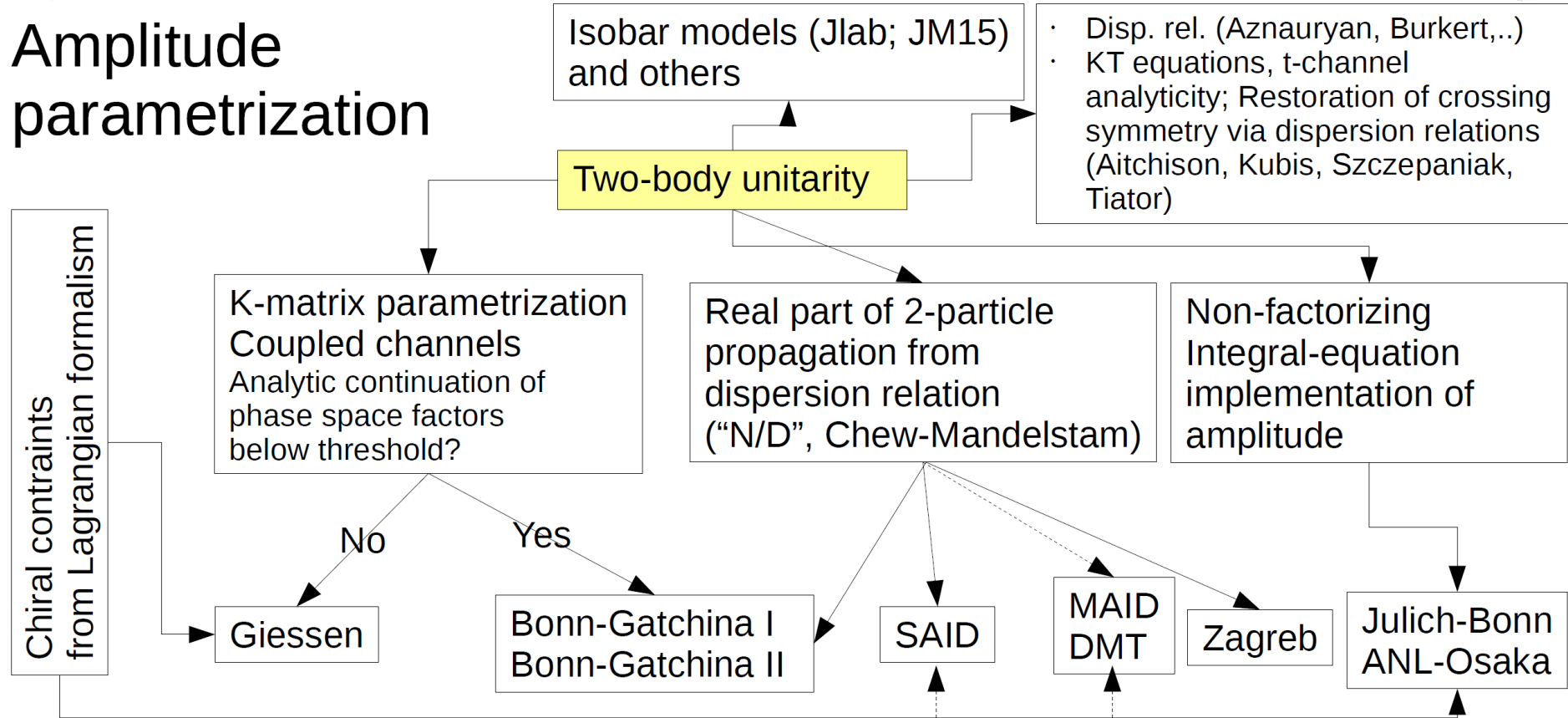


Three-body channels $\sigma N, \pi\Delta, \rho N$

- Resonant sub-channels
- Fit $2 \rightarrow 2$ amplitude to $2 \rightarrow 2$ scattering data
- Include as sub-channel in 3-body amplitude: 2-body input depends only on on-shell $2 \rightarrow 2$ scattering

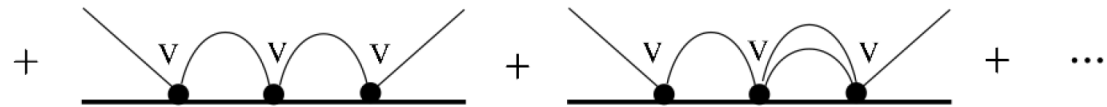
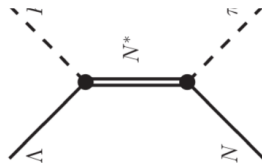


Amplitude parametrization



$$T = V + VGT,$$

Genuine Resonance:

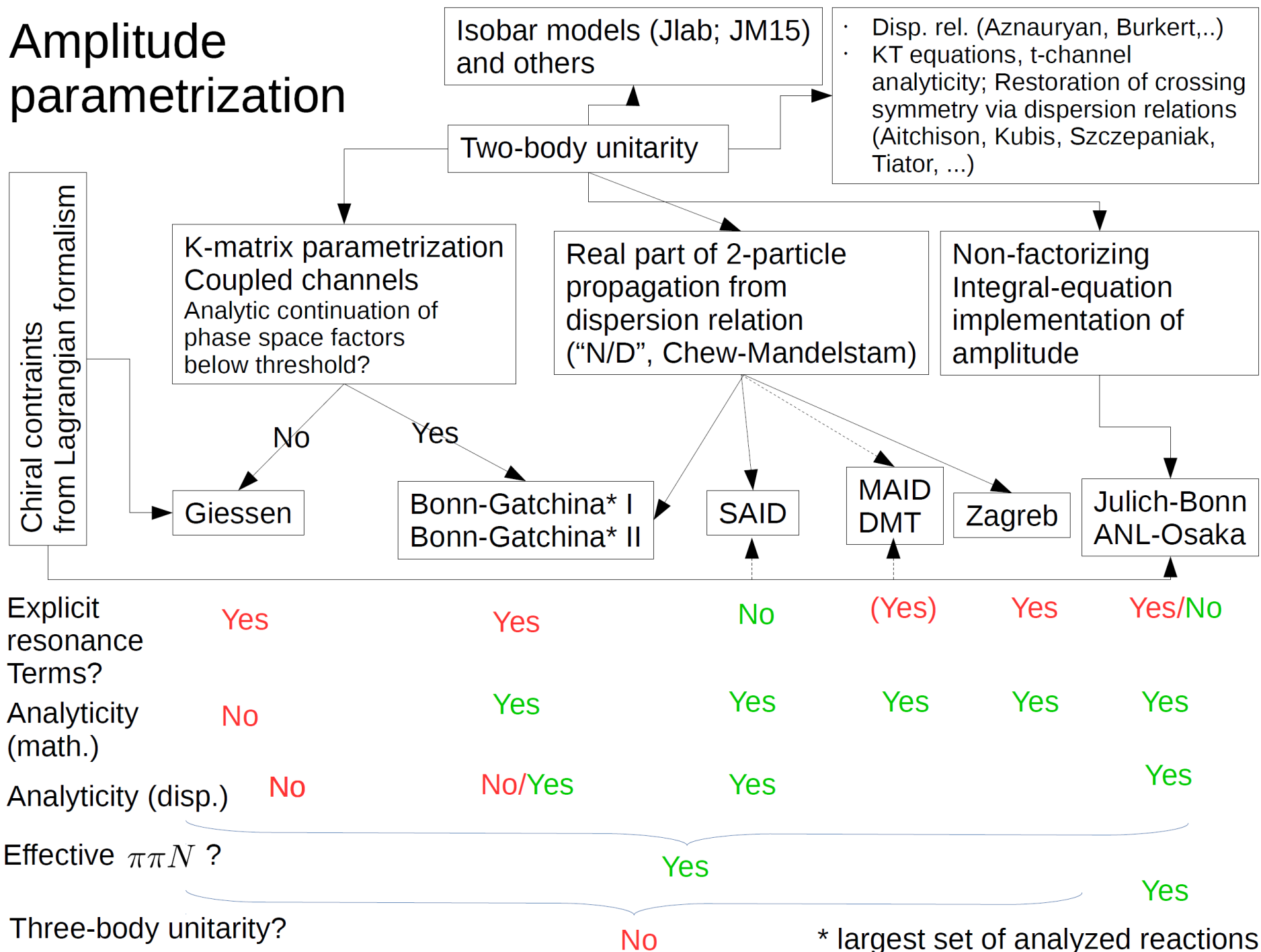


Unitarity loop G :

- $\text{Re } G \rightarrow 0$: K-matrix
- V point-like: SAID

Integral equation: Julich-Bonn, ANL-Osaka

Amplitude parametrization



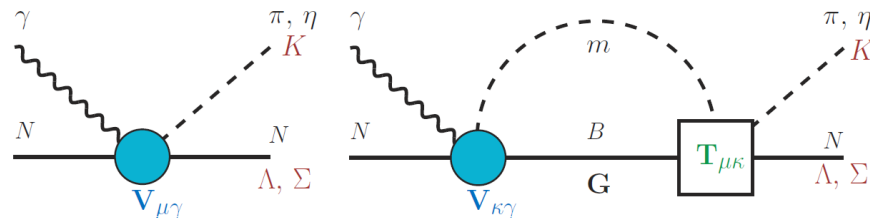
Coupling of the photon (1)

- Direct parametrization of multipoles....

Multipole amplitude

$$M_{\mu\gamma}^{IJ} = V_{\mu\gamma}^{IJ} + \sum_{\kappa} T_{\mu\kappa}^{IJ} G_{\kappa} V_{\kappa\gamma}^{IJ}$$

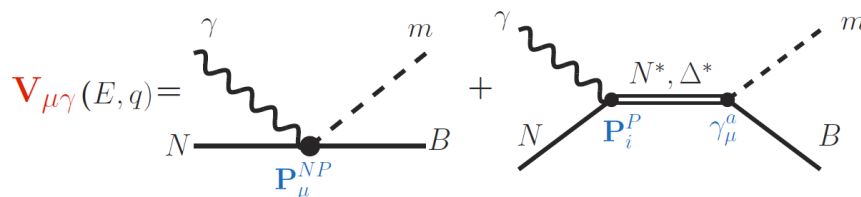
(partial wave basis)



$$m = \pi, \eta, K, B = N, \Delta, \Lambda$$

$T_{\mu\kappa}$: Jülich hadronic T -matrix \rightarrow Watson's theorem fulfilled by construction
 \rightarrow **analyticity of T**: extraction of resonance parameters

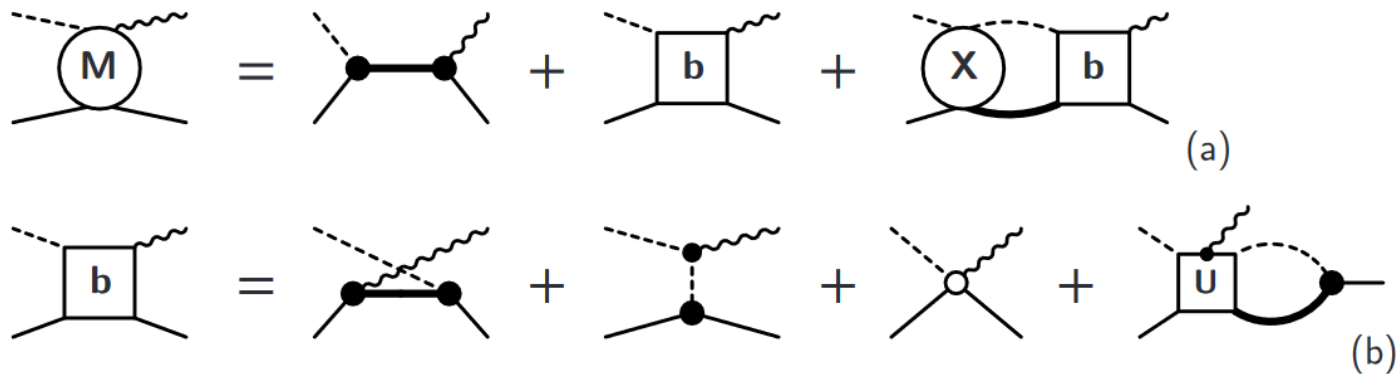
Photoproduction potential: approximated by energy-dependent polynomials (field-theoretical description numerically too expensive)



$$= \frac{\tilde{\gamma}_{\mu}^a(q)}{m_N} P_{\mu}^{NP}(E) + \sum_i \frac{\gamma_{\mu,i}^a(q) P_i^P(E)}{E - m_i^b}$$

Coupling of photon (2)

- ... vs. gauge-invariant photon interaction [[Haberzettl](#)]

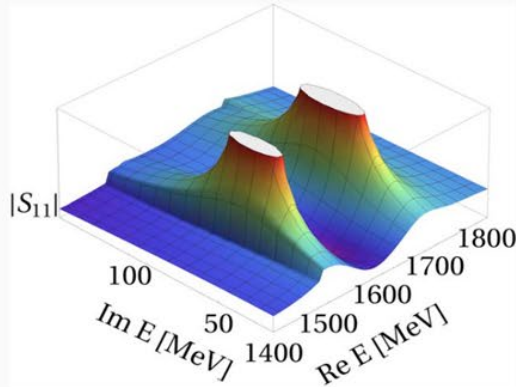


- Requires to make amplitude explicitly covariant
- Requires to calculate many tree level amplitudes
- Requires to calculate many photon-(higher-spin) resonance couplings from Lagrangians
- Realized in Julich-Bonn model [[Huang](#)] and EBAC/ANL-Osaka [[Kamano](#)]
- EBAC also analyzed two-pion final states

Resonance Couplings (typical outcome)

Resonance states: Poles in the T -matrix on the 2nd Riemann sheet

[D. Roenchen, M. D., U.-G. Meißner, EPJ A 54, 110 (2018)]



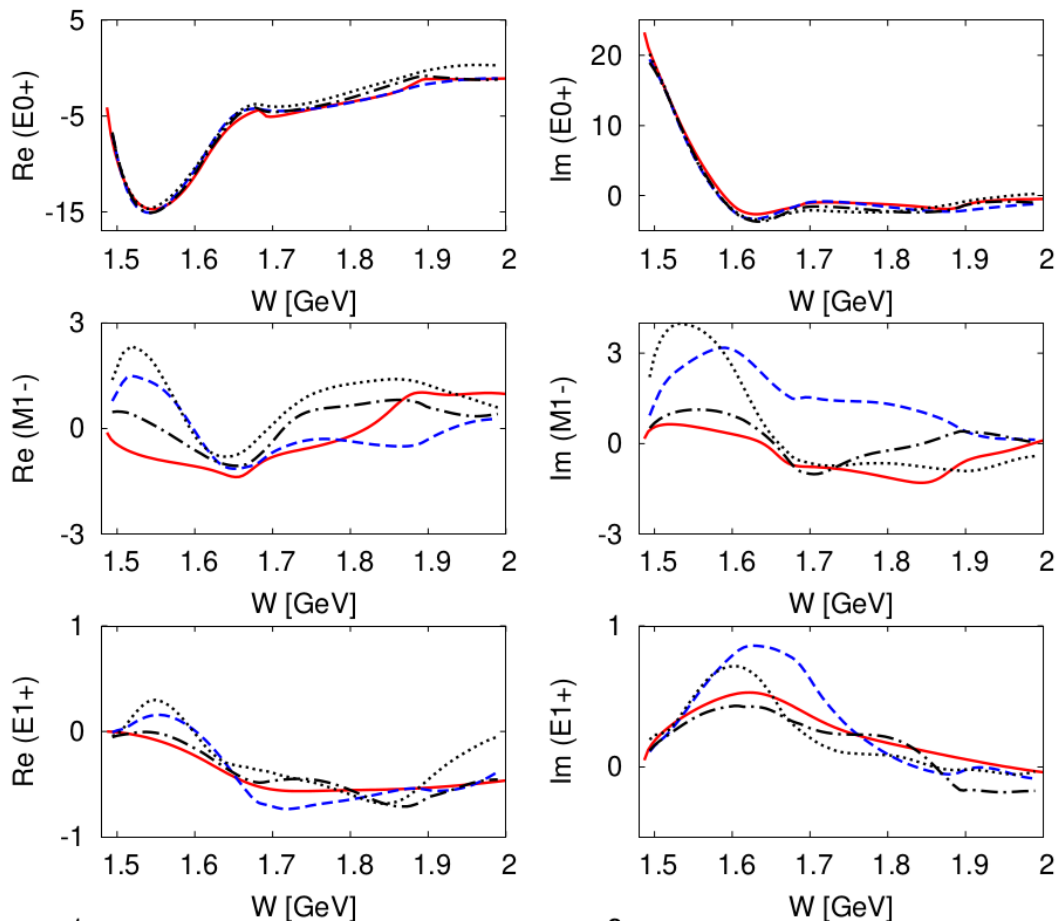
- $\text{Re}(E_0)$ = “mass”, $-2\text{Im}(E_0)$ = “width”
- elastic πN residue ($|r_{\pi N}|, \theta_{\pi N \rightarrow \pi N}$), normalized residues for inelastic channels ($\sqrt{\Gamma_{\pi N} \Gamma_{\mu}} / \Gamma_{\text{tot}}, \theta_{\pi N \rightarrow \mu}$)
- photocouplings at the pole: $\tilde{A}_{\text{pole}}^h = A_{\text{pole}}^h e^{i\vartheta^h}$, $h = 1/2, 3/2$

Inclusion of $\gamma p \rightarrow K^+ \Lambda$ in JüBo (“JuBo2017-1”): 3 additional states

	z_0 [MeV]	$\frac{\Gamma_{\pi N}}{\Gamma_{\text{tot}}}$	$\frac{\Gamma_{\eta N}}{\Gamma_{\text{tot}}}$	$\frac{\Gamma_{K\Lambda}}{\Gamma_{\text{tot}}}$
N(1900)3/2 ⁺	1923 − i 108.4	1.5 %	0.78 %	2.99 %
N(2060)5/2 [−]	1924 − i 100.4	0.35 %	0.15 %	13.47 %
$\Delta(2190)$ 1/2 ⁺	2191 − i 103.0	33.12 %		

- N(1900)3/2⁺: s-channel resonances, seen in many other analyses of kaon photoproduction (BnGa), 3 stars in PDG
- N(2060)5/2[−]: dynamically generated, 2 stars in PDG, seen e.g. by BnGa
- $\Delta(2190)$ 1/2⁺: dyn. gen., no equivalent PDG state

Current state in η photoproduction: Multipoles from different groups



From: **EtaMAID2018**
[Tiator et al., EPJA54 (2018)]

Analyzes:

$$\gamma p \rightarrow \eta p$$

$$\gamma p \rightarrow \eta' p$$

$$\gamma n \rightarrow \eta n$$

$$\gamma n \rightarrow \eta' n$$

EtaMAID2018

BnGa [PLB 772 (2017)]

JuBo (dotted) [EPJA 54 (2018)]

KSU [1804.06031]

Review: Krusche, Wilkins,
[Prog.Part.Nucl.Phys. 80 (2014)]

Ambiguities & complete experiment

- Does the measurement of a set of observables allow to determine the partial-wave amplitudes (up to one global undetermined phase)?
- Polynomial expansion of cross section: Assume only $\ell = 0, 1$ exist. Then:

$$\frac{d\sigma}{d\Omega} = \frac{1}{k^2} [\sin^2 \delta_0 + 6 \sin \delta_0 \sin \delta_1 \cos(\delta_1 - \delta_0) \cos \theta + 9 \sin^2 \delta_1 \cos^2 \theta] \quad (*)$$

- Assume experimental cross section is well described by A, B, C, where

$$\frac{d\sigma}{d\Omega} = \frac{1}{k^2} [A + B \cos \theta + C \cos^2 \theta]$$

- Sign ambiguity: (*) does not change if signs of both δ_0, δ_1 are changed.
- Generalization to systems with spin (usually, photoproduction):
 - "Complete experiment" (up to a global, energy-dependent phase)
 - "Complete truncated-partial-wave experiment"

2.2 One statistical aspect [Landay]

- How many resonances does one need to describe a given data set?
- Search for a “minimal set” (Occam’s razor)
- Too many hypothesis to test in fits (all combinations of all candidates)
- Automatized methods → Model selection techniques
 - “Least absolute shrinkage and selection operator” (LASSO) creates a whole family of models automatically from smaller to larger complexity
 - Additional criteria help to select the minimal model (usually weighing the chi-square against degrees of freedom)

LASSO

$$\sum_{i=1}^n \frac{(y_i - f(x_i, \beta_j))^2}{\sigma_i^2} + \lambda \sum_{j=1}^m |\beta_j|$$

Normal χ^2

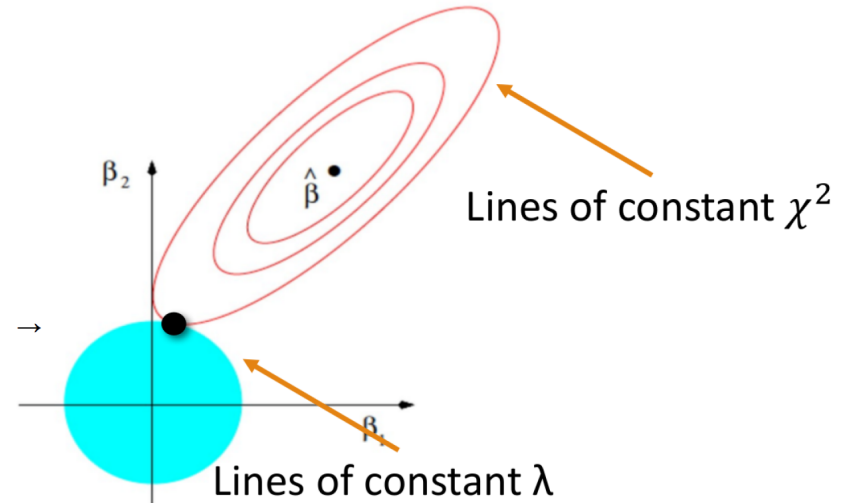
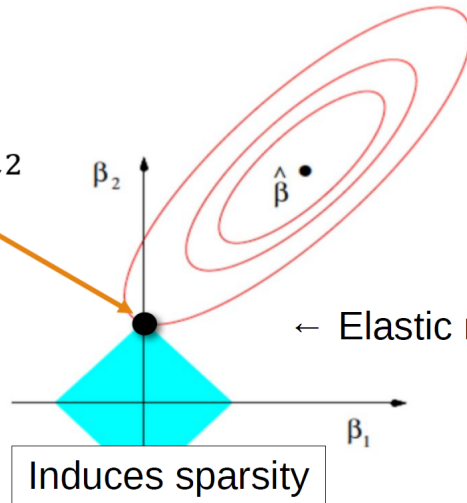
Penalty Term

LASSO ($n = 1$)

$\hat{\beta}_i$: Best parameters without penalty
 $\beta_i = 0$: Best parameters only penalty

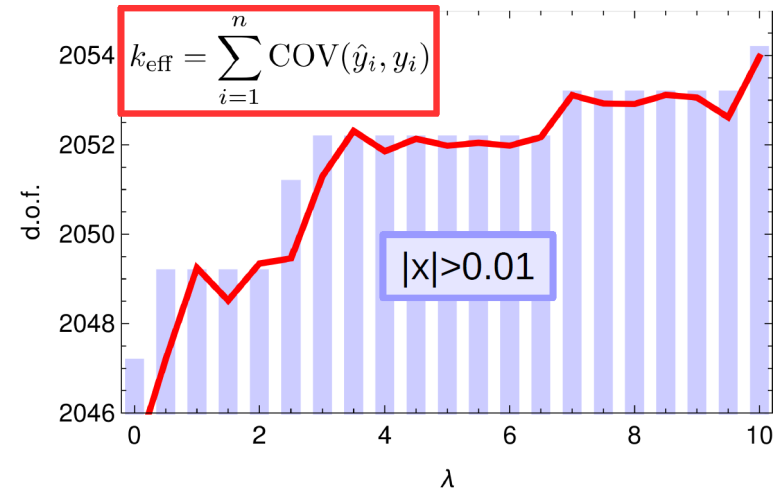
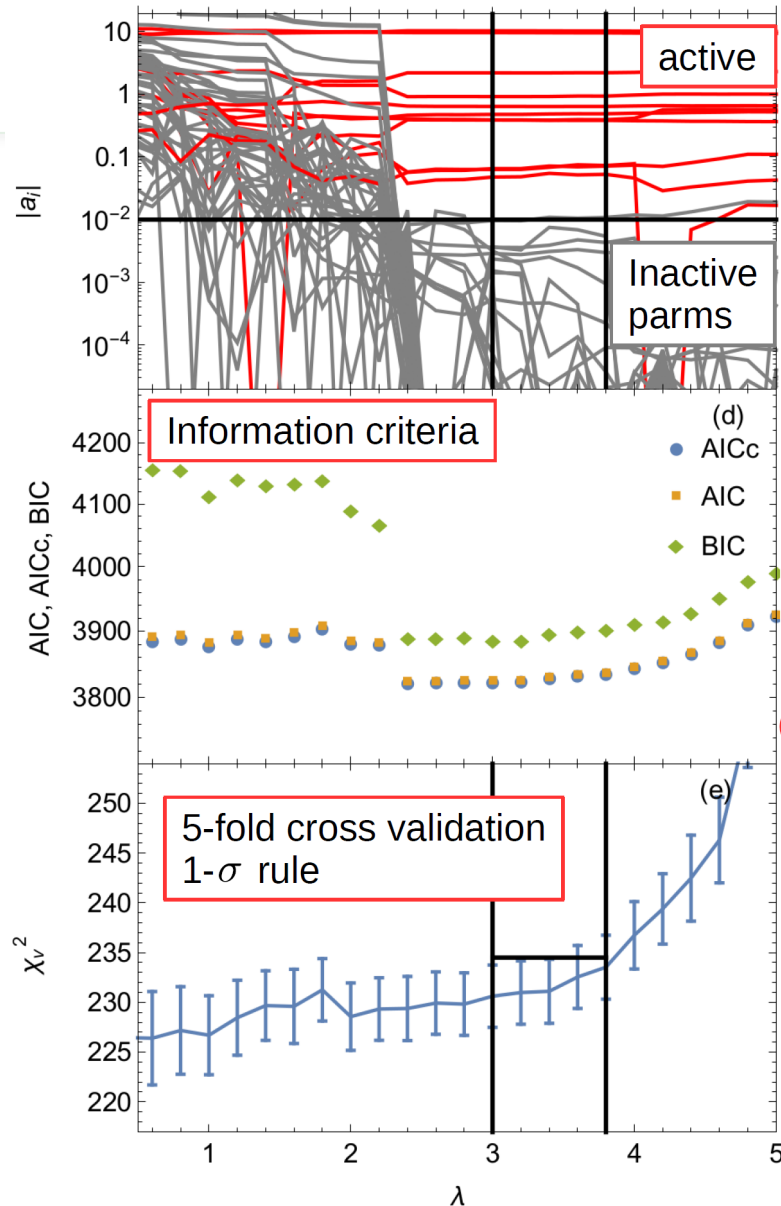
Ridge Regression ($n = 2$)

Simultaneous
minimization of χ^2
and Penalty



See, e.g.: *The Elements of Statistical Learning: Data Mining, Inference, and Prediction*, T. Hastie, R. Tibshirani, J. Friedman, Springer 2009 second ed.

Information theory criteria



$k \rightarrow k_{\text{eff}}$ subsequently

$$AIC = -2 \max \log(L(\hat{\theta}|data)) + 2k = \chi^2 + 2k$$

$$AIC_c = AIC + \frac{2k(k+1)}{n-k-1}$$

$$BIC = -2 \max \log(L(\hat{\theta}|data)) + 2\log(n) = \chi^2 + k \log(n)$$

Close relation to Bayesian model comparison (here: $n \gg k$)

See, e.g.: Andrew A. Neath, Joseph E. Cavanaugh, DOI: 10.1002/wics.199

Synthetic data results

- 10 partial waves
- 10 resonance candidates
- Synthetic data with 4 active resonances

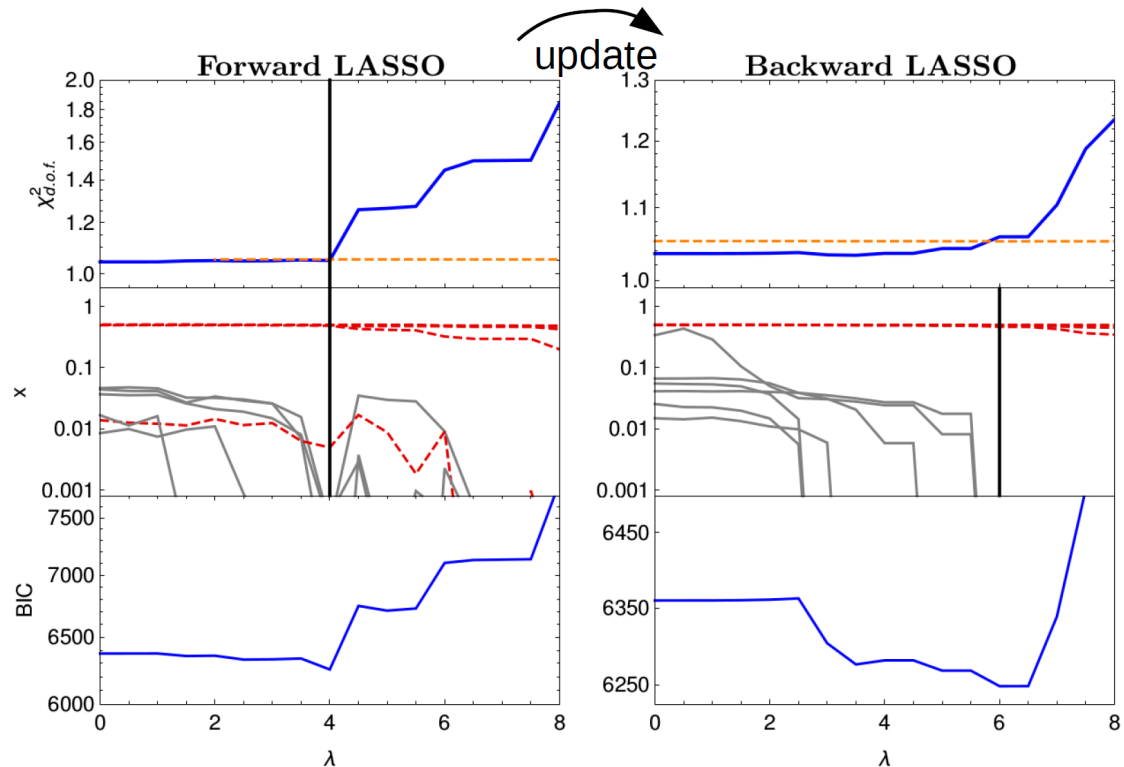
$$W) = e^{i\phi} \left(\frac{k_f(W)}{\Lambda} \right)^{L+1/2} \times \left(a e^{-\alpha^2 \left(\frac{k_f(W)}{\Lambda} \right)^2} - \boxed{x} e^{i\Phi} \frac{\Gamma/2}{W - M + i\Gamma/2} \right) \times$$

- Penalty (group LASSO):

$$P_{gr}(\lambda) = \lambda^4 \sum_{i=1}^{i_{\max}} \sqrt{p_i} |x_i|$$

Large $\lambda \rightarrow$ small λ

Small $\lambda \rightarrow$ large λ



Selected:
4 active resonances
1 inactive resonance

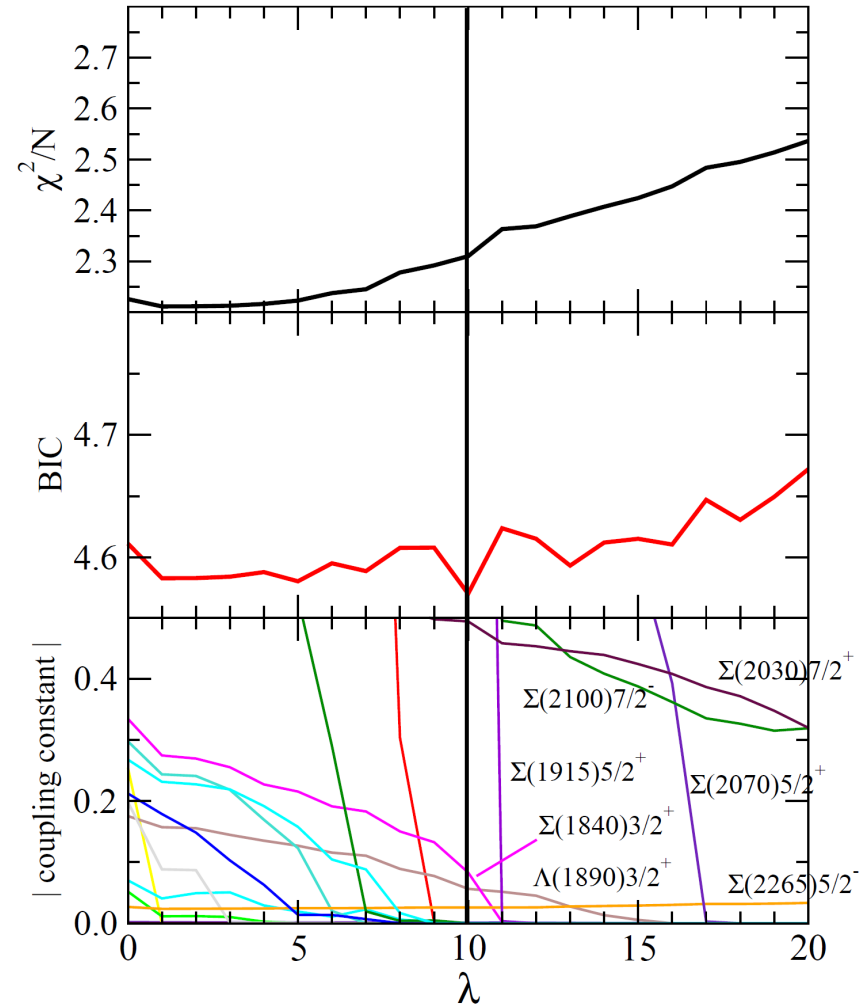
Selected:
4 active resonances
0 inactive resonance

Finds good local minima!

Greediness built in

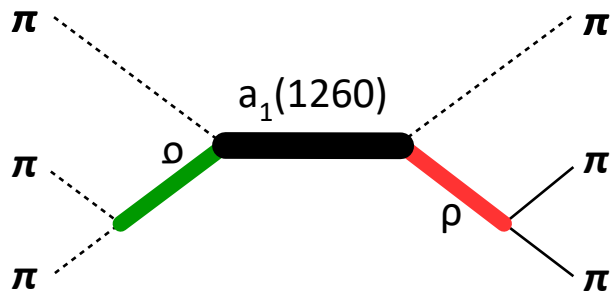
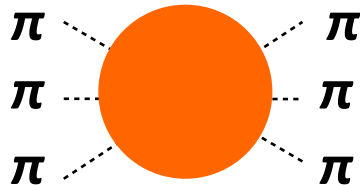
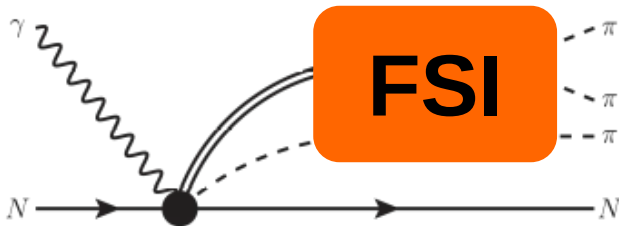
Results for the reaction $\bar{K}N \rightarrow K\Xi$ [Landay]

- Start with an abundant set of resonances
- Fit data for different penalties
- Use information criteria to identify to point of maximal information
- Of 21 PDG candidates, 10 survive.



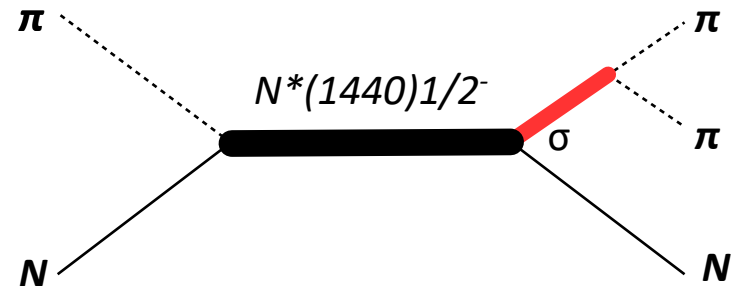
3. Three-body aspects

Light mesons



- Important channel in GlueX @ Jlab: hybrids and exotics
- Finite volume spectrum from lattice QCD:
[Lang \(2014\)](#), [Woss \[HadronSpectrum\] \(2018\)](#)
[Hörz \(2019\)](#), [Culver \(2020\)](#), [Fischer \(2020\)](#),
[Hansen \(2020\)](#),...

Light baryons



- Roper resonance is debated for ~50 years in experiment. Can only be seen in PWA.
- 1st calculation w. meson-baryon operators on the lattice: [Lang et al. \(2017\)](#)

3.1 Three-body unitarity with isobars * [\[Mai\]](#)

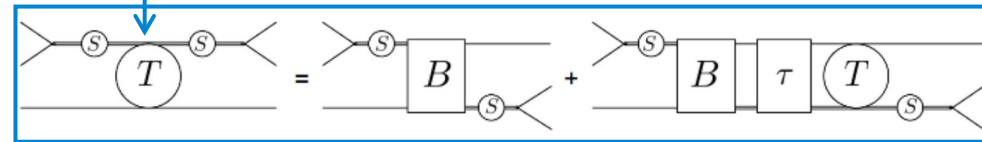
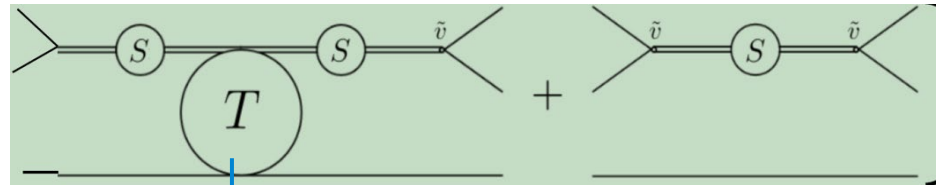
$$\begin{aligned} \langle q_1, q_2, q_3 | (\hat{T} - \hat{T}^\dagger) | p_1, p_2, p_3 \rangle &= i \int_P \langle q_1, q_2, q_3 | \hat{T}^\dagger | k_1, k_2, k_3 \rangle \langle k_1, k_2, k_3 | \hat{T} | p_1, p_2, p_3 \rangle \\ &\times \prod_{\ell=1}^3 \left[\frac{d^4 k_\ell}{(2\pi)^4} (2\pi) \delta^+(k_\ell^2 - m^2) \right] (2\pi)^4 \delta^4 \left(P - \sum_{\ell=1}^3 k_\ell \right) \end{aligned}$$

delta function sets all intermediate particles on-shell

* "Isobar" stands for two-body sub-amplitude which can be resonant or not; can be matched to CHPT expansion to one loop if desired. Isobars are re-parametrization of full 2-body amplitude [\[Bedaque\]](#) [\[Hammer\]](#)

Three-body unitarity

$$\langle q_1, q_2, q_3 | (\hat{T} - \hat{T}^\dagger) | p_1, p_2, p_3 \rangle = i \int_P \langle q_1, q_2, q_3 | \hat{T}^\dagger | k_1, k_2, k_3 \rangle \langle k_1, k_2, k_3 | \hat{T} | p_1, p_2, p_3 \rangle$$

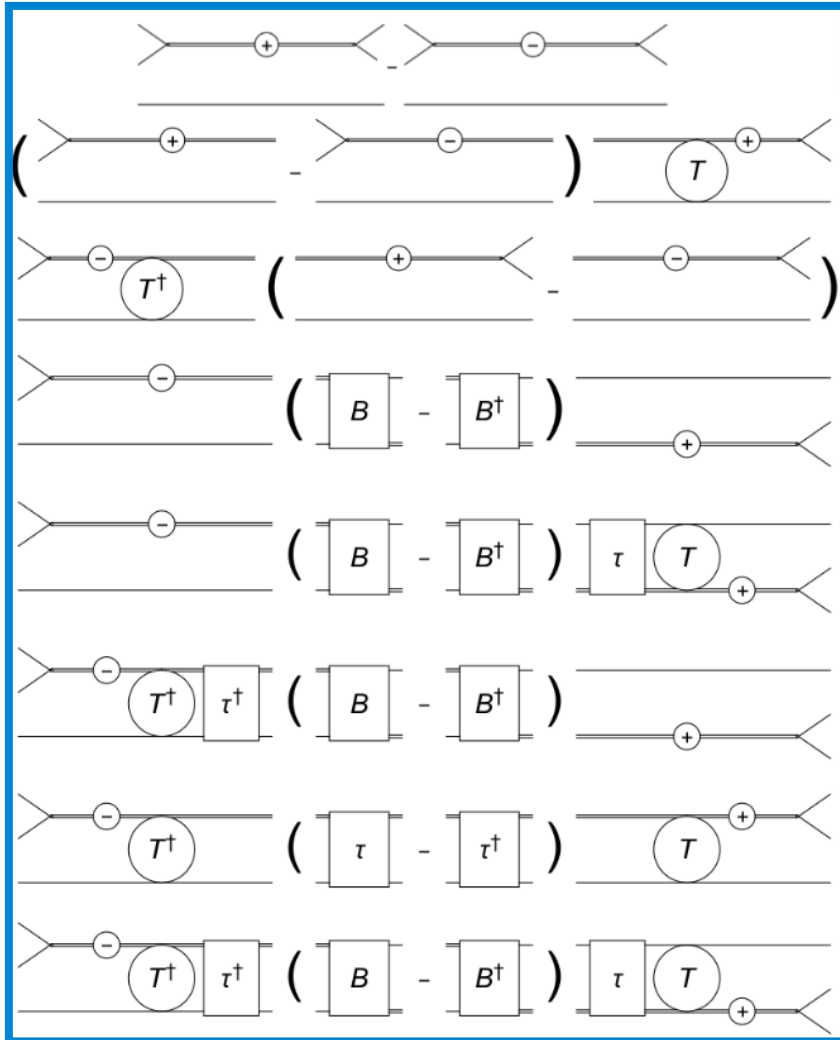


General Ansatz for the isobar-spectator interaction

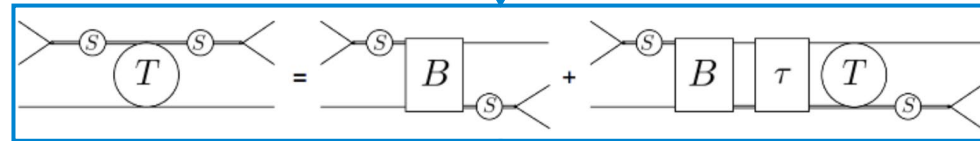
→ **B** & **τ** are **new** unknown functions

Three-body unitarity

$$\langle q_1, q_2, q_3 | (\hat{T} - \hat{T}^\dagger) | p_1, p_2, p_3 \rangle = i \int_P \langle q_1, q_2, q_3 | \hat{T}^\dagger | k_1, k_2, k_3 \rangle \langle k_1, k_2, k_3 | \hat{T} | p_1, p_2, p_3 \rangle$$



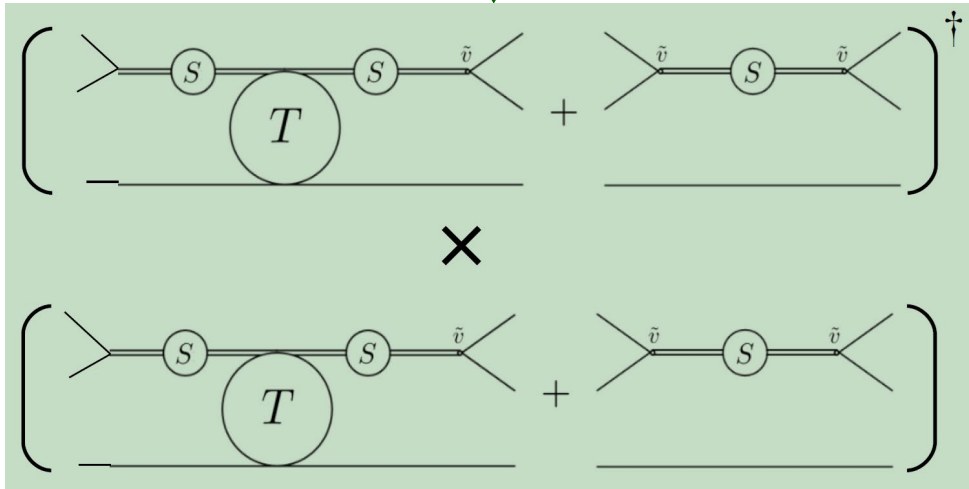
Bethe-Salpeter equation



$$\begin{aligned} \hat{T} - \hat{T}^\dagger &= v(S - S^\dagger)v + vST Sv - vS^\dagger T^\dagger S^\dagger v \\ &= v(S - S^\dagger)v + (vS - vS^\dagger)TSv + vS^\dagger T^\dagger (Sv - S^\dagger v) + vS^\dagger (T - T^\dagger)Sv \end{aligned}$$

Three-body unitarity

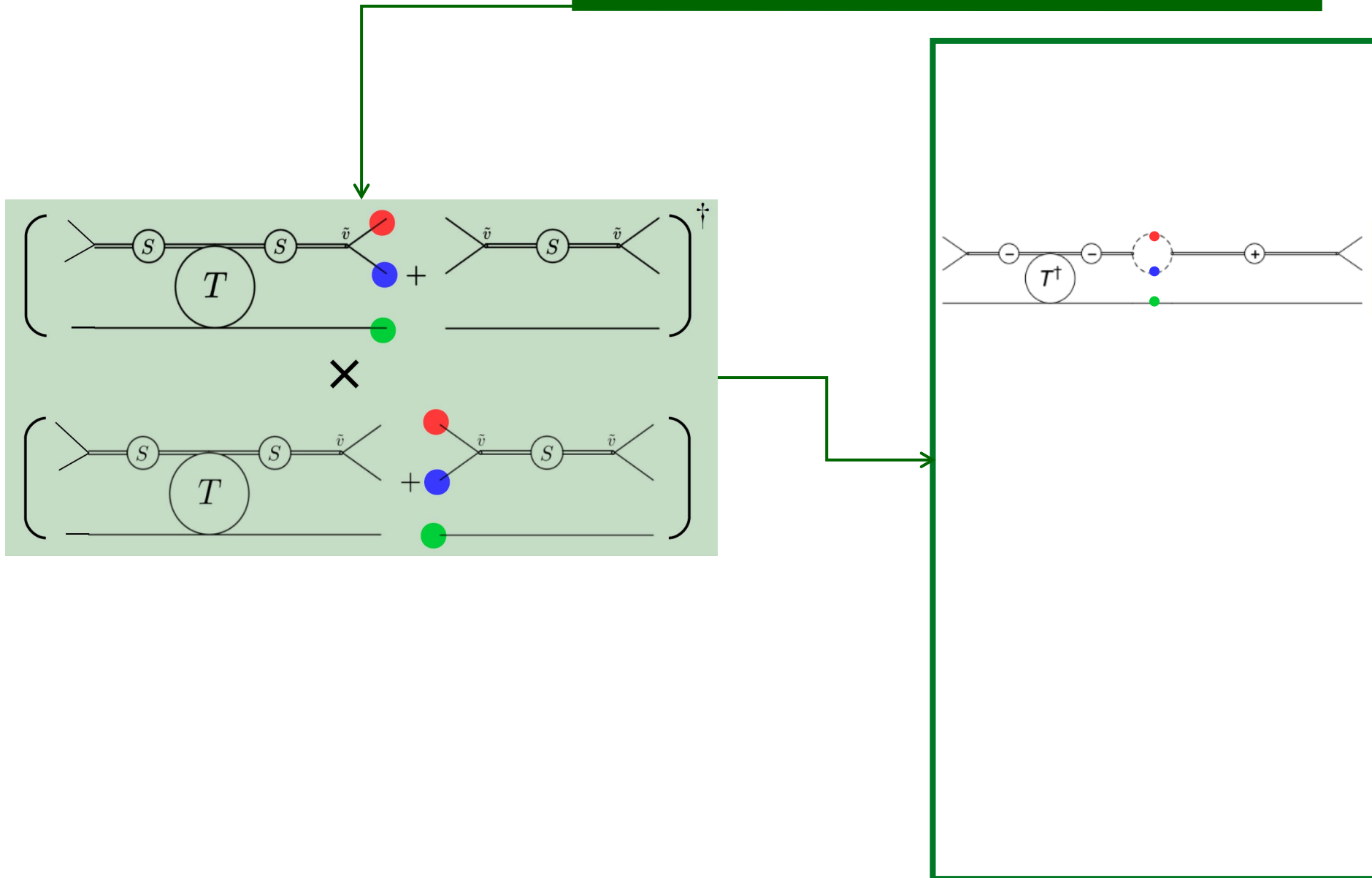
$$\langle q_1, q_2, q_3 | (\hat{T} - \hat{T}^\dagger) | p_1, p_2, p_3 \rangle = i \int_P \langle q_1, q_2, q_3 | \hat{T}^\dagger | k_1, k_2, k_3 \rangle \langle k_1, k_2, k_3 | \hat{T} | p_1, p_2, p_3 \rangle$$



General connected-disconnected structure

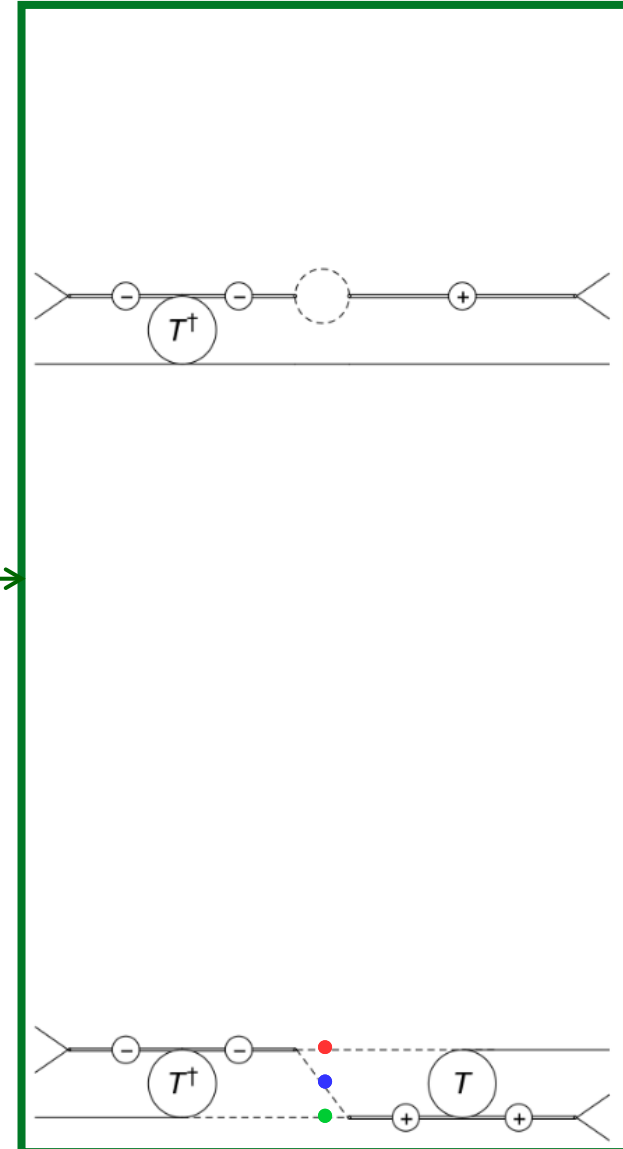
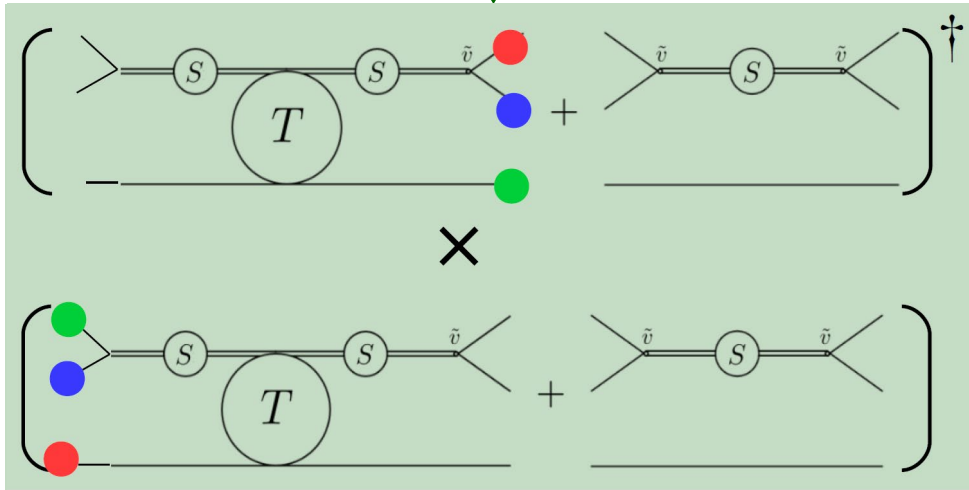
Three-body unitarity

$$\langle q_1, q_2, q_3 | (\hat{T} - \hat{T}^\dagger) | p_1, p_2, p_3 \rangle = i \int_P \langle q_1, q_2, q_3 | \hat{T}^\dagger | k_1, k_2, k_3 \rangle \langle k_1, k_2, k_3 | \hat{T} | p_1, p_2, p_3 \rangle$$



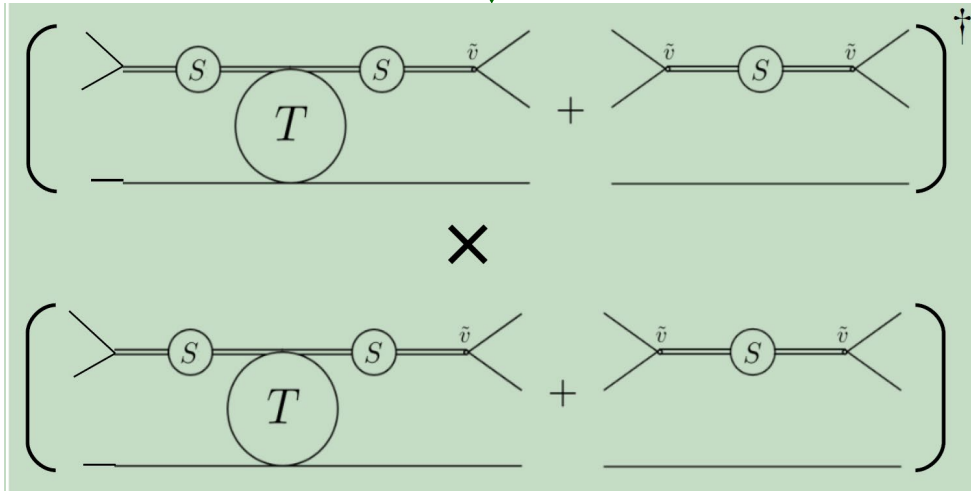
Three-body unitarity

$$\langle q_1, q_2, q_3 | (\hat{T} - \hat{T}^\dagger) | p_1, p_2, p_3 \rangle = i \int_P \langle q_1, q_2, q_3 | \hat{T}^\dagger | k_1, k_2, k_3 \rangle \langle k_1, k_2, k_3 | \hat{T} | p_1, p_2, p_3 \rangle$$

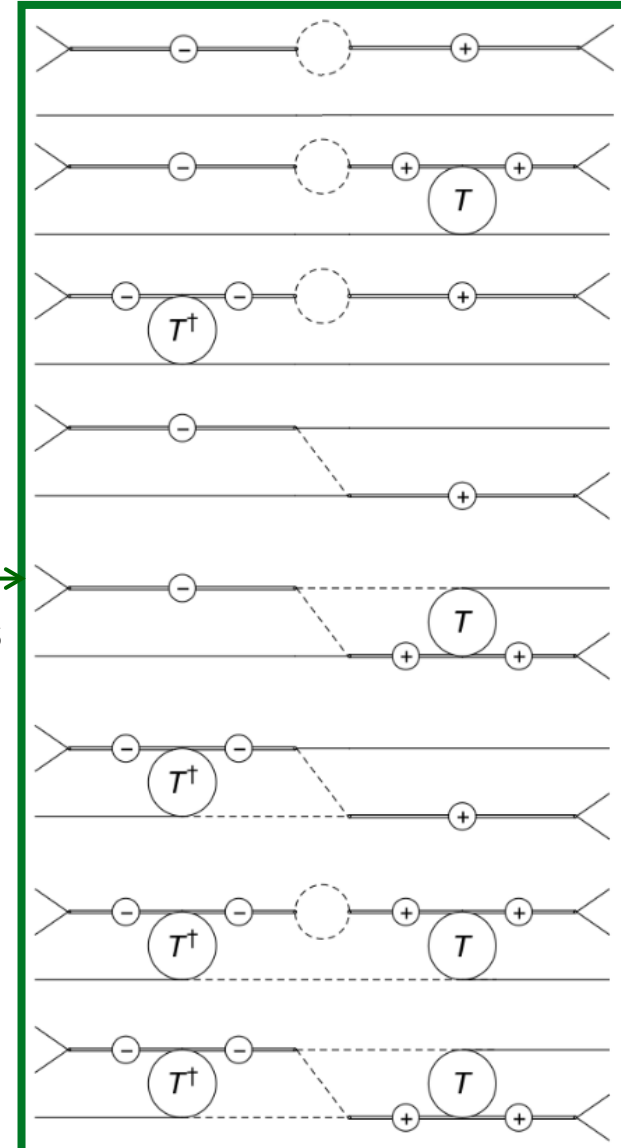


Three-body unitarity

$$\langle q_1, q_2, q_3 | (\hat{T} - \hat{T}^\dagger) | p_1, p_2, p_3 \rangle = i \int_P \langle q_1, q_2, q_3 | \hat{T}^\dagger | k_1, k_2, k_3 \rangle \langle k_1, k_2, k_3 | \hat{T} | p_1, p_2, p_3 \rangle$$

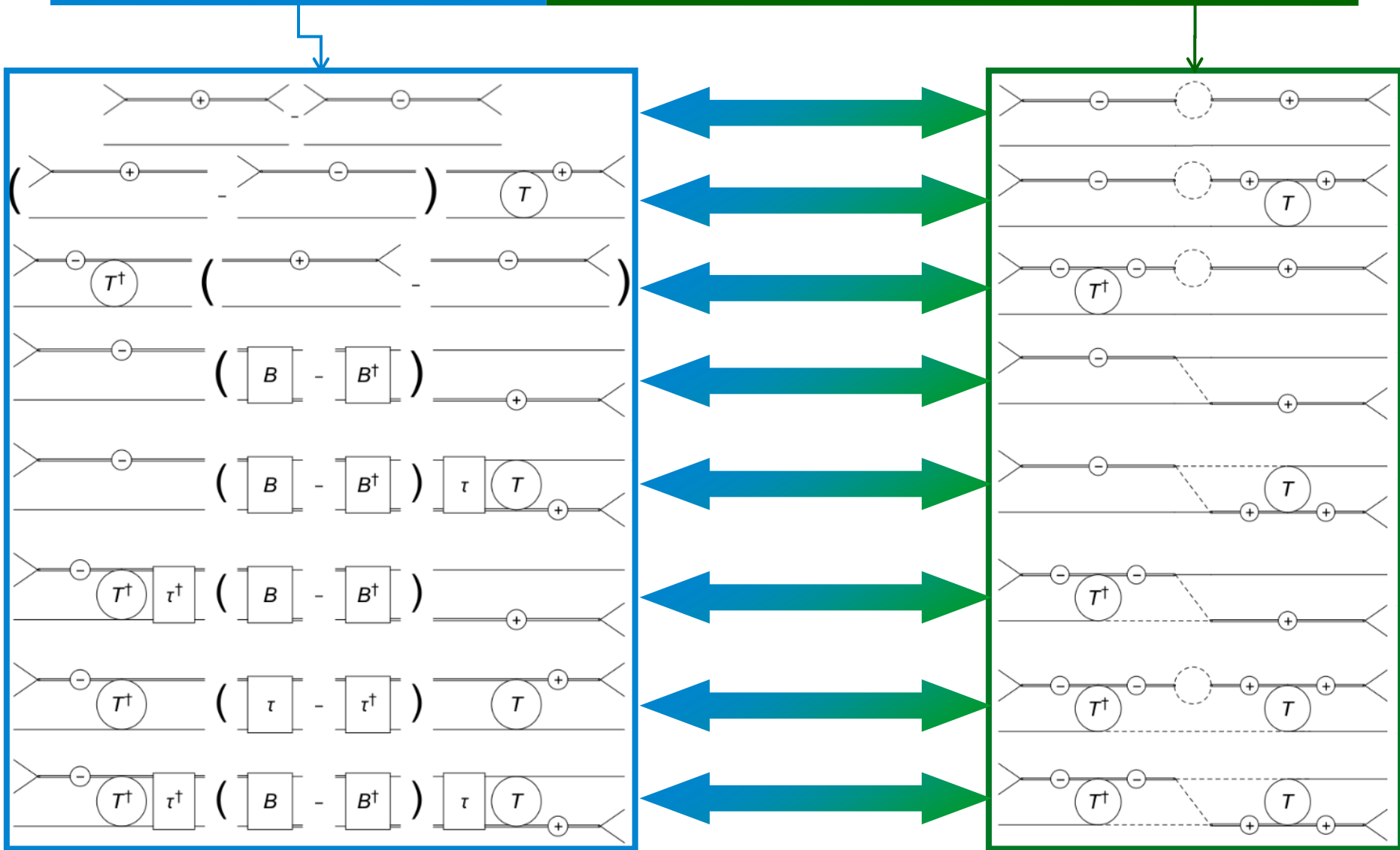


8 topologies



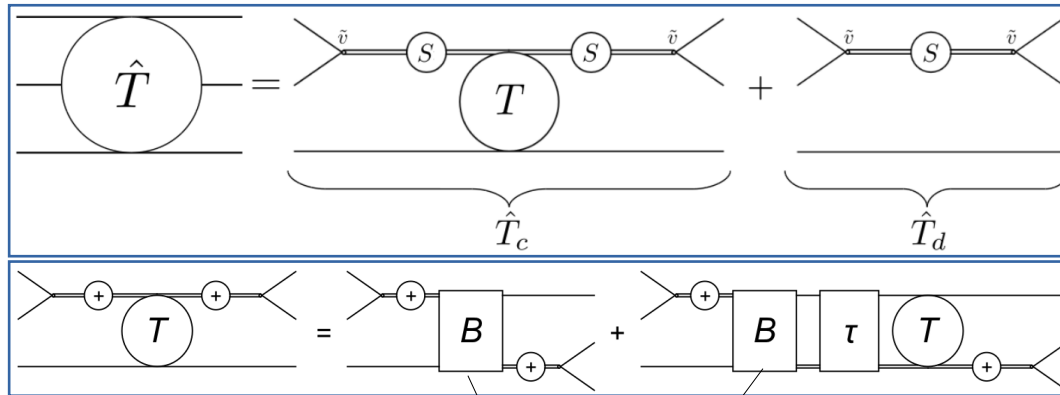
Three-body unitarity

$$\langle q_1, q_2, q_3 | (\hat{T} - \hat{T}^\dagger) | p_1, p_2, p_3 \rangle = i \int_P \langle q_1, q_2, q_3 | \hat{T}^\dagger | k_1, k_2, k_3 \rangle \langle k_1, k_2, k_3 | \hat{T} | p_1, p_2, p_3 \rangle$$



Scattering amplitude (1)

3 → 3 scattering amplitude is a 3-dimensional integral equation



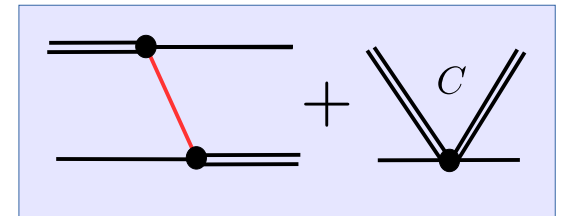
Imaginary parts of **B, S** are fixed by **unitarity/matching**

$$\text{Disc } B(u) = 2\pi i \lambda^2 \frac{\delta(E_Q - \sqrt{m^2 + Q^2})}{2\sqrt{m^2 + Q^2}}$$

- un-subtracted dispersion relation

$$\langle q|B(s)|p\rangle = -\frac{\lambda^2}{2\sqrt{m^2 + Q^2} (E_Q - \sqrt{m^2 + Q^2} + i\epsilon)} + C$$

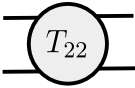
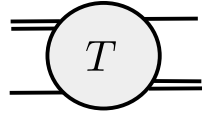
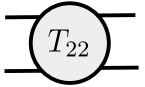
- one- π exchange in TOPT → **RESULT, NOT INPUT!**
- One can map to field theory but does not have to. Result is a-priori dispersive.



Scattering amplitude (2)

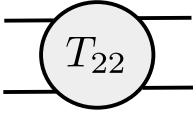
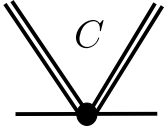
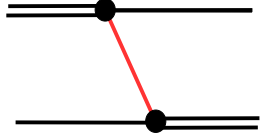
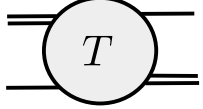
Here: Version in which isobar rewritten in on-shell $2 \rightarrow 2$ scattering amplitude T_{22}

$$\langle q_1, q_2, q_3 | \hat{T}_c(s) | p_1, p_2, p_3 \rangle = \frac{1}{3!} \sum_{n=1}^3 \sum_{m=1}^3 T_{22}(\sigma(q_n)) \langle q_n | T(s) | p_m \rangle T_{22}(\sigma(p_m))$$

$$\langle q | T(s) | p \rangle = \langle q | C(s) | p \rangle + \frac{1}{m^2 - (P - p - q)^2 - i\epsilon}$$

$$- \int \frac{d^3 \ell}{(2\pi)^3} \frac{1}{2E_\ell} T_{22}(\sigma(\ell)) \left(\langle p | C(s) | \ell \rangle + \frac{1}{m^2 - (P - p - \ell)^2 - i\epsilon} \right) \langle \ell | T(s) | p \rangle$$

(S-wave)

3.2 Analytic cont. 3B (1)

SMC

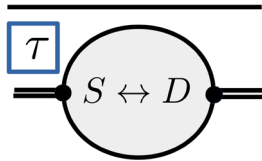
$$T_{LL'}^J(q_1, p) = (B_{LL'}^J(q_1, p) + C_{LL'}^J(q_1, p)) + \int_0^\Lambda \frac{dl l^2}{(2\pi)^3 2E_l} (B_{LL''}^J(q_1, l) + C_{LL''}^J(q_1, l)) \tau(\sigma(l)) T_{L''L'}^J(l, p)$$

$$\tau^{-1}(\sigma) = K^{-1} - \Sigma,$$

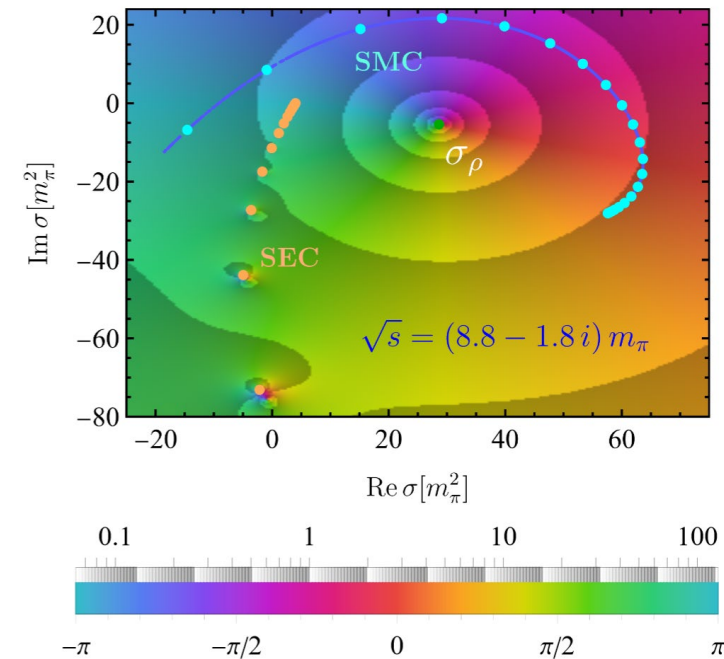
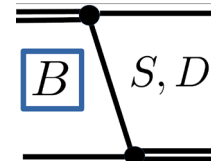
$$\Sigma = \int_0^\infty \frac{dk k^2}{(2\pi)^3} \frac{1}{2E_k} \frac{\sigma^2}{\sigma'^2} \frac{\tilde{v}(k)^* \tilde{v}(k)}{\sigma - 4E_k^2 + i\epsilon}$$

$$B_{\lambda\lambda'}(p, p') = \frac{v_\lambda^*(P - p - p', p) v_{\lambda'}(P - p - p', p')}{2E_{p'+p}(\sqrt{s} - E_p - E_{p'} - E_{p'+p} + i\epsilon)}$$

SEC



Singularities

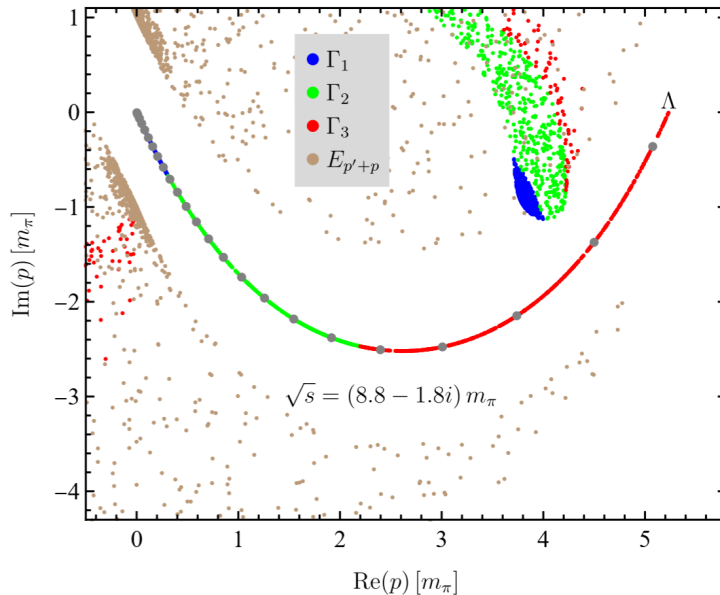
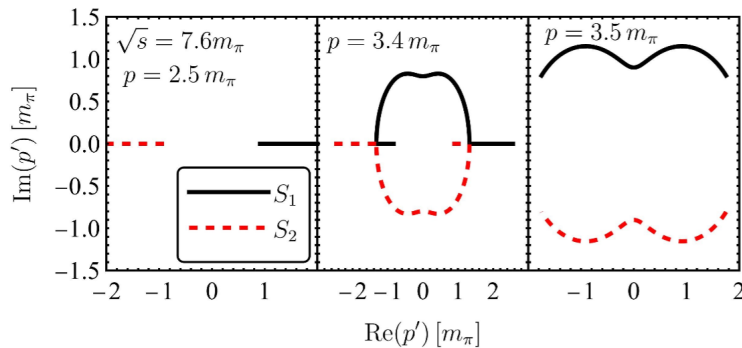


- Two contours (SMC and SEC)
- Deform both “adiabatically” to go to complex s
- Set of rules:
 - Contours cannot intersect with each others
 - Contours cannot intersect with (3-body) cuts
- Passing singularities left or right determines sheet

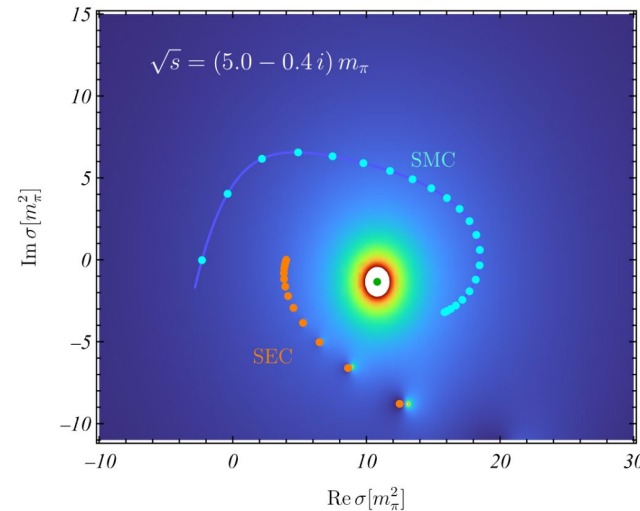
Analytic continuation 3B (2)

- Three-body cuts

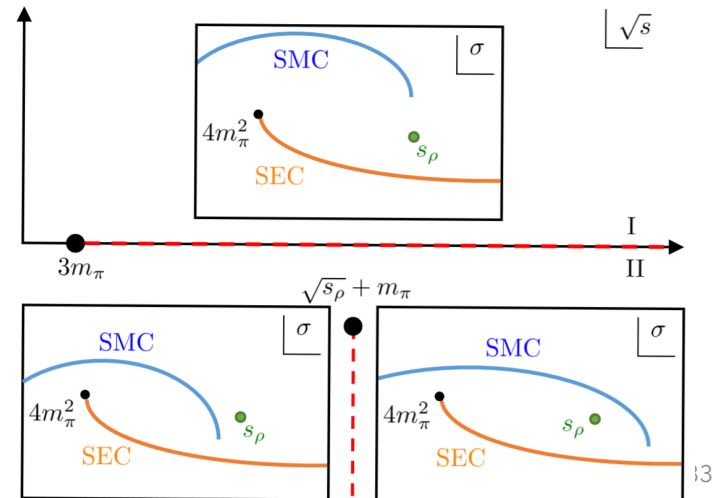
$$\sqrt{s} - E_p - E_{p'} - E_{p+p'} + i\epsilon = 0$$



- Complex branch points

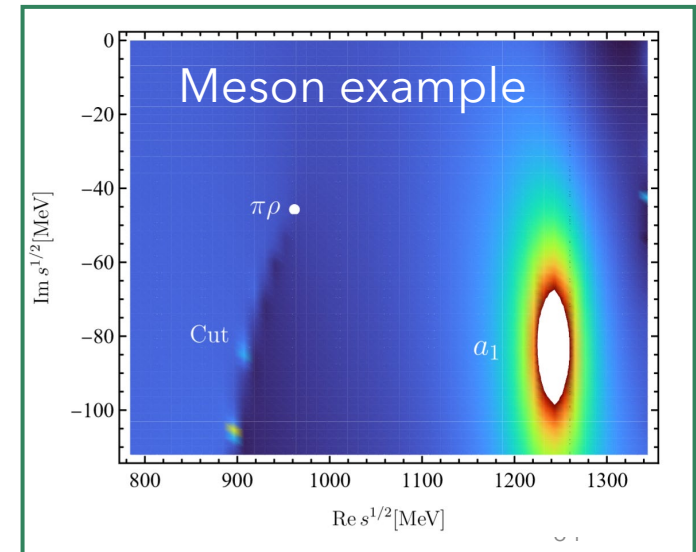
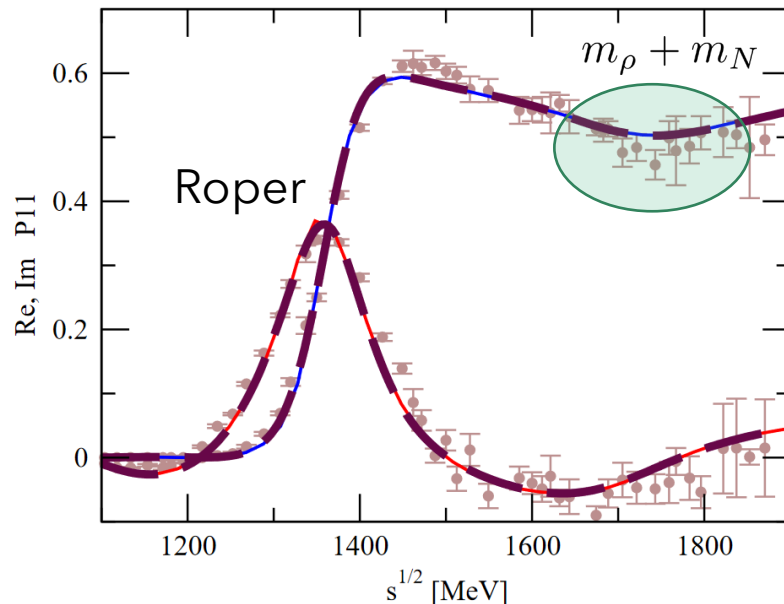
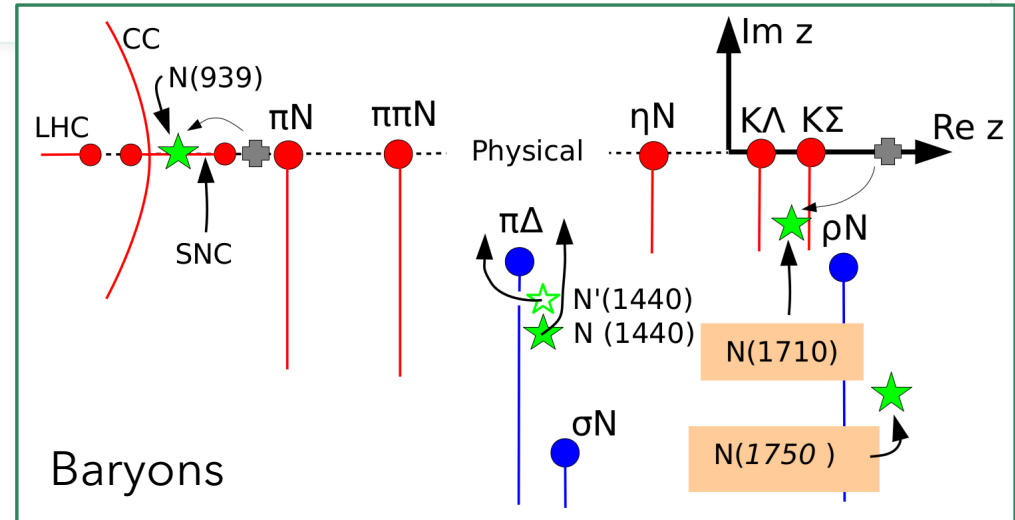


Integration limits at poles induce branch points



Analytic continuation 3B (3)

- Real and complex branch points ✓
- Poles appear doubled due to new Riemann sheets due to (complex) thresholds ✓
- Circular cut (CC) and short (nucleon) cut (SNC) exist only in partial waves
- Complex branch points can mimic resonances (ρN) [Ceci]



Summary

- Resonances are not necessarily bumps in cross sections
- Bumps in cross sections are not necessarily resonances
 - Threshold cusps; complex branch points; triangle singularities, statistical fluctuations
- Some quark models and some recent IQCD calculations predict more resonances than found in experiment
 - Large-scale experimental effort at JLab, Elsa, Mami,... together with pheno-analyses found convincing signals of many new states
 - Future: Ongoing efforts; new experiments (BGO-OD); electromagnetic properties through electroproduction reactions (Jlab 12-GeV upgrade)
- From a phenomenological point of view, the challenge in baryon spectroscopy is rather data consistency and systematic error than amplitude parametrization → New statistical methods needed

Spare slides

Physics opportunities with meson beams

Physics opportunities with meson beams

[\[Paper link\]](#)

William J. Briscoe, Michael Döring, Helmut Haberzettl, D. Mark Manley,
Megumi Naruki, Igor I. Strakovsky and Eric S. Swanson

Eur. Phys. J. A (2015) **51**: 129

DOI 10.1140/epja/i2015-15129-5

Physics Opportunities with Meson Beams for EIC

[\[follow-up\]](#) (2021)

Strange Hadron Spectroscopy with Secondary KL Beam in Hall D

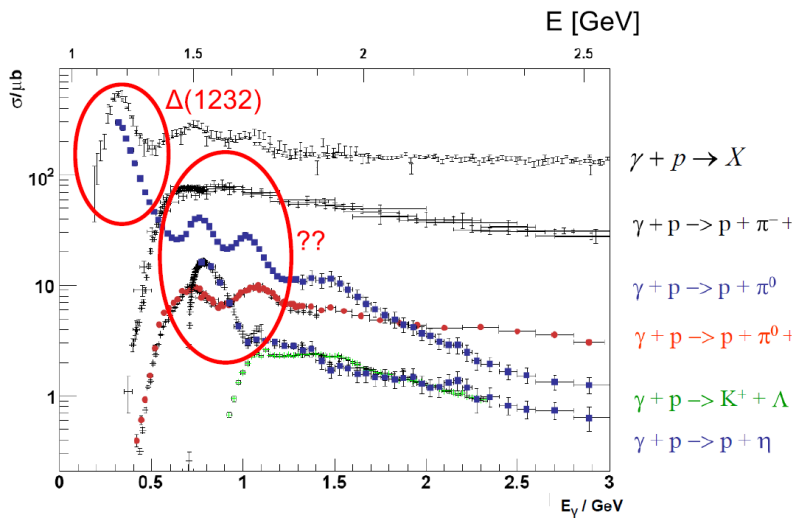
KLF Collaboration • [Moskov Amaryan \(Old Dominion U.\)](#) [Show All\(152\)](#)

Aug 18, 2020

[\[Preprint link\]](#)

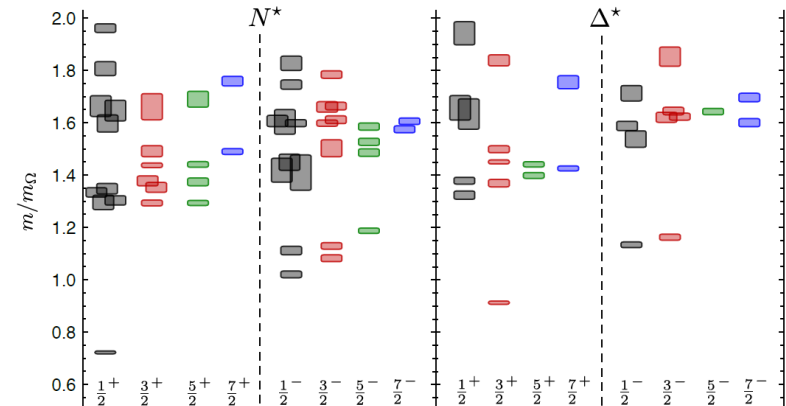
Baryons in photoproduction

Experimental study of hadronic reactions



source: ELSA; data: ELSA, JLab, MAMI

Theoretical predictions of excited hadrons
e.g. from lattice calculations:
(with some limitations)



$m_\pi = 396$ MeV [Edwards et al., Phys.Rev. D84 (2011)]

$$\gamma^{(*)} N \rightarrow \begin{cases} \pi N \\ \eta N, K\Lambda, K\Sigma, \omega N, \phi N, \dots \\ \pi\pi N, \pi\eta N, \dots \end{cases}$$

SAID Data Base @ GW:

<https://gwdac.phys.gwu.edu/>

New:

<https://jbw.phys.gwu.edu/>

PDG Changes

- Changes from one PDG edition to another
- New states in red
- Upgrade existing states
- Removal older & lower rated states
- All changes come from Partial-wave analysis (PWA) of photon-induced reactions.

Table from [\[Crede\]](#)

Table 9. (Colour online) Baryon Summary Table for N^* and Δ resonances including recent changes from PDG 2010 [\[2\]](#) to PDG 2012 [\[3\]](#).

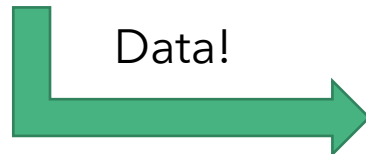
N^*	$J^P (L_{2I,2J})$	2010	2012	Δ	$J^P (L_{2I,2J})$	2010	2012
p	$1/2^+ (P_{11})$	****	****	$\Delta(1232)$	$3/2^+ (P_{33})$	****	****
n	$1/2^+ (P_{11})$	****	****	$\Delta(1600)$	$3/2^+ (P_{33})$	***	***
$N(1440)$	$1/2^+ (P_{11})$	****	****	$\Delta(1620)$	$1/2^- (S_{31})$	****	****
$N(1520)$	$3/2^- (D_{13})$	****	****	$\Delta(1700)$	$3/2^- (D_{33})$	****	****
$N(1535)$	$1/2^- (S_{11})$	****	****	$\Delta(1750)$	$1/2^+ (P_{31})$	*	*
$N(1650)$	$1/2^- (S_{11})$	****	****	$\Delta(1900)$	$1/2^- (S_{31})$	**	**
$N(1675)$	$5/2^- (D_{15})$	****	****	$\Delta(1905)$	$5/2^+ (F_{35})$	****	****
$N(1680)$	$5/2^+ (F_{15})$	****	****	$\Delta(1910)$	$1/2^+ (P_{31})$	****	****
$N(1685)$			*				
$N(1700)$	$3/2^- (D_{13})$	***	***	$\Delta(1920)$	$3/2^+ (P_{33})$	***	***
$N(1710)$	$1/2^+ (P_{11})$	***	***	$\Delta(1930)$	$5/2^- (D_{35})$	***	***
$N(1720)$	$3/2^+ (P_{13})$	****	****	$\Delta(1940)$	$3/2^- (D_{33})$	*	**
$N(1860)$	$5/2^+$		**				
$N(1875)$	$3/2^-$		***				
$N(1880)$	$1/2^+$		**				
$N(1895)$	$1/2^-$		**				
$N(1900)$	$3/2^+ (P_{13})$	**	***	$\Delta(1950)$	$7/2^+ (F_{37})$	****	****
$N(1990)$	$7/2^+ (F_{17})$	**	**	$\Delta(2000)$	$5/2^+ (F_{35})$	**	**
$N(2000)$	$5/2^+ (F_{15})$	**	**	$\Delta(2150)$	$1/2^- (S_{31})$	*	*
$N(2080)$	D_{13}	**		$\Delta(2200)$	$7/2^- (G_{37})$	*	*
$N(2090)$	S_{11}	*		$\Delta(2300)$	$9/2^+ (H_{39})$	**	**
$N(2040)$	$3/2^+$		*				
$N(2060)$	$5/2^-$		**				
$N(2100)$	$1/2^+ (P_{11})$	*	*	$\Delta(2350)$	$5/2^- (D_{35})$	*	*
$N(2120)$	$3/2^-$		**				
$N(2190)$	$7/2^- (G_{17})$	****	****	$\Delta(2390)$	$7/2^+ (F_{37})$	*	*
$N(2200)$	D_{15}	**		$\Delta(2400)$	$9/2^- (G_{39})$	**	**
$N(2220)$	$9/2^+ (H_{19})$	****	****	$\Delta(2420)$	$11/2^+ (H_{3,11})$	****	****
$N(2250)$	$9/2^- (G_{19})$	****	****	$\Delta(2750)$	$13/2^- (I_{3,13})$	**	**
$N(2600)$	$11/2^- (I_{1,11})$	***	***	$\Delta(2950)$	$15/2^+ (K_{3,15})$	**	**
$N(2700)$	$13/2^+ (K_{1,13})$	**	**				

The role of meson beams in baryon spectroscopy

(Non-strange, light baryon sector)

- Pion-induced reactions

$$\pi N \rightarrow \begin{cases} \pi N \\ \eta N, K\Lambda, K\Sigma \\ \pi\pi N, \pi\eta N, \dots \end{cases}$$



- **Two** complex amplitudes (g,h)

- Photon-induced reactions

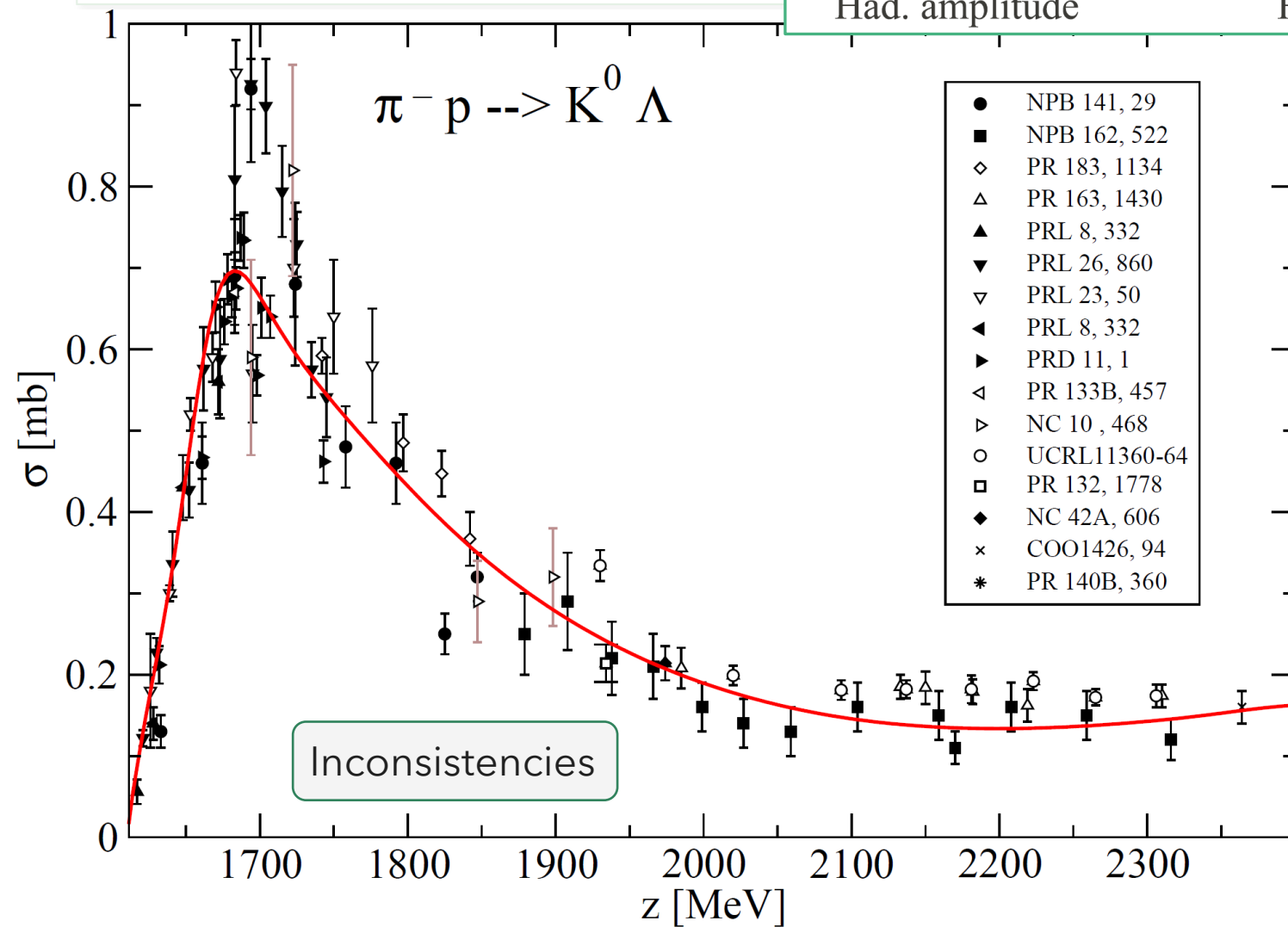
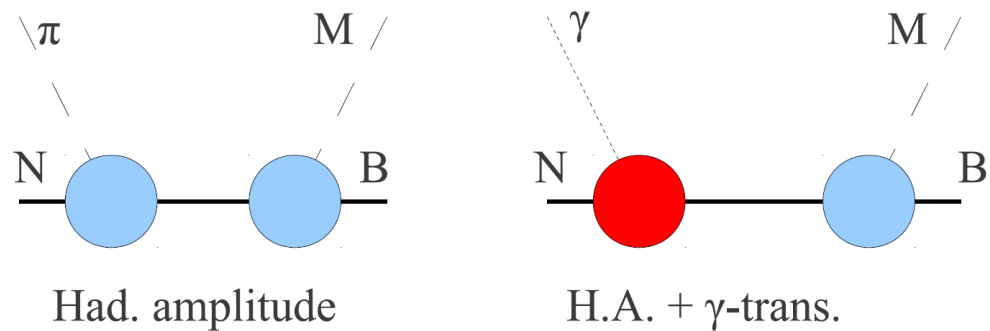
$$\gamma^{(*)} N \rightarrow \begin{cases} \pi N \\ \eta N, K\Lambda, K\Sigma \\ \pi\pi N, \pi\eta N, \dots \end{cases}$$

$$\begin{cases} \pi N \\ \eta N, K\Lambda, K\Sigma \\ \pi\pi N, \pi\eta N, \dots \end{cases} \leftrightarrow \begin{cases} \pi N \\ \eta N, K\Lambda, K\Sigma \\ \pi\pi N, \pi\eta N, \dots \end{cases}$$

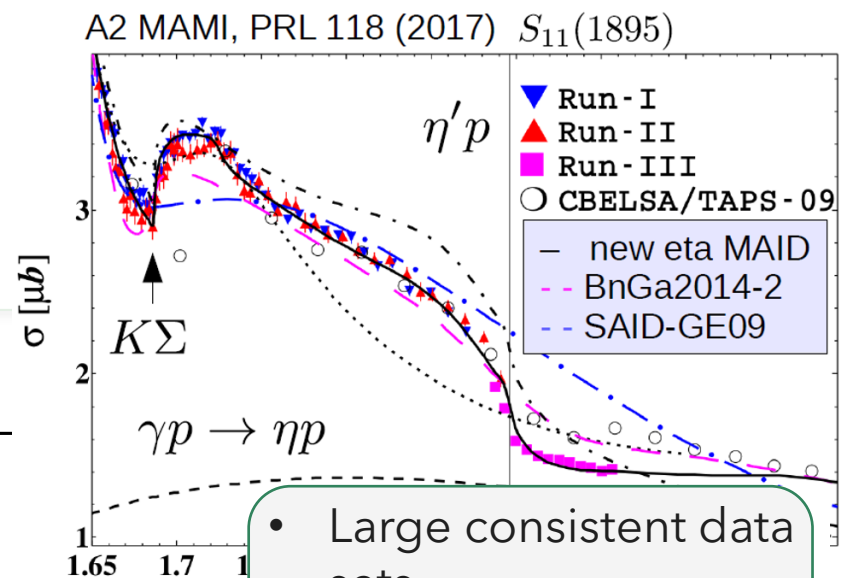
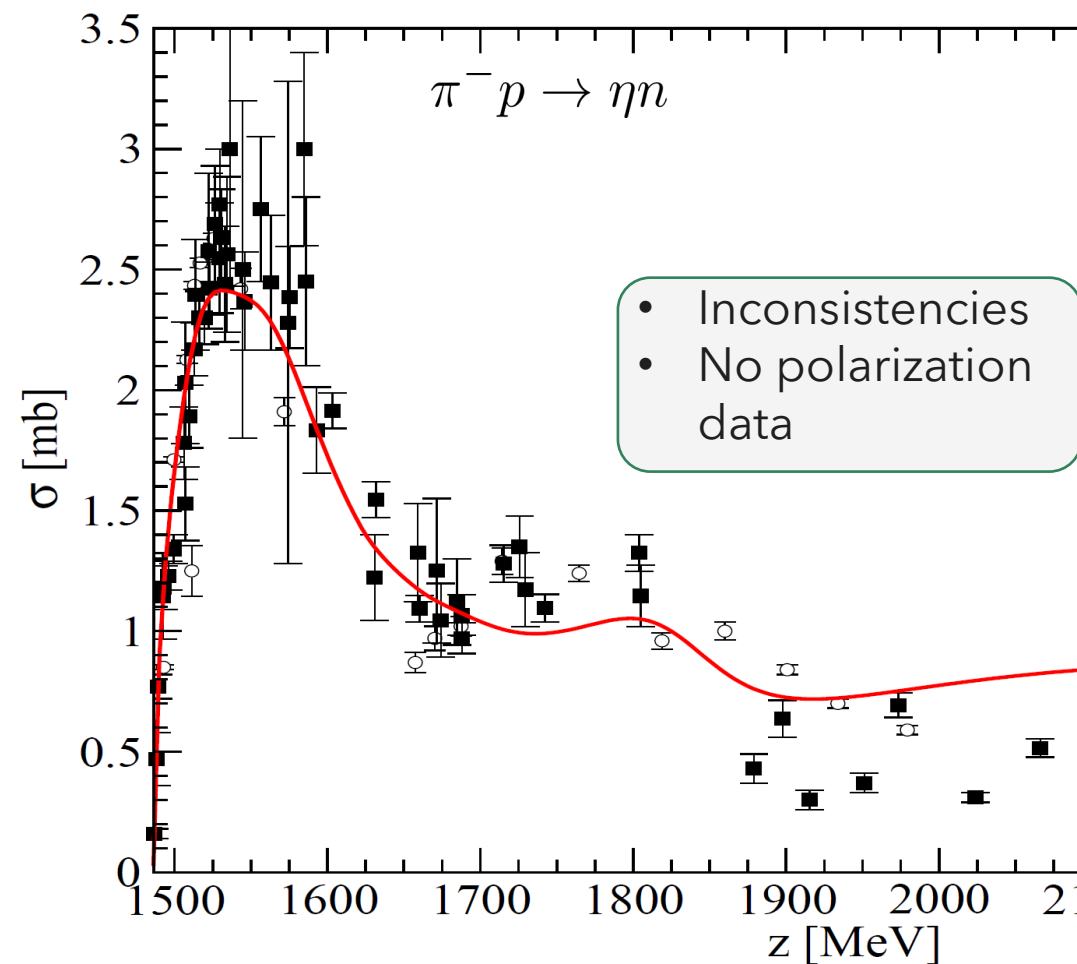
- **Final-state interaction** as sub-process
- **Four** (photo) or **six** (electro) complex amplitudes (CGNL, ...)

Photon-induced reactions have more d.o.f. and their analysis depends on meson-induced reaction data (except complete experiment).

Data



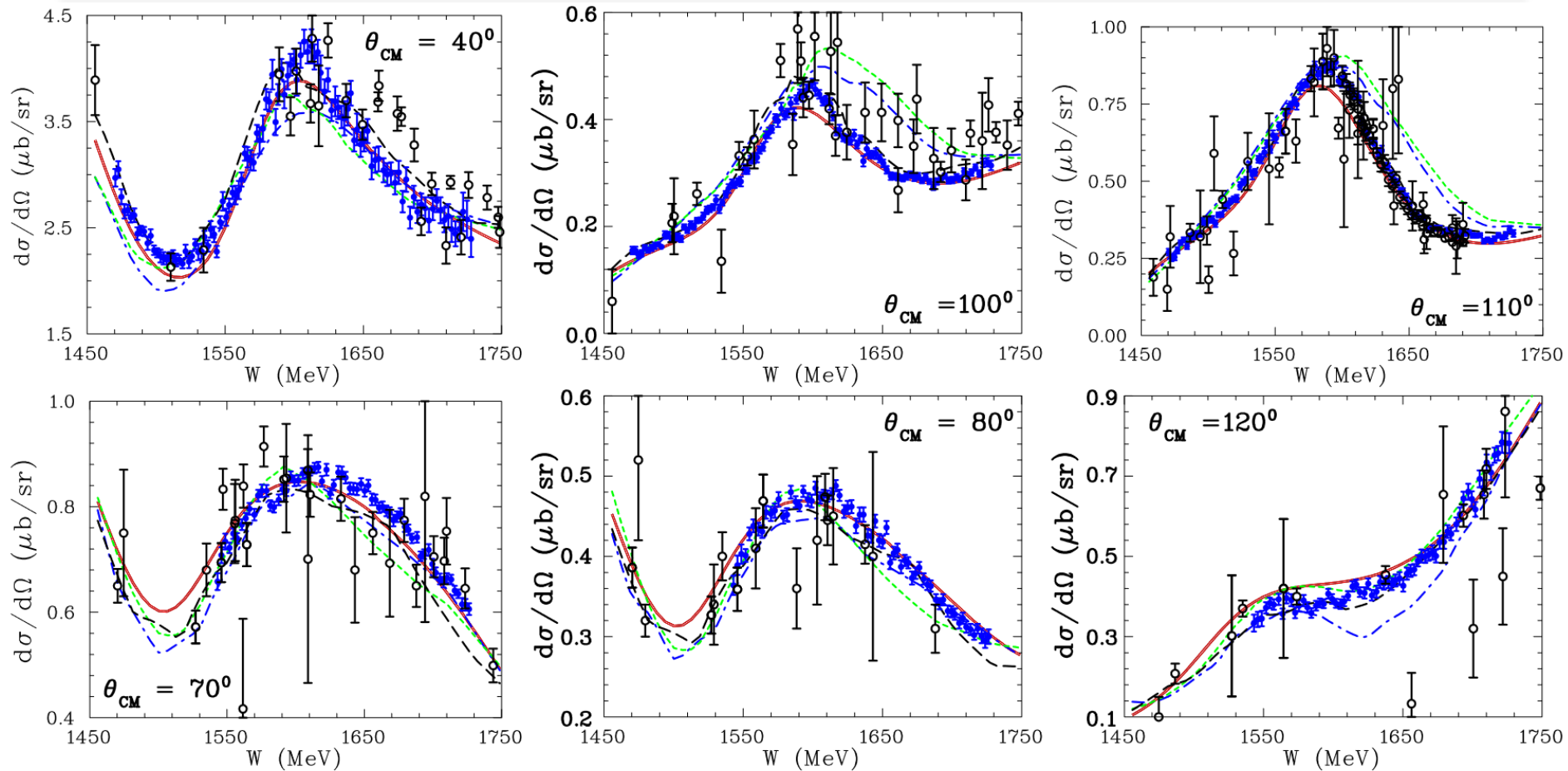
Data: η production



- Large consistent data sets
- Many different polarization data

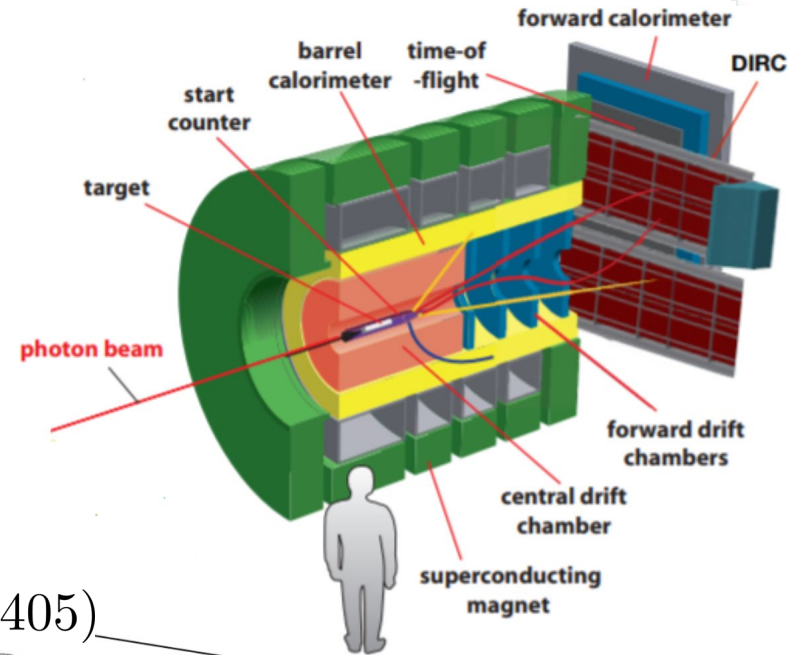
Example of recent improvements

Goal: Reduction of systematic uncertainties/ large body of consistent data



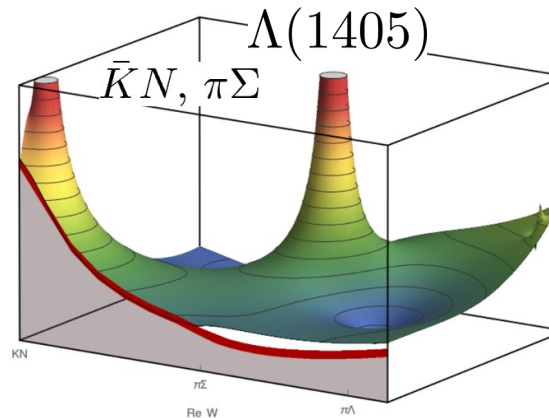
EPECUR experiment [[Alekseev 2015](#)] (**blue**) compared to previous measurements (**black**)

K-Long Facility



- Hyperon spectroscopy: Increased activity and analyses by

- Kent state group,
- JPAC,
- Bonn-Gatchina,
- ANL-Osaka,...

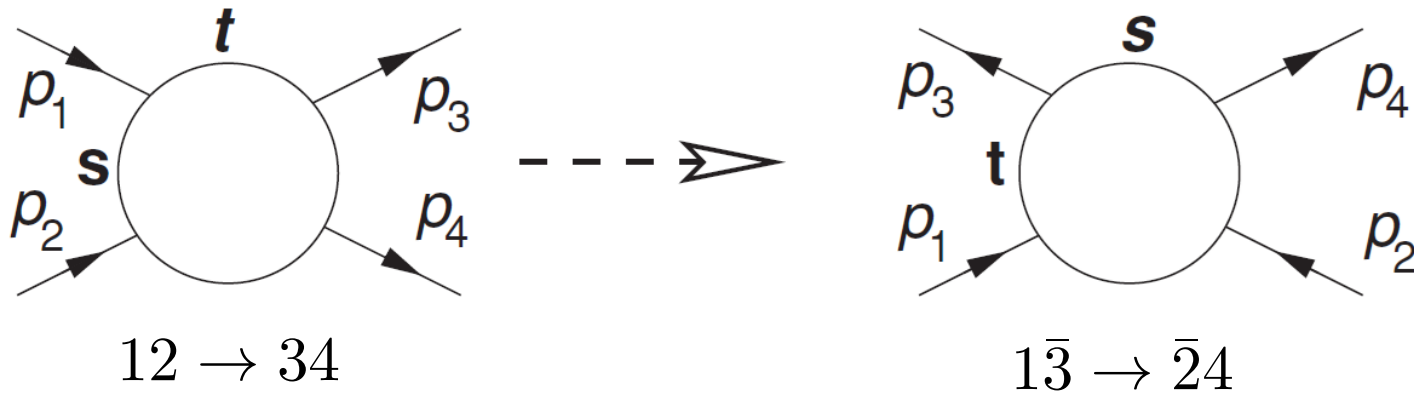


From: [Mai]

- Strange meson spectroscopy
 - Broader physics scope [Proposal]
- To accomplish physics program, 200 days running is approved

Crossing Symmetry

- Consider another process by turning the scattering around:

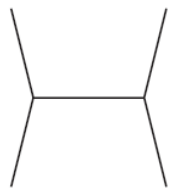


- negative 0-components appear: $p_{30} \leq -m_3$ and $p_{20} \leq -m_2$
- interpretation of crossed process: anti-particle with $\bar{p}_3 = -p_3$
- Crossed diagram describes another process; so called t -channel reaction:

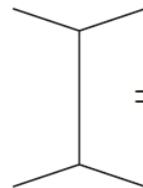
$$t = (p_1 - p_3)^2 = (p_1 + \bar{p}_3)^2 \geq (m_1 + m_3)^2$$

Crossed processes in λ^3

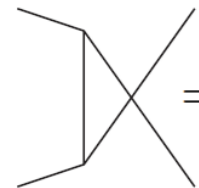
- s, t, and u-channel processes in λ^3 theory:


$$= \frac{\lambda^2}{m^2 - s},$$

The diagram shows a horizontal internal line with two external lines on each end, representing an s-channel process.


$$= \frac{\lambda^2}{m^2 - t},$$

The diagram shows a vertical internal line with two external lines on each end, representing a t-channel process.


$$= \frac{\lambda^2}{m^2 - u}$$

The diagram shows a crossed internal line with two external lines on each end, representing a u-channel process.

***u*-channel reactions**

- Analogously, if $p_{40} \leq -m_4$, $p_{20} \leq -m_2$: $1 + \bar{4} \rightarrow 3 + \bar{2}$

$$u = (p_1 - p_4)^2 = (p_1 + \bar{p}_4)^2 \geq (m_1 + m_4)^2$$

- In summary:

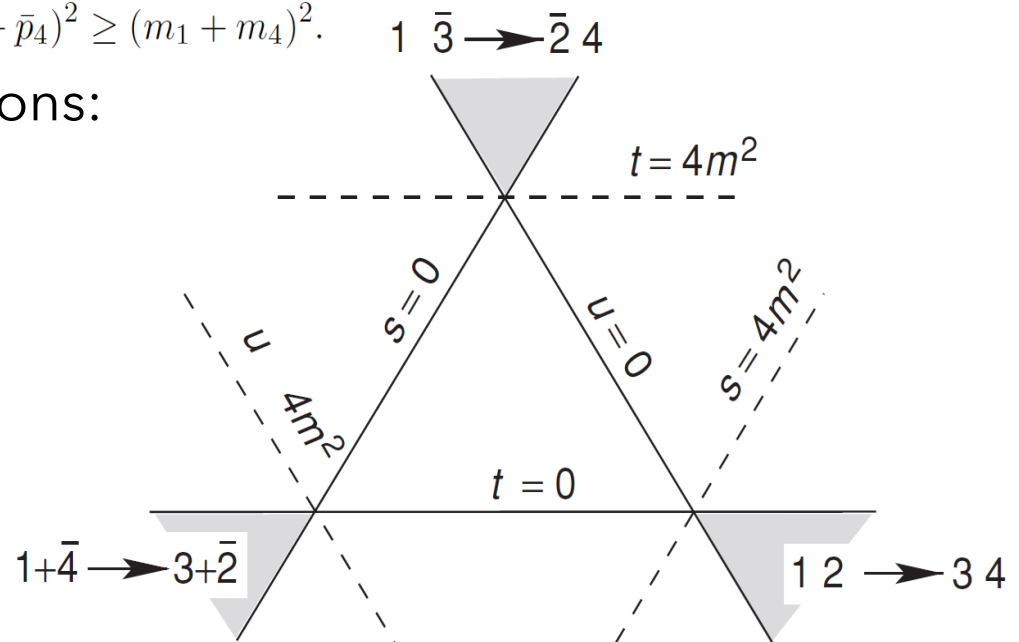
$$s\text{-channel : } 1 + 2 \rightarrow 3 + 4, \quad s = (p_1 + p_2)^2 \geq (m_1 + m_2)^2;$$

$$t\text{-channel : } 1 + \bar{3} \rightarrow \bar{2} + 4, \quad t = (p_1 + \bar{p}_3)^2 \geq (m_1 + m_3)^2;$$

$$u\text{-channel : } 1 + \bar{4} \rightarrow 3 + \bar{2}, \quad u = (p_1 + \bar{p}_4)^2 \geq (m_1 + m_4)^2.$$

- There are 3 unitarity relations:

- s-channel unitarity
- t-channel unitarity
- u-channel unitarity



Analytic structure in the Mandelstam plane

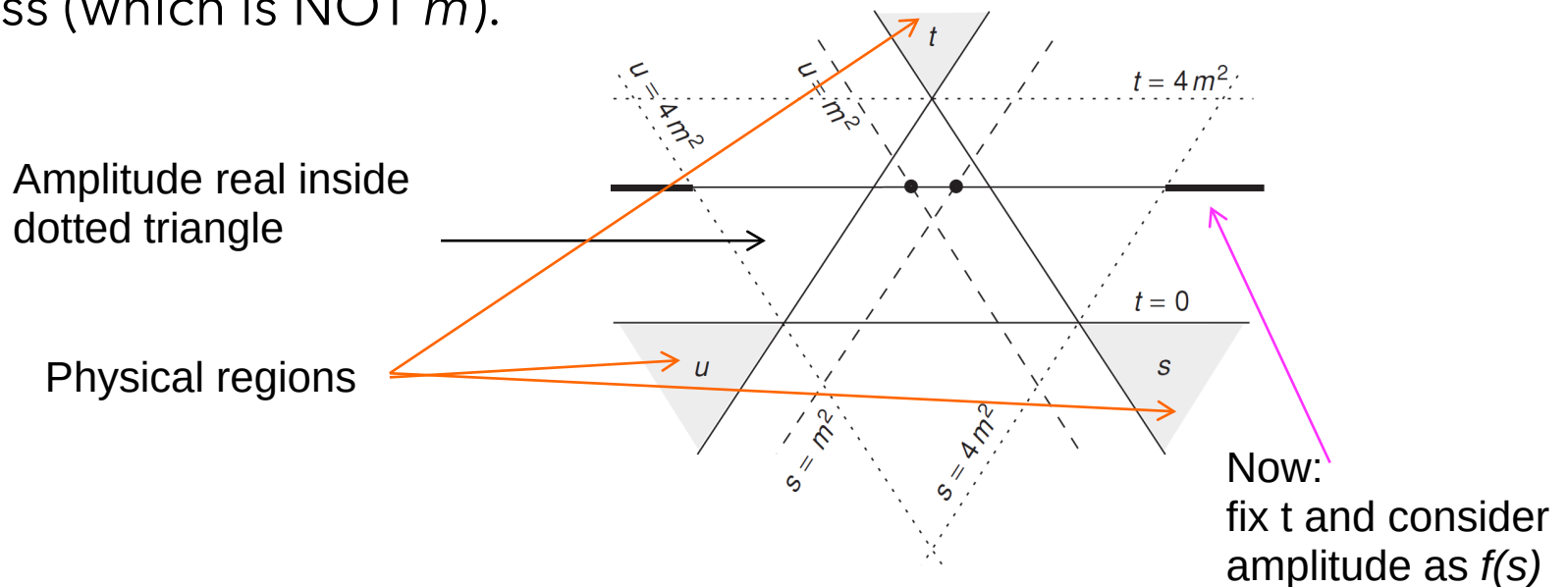
- Again, s-, t-, and u-channel processes:

$$\text{Diagram 1} = \frac{\lambda^2}{m^2 - s},$$

$$\text{Diagram 2} = \frac{\lambda^2}{m^2 - t},$$

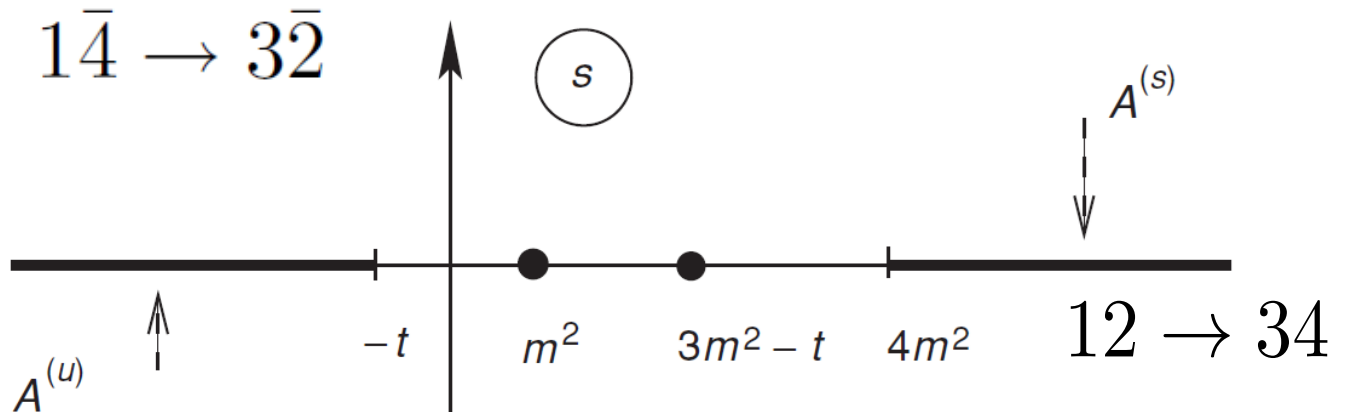
$$\text{Diagram 3} = \frac{\lambda^2}{m^2 - u}$$

- Induce poles in the amplitude, at position of physical particle mass (which is NOT m).



Left- and right-hand cut

- The only non-analyticities on the first Riemann sheet:



Dispersive representation of the amplitude

[Gribov]

• Cauchy's Theorem:

$$\int_C \frac{dz}{2\pi i} \frac{A(z)}{z-s} = A(s)$$

$\lambda^2/(m^2 - t)$ does not fall with $s \rightarrow$ once-subtracted dispersion relation:

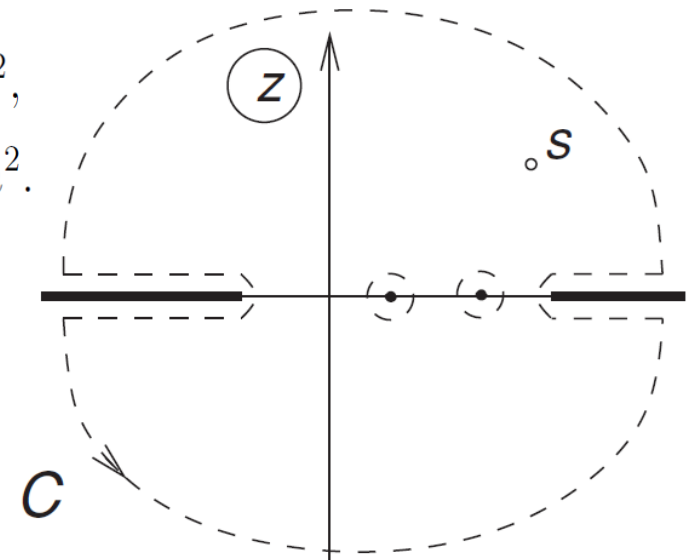
$$A(s) - A(0) = \int_C \frac{dz}{2\pi i} \left[\frac{A(z)}{z-s} - \frac{A(z)}{z} \right] = \frac{s}{\pi} \int_C \frac{dz}{2i} \frac{A(z)}{z(z-s)}$$

$$\text{Im}_s A \equiv \frac{1}{2i} [A(s+i0, t) - A(s-i0, t)], \quad s > 4m^2,$$

$$\text{Im}_u A \equiv \frac{1}{2i} [A(u+i0, t) - A(u-i0, t)], \quad u > 4m^2.$$

\rightarrow Simplify the expression!

Similar: Derive the real part of two-particle propagator G from its imaginary part (much simpler: no poles, no left-hand cut)



Example: Pion-nucleon scattering [Gribov]

forward scattering $t=0$:

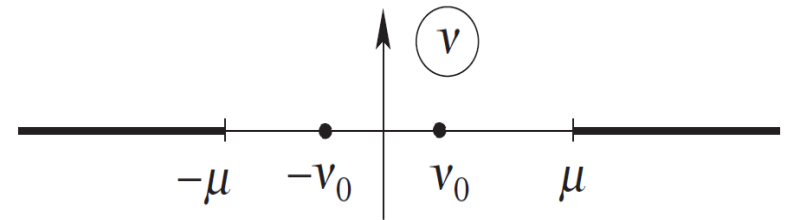
$$s = (p + k)^2 = M^2 + \mu^2 + 2M\nu,$$

$$u = (p - k')^2 = M^2 + \mu^2 - 2M\nu = 2(M^2 + \mu^2) - s$$

ν Energy of the pion in nucleon rest frame

$$\nu = \frac{s - u}{2M} = \frac{s - (M^2 + \mu^2)}{M}$$

$$f(\nu) = \frac{r}{\nu_0 - \nu} + \frac{1}{\pi} \int_{\mu}^{\infty} \frac{d\nu' \operatorname{Im} f(\nu')}{\nu' - \nu} \\ + \frac{r}{\nu_0 + \nu} + \frac{1}{\pi} \int_{-\mu}^{-\infty} \frac{d\nu' \operatorname{Im} f(\nu')}{\nu' - \nu}$$



$$A = \bar{\mathbf{U}}(p') \phi_{\alpha}(k') (f_{+}(\nu) \delta_{\alpha\beta} \cdot \mathbf{I} + f_{-}(\nu) \varepsilon_{\alpha\beta\gamma} \cdot \boldsymbol{\tau}_{\gamma}) \phi_{\beta}(k) \mathbf{U}(p)$$

As $f(-\nu) = f(\nu)$

for $f = f_{+} \rightarrow$

$$f(\nu) = f(0) + \frac{2r}{\nu_0} \frac{\nu^2}{\nu_0^2 - \nu^2} + \frac{\nu^2}{\pi} \int_{\mu}^{\infty} \frac{d\nu'^2}{\nu'^2} \frac{\operatorname{Im} f(\nu')}{(\nu'^2 - \nu^2)}$$

Right-hand and left-hand cuts

- Pole positions of wide resonances might be distorted if “left-hand cut” is not taken properly into account (and: analyticity in s , not \sqrt{s})

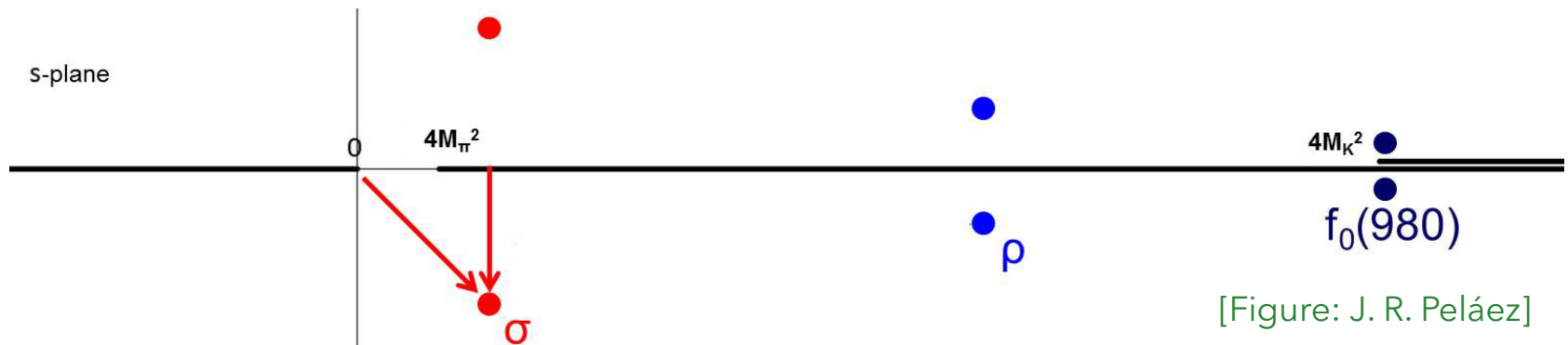
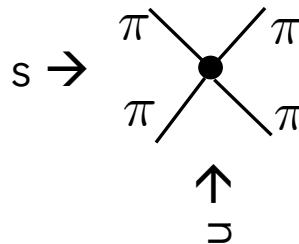


[Figure: J. R. Peláez]

- Build in crossing symmetry manifestly through Roy-(like equations)

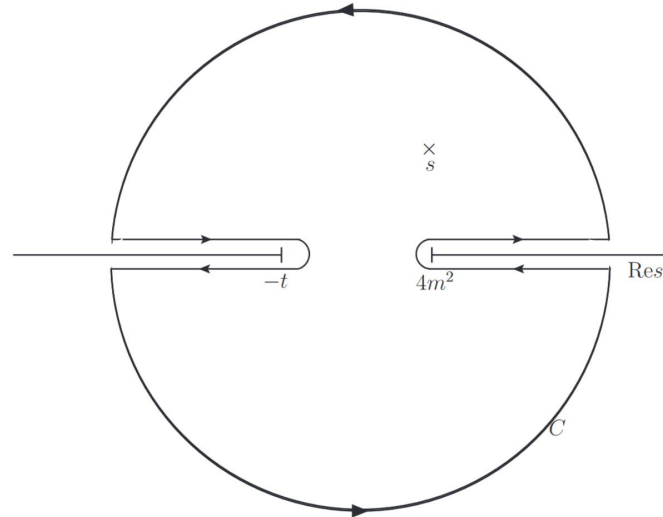
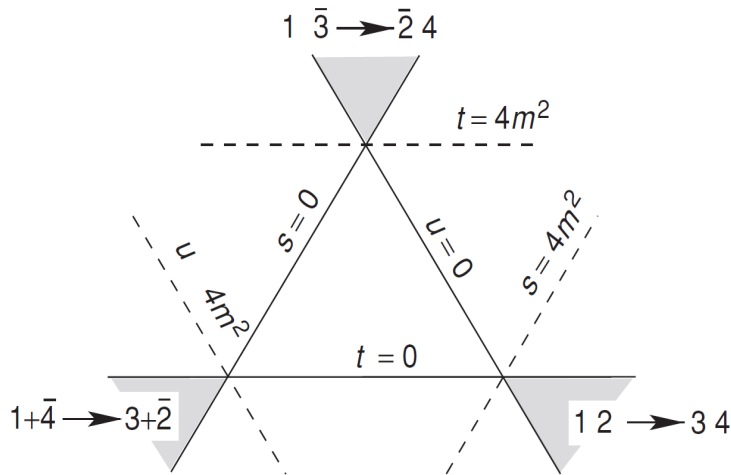
[Peláez]



Advantage: $\pi\pi$ scattering in u -channel is still $\pi\pi$
 πN : [Hoferichter]

Roy(-like) equations

[Figure & formulas:
J. R. Peláez] [Gribov]



$$T(s, t, u) = \frac{1}{\pi} \int_{4m^2}^{\infty} ds' \frac{\text{Im} T(s', t, u')}{s' - s} + \frac{1}{\pi} \int_{-\infty}^{-t} ds' \frac{\text{Im} T(s', t, u')}{s' - s}$$

Subtraction

Unphysical region

Crossing relations:

$$T^{(I)}(s, t) = T^{(I)}(0, t) + \frac{s}{\pi} \int_{4M_{\pi}^2}^{\infty} ds' \left[\frac{\text{Im} T^{(I)}(s', t)}{s'(s' - s)} - \frac{\text{Im} T^{(I)}(u', t)}{u'(u' - s)} \right]$$

$$T^{(I)}(u', t, s') = \sum_{I'} C_{su}^{II'} T^{(I')}(s', t, u'), \quad T^{(I)}(0, t) = \sum_{I''} C_{st}^{II''} T^{(I'')}(t, 0)$$

Only physical Region!

$s \leftrightarrow u$ crossing

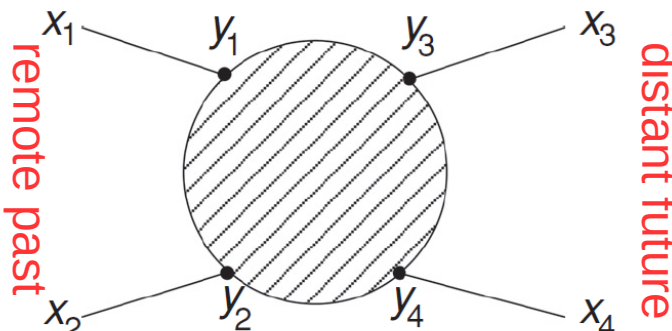
Partial-wave expansion

$$\text{Roy-Eq.: } t_{\ell}^{(I)}(s) = \overline{S} T_{\ell}^I(s) + \sum_{I'=0}^2 \sum_{\ell'=0}^{\ell_{\max}} \int_{4M_{\pi}^2}^{s_{\max}} ds' \overline{K}_{\ell\ell'}^{II'}(s, s') \text{Im } t_{\ell'}^{I'}(s') + \overline{D} T_{\ell}^I(s)$$

Coupled partial waves

Causality and analyticity (1)

- 4-point Green function $A(x_1, x_2; x_3, x_4)$

$$A(x_1, x_2; x_3, x_4) =$$


$$= \int f(y_1, y_2, y_3, y_4) \left\{ \prod_{i=1}^4 D(y_i - x_i) d^4 y_i \right\}$$

- $D(y-x)$: free particle propagation

$$D(y_\mu - x_\mu) = \int \frac{d^3 \mathbf{p}}{(2\pi)^3} \int \frac{dp_0}{2\pi i} \frac{\exp\{-ip^\mu(y-x)_\mu\}}{m^2 - p^2 - i\epsilon}$$

[Gribov]

Causality and analyticity (2)

- As $y_0 > x_0$, pole at $p_0 = \sqrt{m^2 + \mathbf{p}^2}$

$$\begin{aligned}
 D(y_\mu - x_\mu) &= \int \frac{d^3 \mathbf{p}}{(2\pi)^3} \frac{\exp \{-ip^\mu (y - x)_\mu\}}{2p_0} \\
 &= \int \frac{d^3 \mathbf{p}}{(2\pi)^3} \psi_{\mathbf{p}}(y) \cdot \psi_{\mathbf{p}}^*(x), \quad y_0 > x_0
 \end{aligned}$$

- while for final state $x_{03} > y_{03}$, $x_{04} > y_{04}$

$$D(y_\mu - x_\mu) = \int \frac{d^3 \mathbf{p}}{(2\pi)^3} \psi_{\mathbf{p}}(x) \cdot \psi_{\mathbf{p}}^*(y), \quad x_0 > y_0$$

- Truncates amplitude f gets multiplied by product of wave functions.

Causality and analyticity (3): Amplitude in momentum space

- Fourier transform of f :

$$\mathcal{M}(p_i) = \int f(y_1, y_2, y_3, y_4) e^{-i(p_1 y_1 + p_2 y_2) + i(p_3 y_3 + p_4 y_4)} \prod d^4 y_i$$

- Make it simple:

- Forward scattering $p_1 \approx p_3, p_2 \approx p_4$
- Solve some integrals \rightarrow only dependence on relative positions, here chosen: $y_{13} = y_1 - y_3$

$$\mathcal{M} \implies (2\pi)^4 \delta(p_1 + p_2 - p_3 - p_4) \int e^{ip_1(y_3 - y_1)} f(y_{13}; p_2) d^4 y_{13}$$

- Forward scattering \rightarrow Only dependence on one variable

Causality and analyticity (4):

- The amplitude is proportional to the absorption of a particle in y_1 and creation in y_3 (and reversely for anti-particle):

$$f(y_3, y_1) \propto \langle T \psi(y_3) \bar{\psi}(y_1) \rangle \quad \Delta y^\mu = y_3^\mu - y_1^\mu$$

$$\equiv \vartheta(\Delta y_0) \cdot \psi(y_3) \bar{\psi}(y_1) \pm \vartheta(-\Delta y_0) \cdot \bar{\psi}(y_1) \psi(y_3)$$

$$= \vartheta(\Delta y_0) [\psi(y_3) \bar{\psi}(y_1) \mp \bar{\psi}(y_1) \psi(y_3)] \pm \bar{\psi}(y_1) \psi(y_3)$$

(compare to the time evolution operator U in QM which is a time-ordered product;
the S-matrix is actually a time-evolution operator)


- Consider now a space-like interval $(\Delta y)^2 < 0$.
- The operators $\psi(y_3) \bar{\psi}(y_1)$ have to commute; otherwise, a person at y_3 could tell what was measured at $y_1 \rightarrow$ Causality!
- Then: $f(y_3, y_1) \propto \vartheta(\Delta y_0) \vartheta((\Delta y)^2) \cdot f_1 \pm \bar{\psi}(y_1) \psi(y_3)$
- Insert one in the last term:

$$\langle 0 | \bar{\psi}(y_1) \psi(y_3) | 0 \rangle = \sum_n \langle 0 | \bar{\psi}(y_1) | n \rangle \cdot \langle n | \psi(y_3) | 0 \rangle = \sum_n |C_n|^2 e^{-iP_n(y_1 - y_3)}$$

Causality and analyticity (5)

- We still have to integrate over y to get M (see previous slides):

$$\sum_n |C_n^2| \int d^4 y_{31} e^{ip_1 y_{31}} \cdot e^{iP_n y_{31}} \propto \delta(p_{0,1} + P_{0,n}) = 0$$

- This has to be zero because all incoming, outgoing, intermediate particles have positive energy, e.g., $P_{0,n} > 0$
- Finally, as $p_1 y \equiv E_1 t - \mathbf{p}_1 \cdot \mathbf{y} = E_1 \cdot (t - v_1 z)$
 Projection of \mathbf{y} in \mathbf{p}_1 direction

$$\mathcal{M}(E_1) = \int d^4 y f_1(y) \cdot \vartheta(y_0) \vartheta(y_\mu^2) e^{ip_1 y} = \int d^3 \mathbf{y} \int_{\sqrt{\mathbf{y}^2}}^{\infty} dt e^{iE_1(t-v_1 z)} f_1(y)$$

- Make use of all delta-functions \rightarrow

$$t > 0, \quad t > \sqrt{z^2 + \mathbf{y}_\perp^2} \geq |z| > |v_1 z| \implies (t - v_1 z) > 0$$

- If $\text{Im } E_1 > 0$ and f increases less than expon., M converges in the upper half plane.

Causality and analyticity (6)

- Implies the so-called *polynomial boundary* for $M(s)$

$$|\mathcal{M}(s)| < |s|^N$$

- Absolut converging integral \rightarrow Integration and differentiation can be interchanged.

- Cauchy relations:

$$u = u(x, y), v = v(x, y), z = x + iy \rightarrow \frac{\partial u}{\partial x} = \frac{\partial v}{\partial y}, \frac{\partial u}{\partial y} = -\frac{\partial v}{\partial x}$$

- hold in the upper half plane with

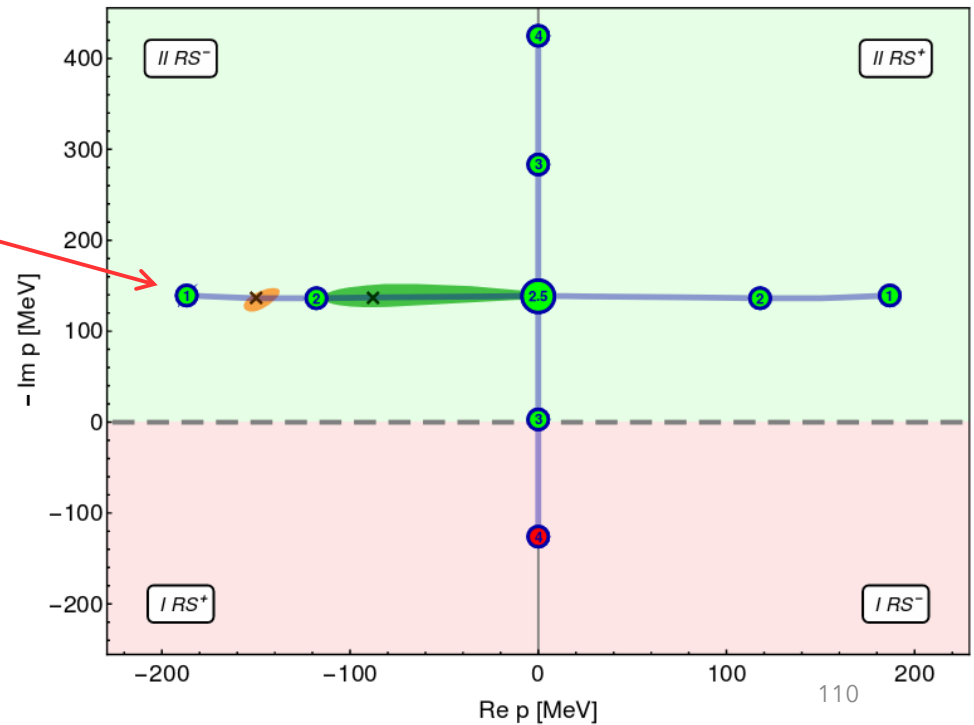
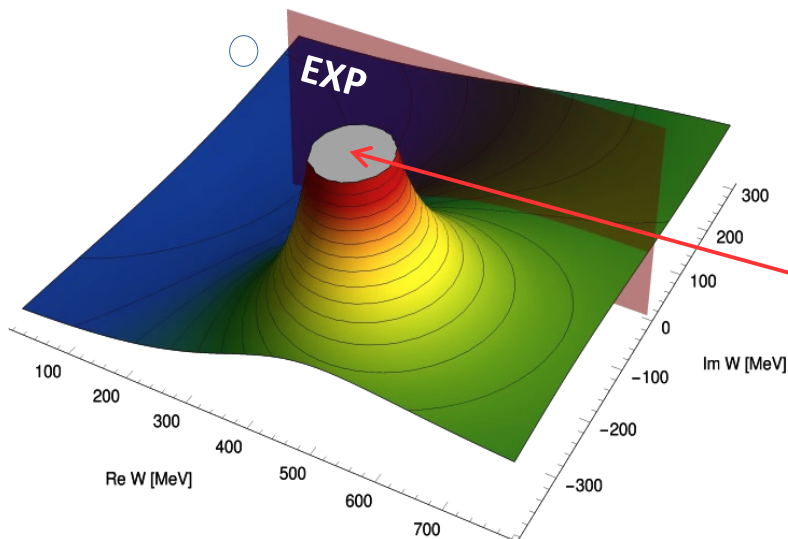
$$u = \operatorname{Re} \mathcal{M}, v = \operatorname{Im} \mathcal{M}, z = E_1$$

- Cauchy relations fulfilled \leftrightarrow function analytic.

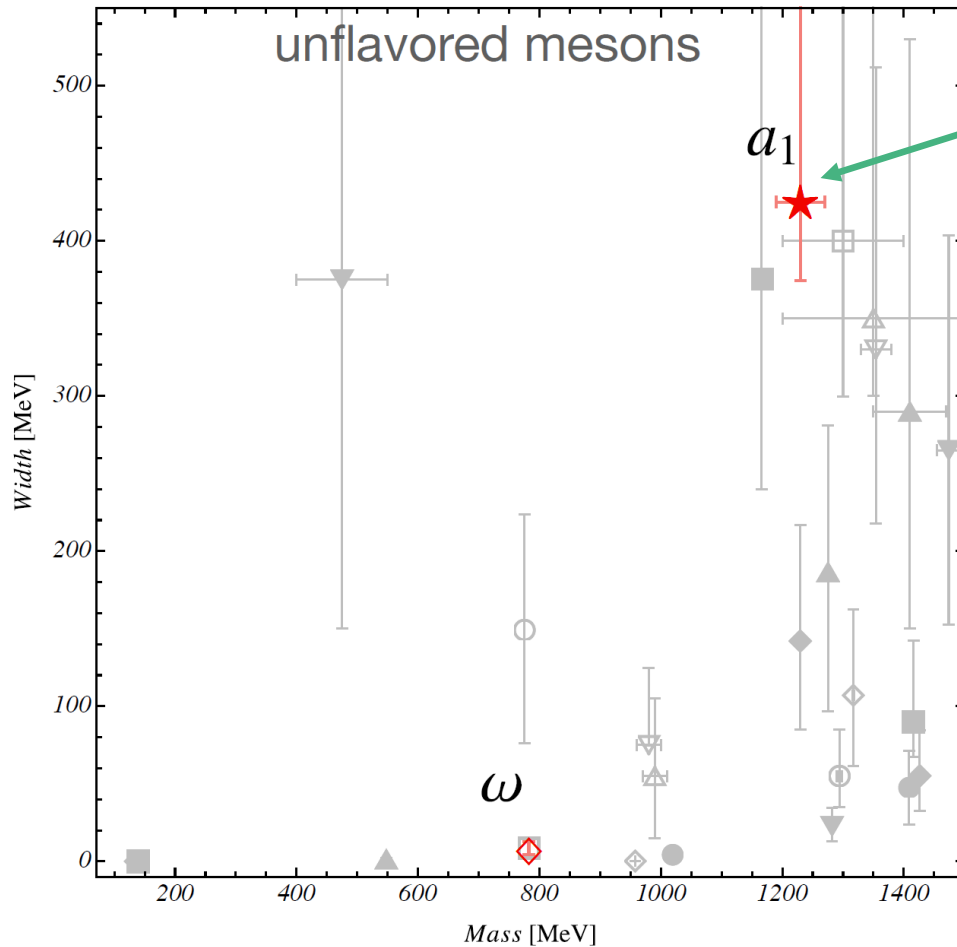
Conclusion: Causality ensures that there are no resonance poles in the upper energy half-plane (1st Riemann sheet)

Chiral trajectories in lattice QCD

- A lattice calculation at $M_\pi=227$ MeV and 315 MeV [GWQCD, [1803.02897](#)]
- σ becomes a (virtual) bound state @ $M_\pi = (345) 415$ MeV



Light unflavored mesons



We concentrate on this resonance!
(because 3-body)

Huge body of work on 2-body
coupled channel resonances from
Lattice QCD (HadSpec collaboration,
BGR group, Bonn group, ...) [\[Briceno\]](#)

Exotic quantum numbers

- A $q\bar{q}$ pair cannot form all possible $(I^G)J^{PC}$ [Meyer]
 - Finding a meson with exotic quantum numbers reveals explicit gluon dynamics at low energies (exp. programs @ COMPASS, GlueX,...)
 - Exp. evidence for $\pi_1(1600)$ rather solid [PDG]
- Which are the allowed forbidden quantum numbers/naming?

Allowed

L	S	J^{PC}	L	S	J^{PC}	L	S	J^{PC}
0	0	0^{-+}	1	0	1^{+-}	2	0	2^{-+}
0	1	1^{--}	1	1	0^{++}	2	1	1^{--}
			1	1	1^{++}	2	1	2^{--}
			1	1	2^{++}	2	1	3^{--}

Some exotics ($J^{PC} = 1^{-+}, \dots$)

J^P	normal meson name	(I^G)	exotic meson name	(I^G)
0^+	a_0	(1^-)	b_0	(1^+)
1^-	ρ	(1^+)	π_1	(1^-)
2^+	a_2	(1^-)	b_2	(1^+)

[Meyer]

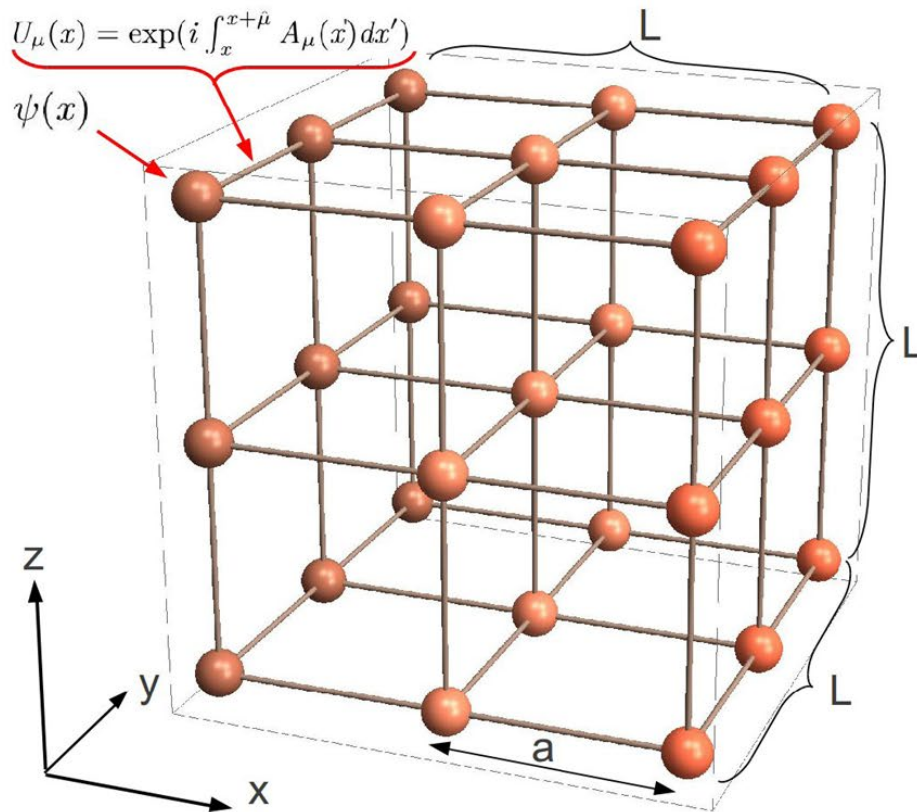
- How can we determine these quantum numbers?

$$P(q\bar{q}) = -(-1)^L$$

$$C(q\bar{q}) = (-1)^{L+S}$$

$$G(q\bar{q}) = (-1)^{L+S+I}$$

3.3 Scattering on a lattice

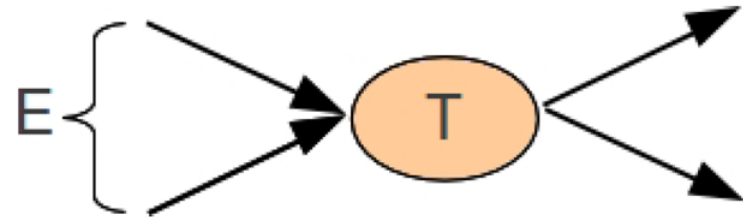


- Side length L ,
periodic boundary conditions
 $\Psi(\vec{x}) \stackrel{!}{=} \Psi(\vec{x} + \hat{e}_i L)$
→ **finite volume effects**
→ **Infinite volume $L \rightarrow \infty$ extrapolation**
- Lattice spacing a
→ **finite size effects**
Modern lattice calculations:
 $a \simeq 0.07 \text{ fm} \rightarrow p \sim 2.8 \text{ GeV}$
→ (much) larger than typical hadronic scales;
not considered here.
- Unphysically large
quark/hadron masses
→ **(chiral) extrapolation**
required.

3.1 Two-body scattering & Lüscher equation

- Unitarity of the scattering matrix S : $SS^\dagger = \mathbb{1}$ $[S = \mathbb{1} - i \frac{p}{4\pi E} T]$.

$$\text{Im } T^{-1}(E) = \sigma \equiv \frac{p}{8\pi E}$$



- → Generic (Lippman-Schwinger) equation for unitarizing the T -matrix:

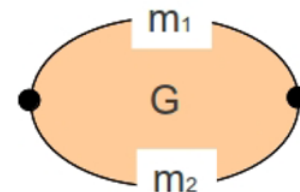
$$T = V + V G T \quad \text{Im } G = -\sigma$$

V : (Pseudo)potential, σ : phase space.

- G : Green's function:

$$G = \int \frac{d^3 \vec{q}}{(2\pi)^3} \frac{f(|\vec{q}|)}{E^2 - (\omega_1 + \omega_2)^2 + i\epsilon},$$

$$\omega_{1,2}^2 = m_{1,2}^2 + \vec{q}^2$$

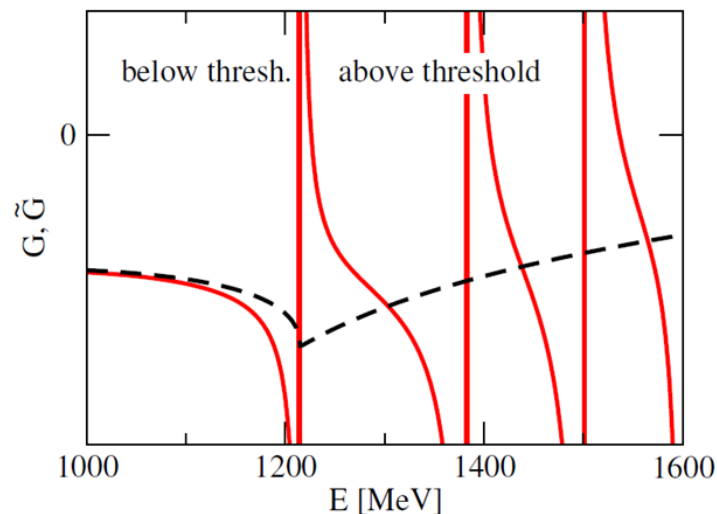
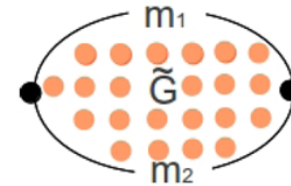


Periodic boundaries and discretization

$$\Psi(\vec{x}) \stackrel{!}{=} \Psi(\vec{x} + \hat{\mathbf{e}}_i L) = \exp(i L q_i) \Psi(\vec{x}) \implies q_i = \frac{2\pi}{L} n_i, \quad n_i \in \mathbb{Z}, \quad i = 1, 2, 3$$

$$\int \frac{d^3 \vec{q}}{(2\pi)^3} g(|\vec{q}|^2) \rightarrow \frac{1}{L^3} \sum_{\vec{n}} g(|\vec{q}|^2), \quad \vec{q} = \frac{2\pi}{L} \vec{n}, \quad \vec{n} \in \mathbb{Z}^3$$

$$G \rightarrow \tilde{G} = \frac{1}{L^3} \sum_{\vec{q}} \frac{f(|\vec{q}|)}{E^2 - (\omega_1 + \omega_2)^2}$$



- $E > m_1 + m_2$: \tilde{G} has poles at free energies in the box, $E = \omega_1 + \omega_2$
- $E < m_1 + m_2$: $\tilde{G} \rightarrow G$ exponentially with L (regular summation theorem).

The Lüscher equation

- Measured eigenvalues of the Hamiltonian (tower of *lattice levels* $E(L)$)
 → Poles of scattering equation \tilde{T} in the finite volume → determines V :

$$\tilde{T} = (1 - V \tilde{G})^{-1} V \rightarrow V^{-1} - \tilde{G} \stackrel{!}{=} 0 \rightarrow V^{-1} = \tilde{G}$$

- The interaction V determines the T -matrix in the infinite volume limit:

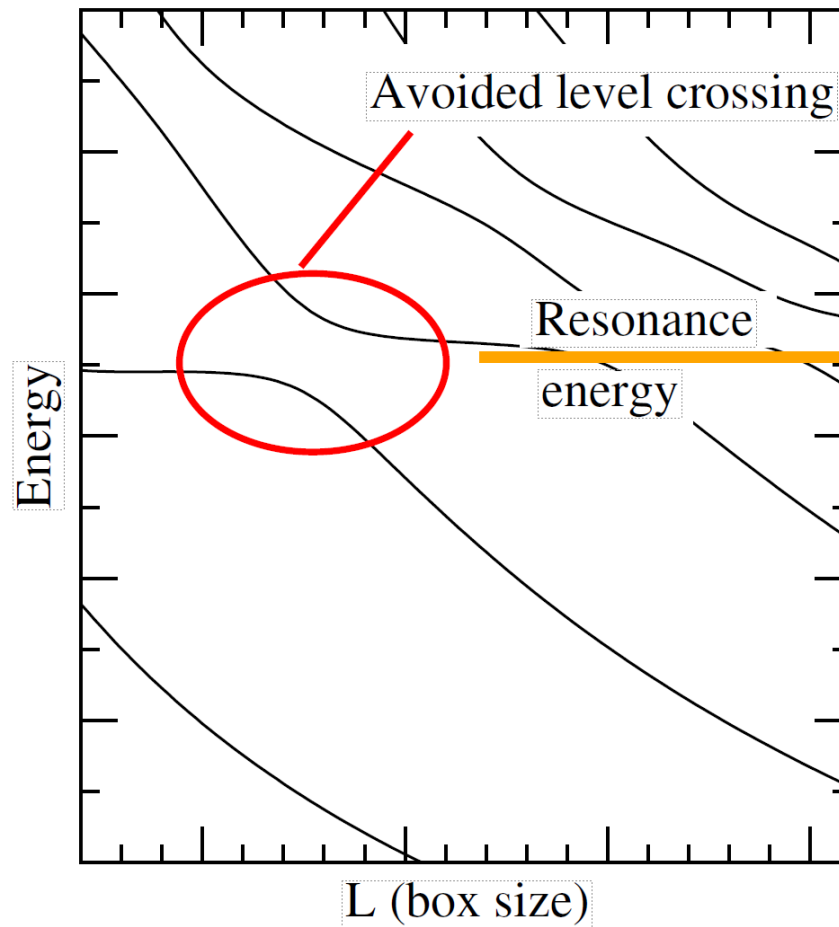
$$T = (V^{-1} - G)^{-1} = (\tilde{G} - G)^{-1}$$

- Re-derivation of Lüscher's equation (T determines the phase shift δ):

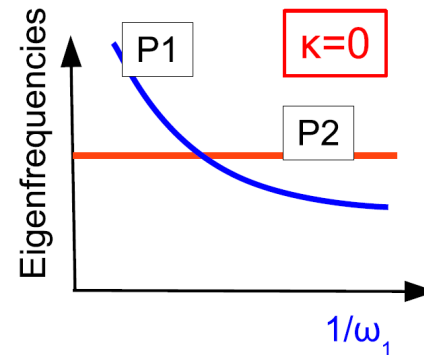
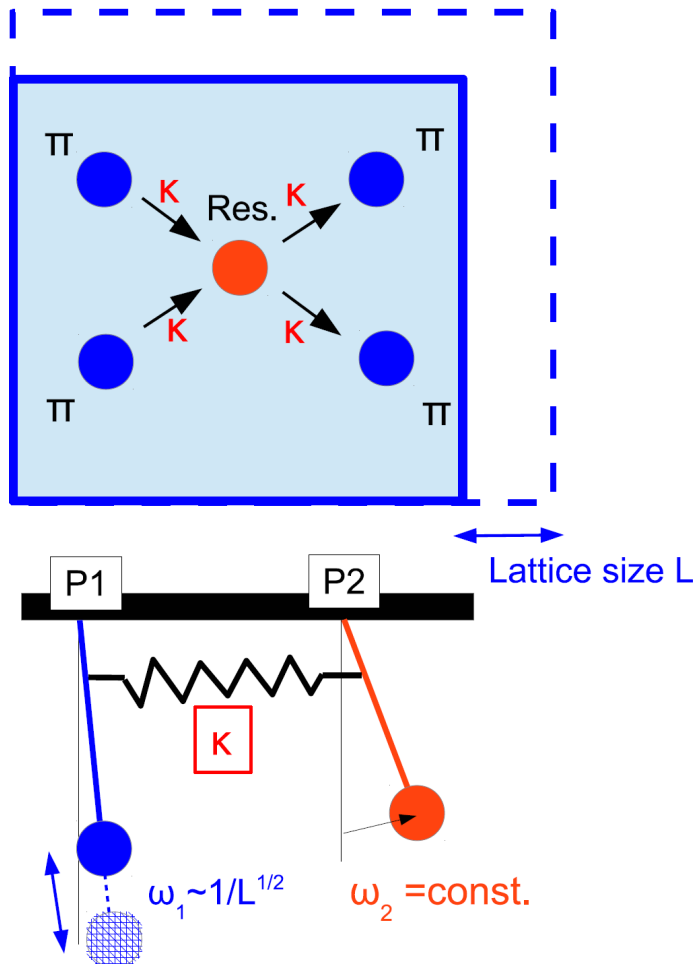
$$p \cot \delta(p) = -8\pi\sqrt{s} (\tilde{G}(E) - \text{Re } G(E))$$

- V and dependence on renormalization have disappeared (!)
- p : c.m. momentum
- E : scattering energy
- $\tilde{G} - \text{Re } G$: known kinematical function
 ($\simeq \mathcal{Z}_{00}$ up to exponentially suppressed contributions)
- One phase at one energy.**

2-body resonances in a box



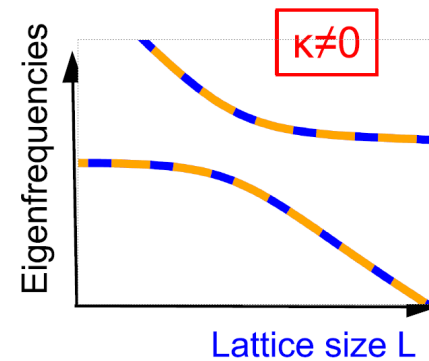
An analogy for avoided level crossing



$$E = 2\sqrt{m_\pi^2 + \left(\frac{2\pi\mathbf{n}}{L}\right)^2}$$

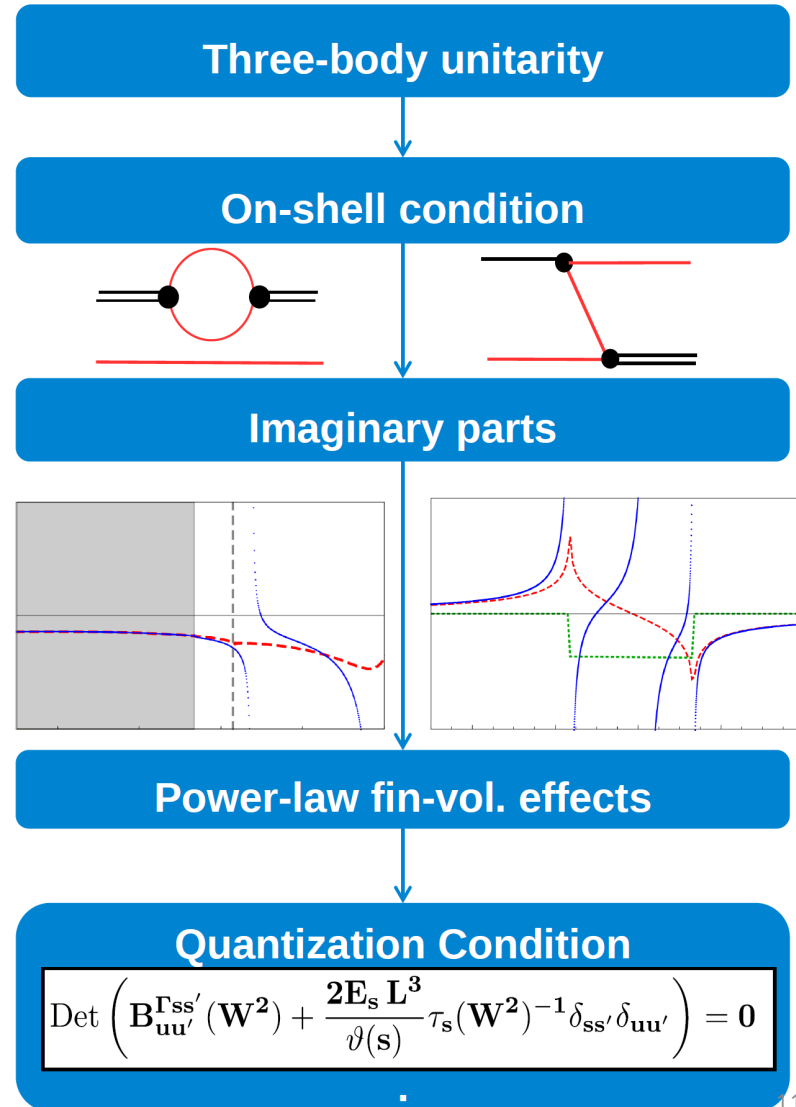
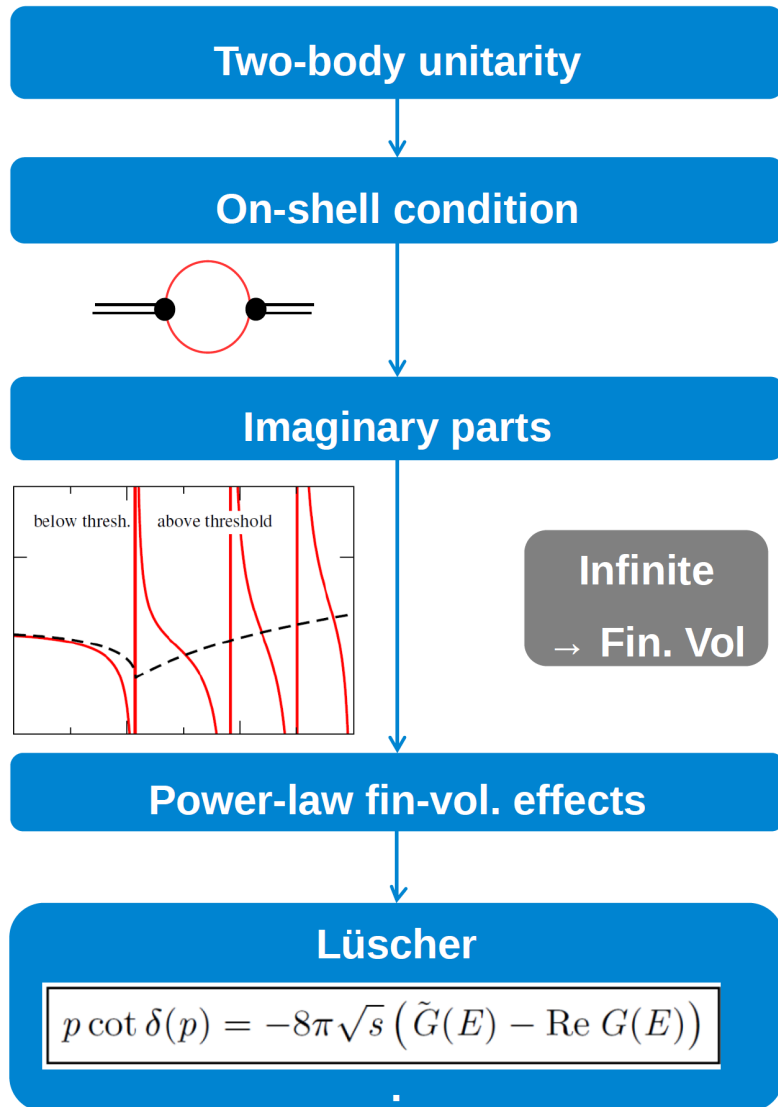
$\mathbf{n} \in \mathbb{Z}^3$

Resonance (system P2)
decouples from pions in a box
(system P1)



Resonance couples to boxed pions

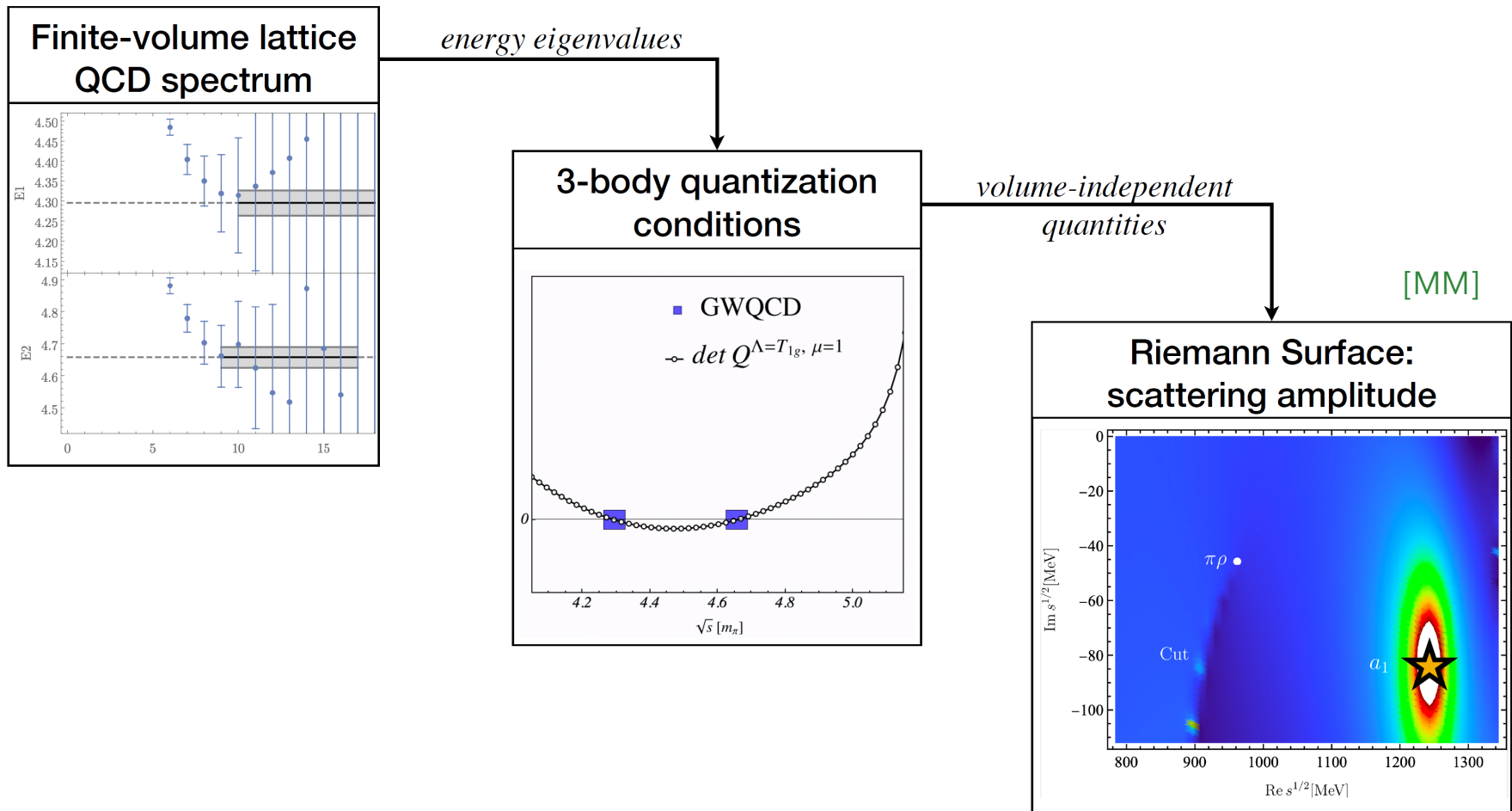
Three-body quantization condition



Extraction of $a_1(1260)$ from IQCD

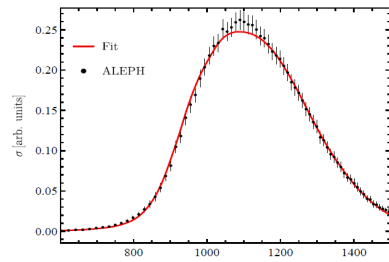
[Mai/GWQCD]

- First-ever three-body resonance from 1st principles (with explicit three-body dynamics).

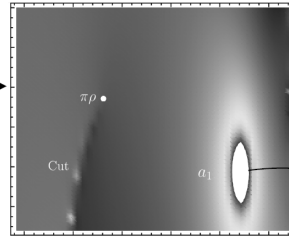


Extraction of $a_1(1260)$ from IQCD

[Mai/GWQCD]

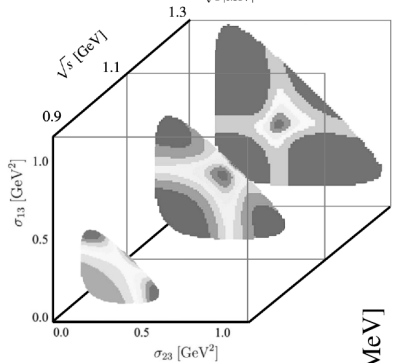


\mathcal{C}

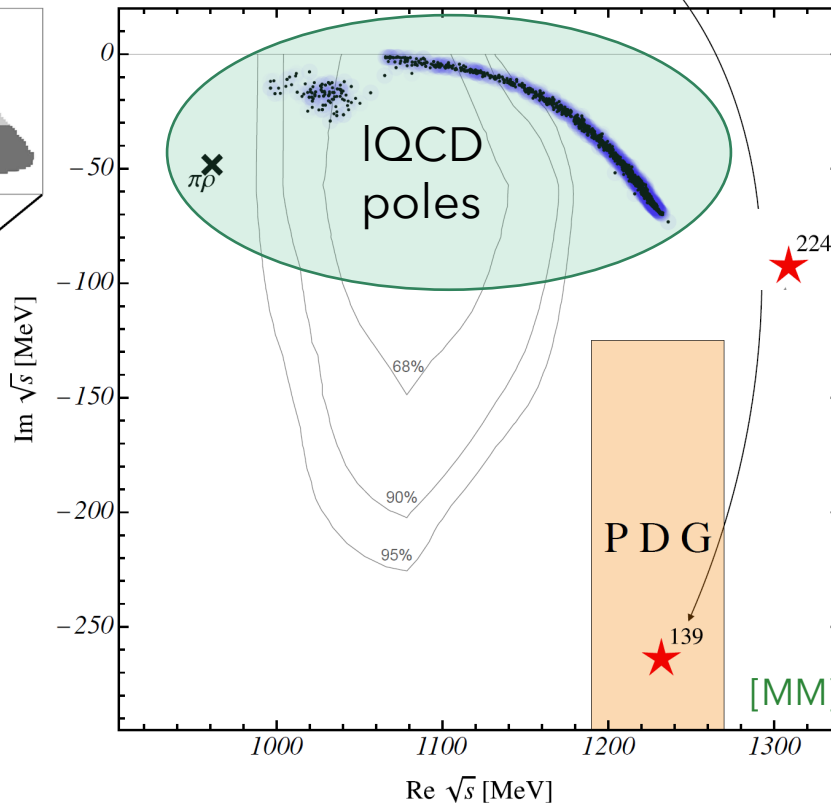


What does phenomenology says?

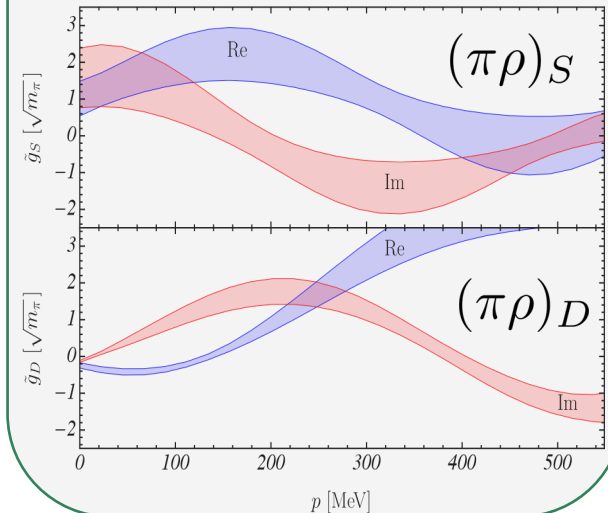
- $\tau \rightarrow (\pi\pi\pi)\nu_\tau$ from ALEPH@CERN
- fit to line shape to fix \mathcal{C}



[Sadasivan]



"Branching ratios" in 3B decays are momentum - dependent, complex pole residues



Review 2B-lattice:
[Briceno]
Reviews 3B-lattice:
[Hansen] [Mai]